Online ISSN: 2249-4596
Print ISSN: 0975-5861
DOI: 10.17406/GJRE

Global Journal

of Researches in Engineering: A

Mechanical & Mechanics Engineering

Highlights

- Conventional Engineering Laws
- Basis of Floating Ash Cenospheres
- Numerical Thermal Stress Analysis
- Optimization of a Static Wavy Flag

Discovering Thoughts, Inventing Future

VOLUME 22 ISSUE 2 VERSION 1.0

Global Journal of Researches in Engineering: A
Mechanical and Mechanics Engineering

Global Journal of Researches in Engineering: A
Mechanical and Mechanics Engineering

Volume 22 Issue 2 (Ver. 1.0)

Open Association of Research Society

Incorporation No.: 0423089
License No.: 42125/022010/1186
Registration No.: 430374
Import-Export Code: 1109007027
Employer Identification Number (EIN):
USA Tax ID: 98-0673427

Global Journals Inc.

*(A Delaware USA Incorporation with "Good Standing"; **Reg. Number: 0423089**)*

Sponsors: Open Association of Research Society
Open Scientific Standards

Publisher's Headquarters office

Global Journals® Headquarters
945th Concord Streets,
Framingham Massachusetts Pin: 01701,
United States of America
USA Toll Free: +001-888-839-7392
USA Toll Free Fax: +001-888-839-7392

Offset Typesetting

Global Journals Incorporated
2nd, Lansdowne, Lansdowne Rd., Croydon-Surrey,
Pin: CR9 2ER, United Kingdom

Packaging & Continental Dispatching

Global Journals Pvt Ltd
E-3130 Sudama Nagar, Near Gopur Square,
Indore, M.P., Pin:452009, India

Find a correspondence nodal officer near you

To find nodal officer of your country, please email us at *local@globaljournals.org*

eContacts

Press Inquiries: *press@globaljournals.org*
Investor Inquiries: *investors@globaljournals.org*
Technical Support: *technology@globaljournals.org*
Media & Releases: *media@globaljournals.org*

Pricing (Excluding Air Parcel Charges):

Yearly Subscription (Personal & Institutional)
250 USD (B/W) & 350 USD (Color)

Editorial Board

Global Journal of Research in Engineering

Prof. (LU), (UoS) Dr. Miklas Scholz

Cand Ing, BEng (equiv), PgC, MSc, Ph.D., CWEM, CEnv, CSci, CEng, FHEA, FIEMA, FCIWEM, FICE, Fellow of IWA, VINNOVA Fellow, Marie Curie Senior, Fellow, Chair in Civil Engineering (UoS) Wetland Systems, Sustainable Drainage, and Water Quality

Dr. Yudong Zhang

B.S., M.S., Ph.D. Signal and Information Processing, Southeast University Professor School of Information Science and Technology at Nanjing Normal University, China

Dr. Minghua He

Department of Civil Engineering Tsinghua University Beijing, 100084, China

Dr. Philip G. Moscoso

Technology and Operations Management IESE Business School, University of Navarra Ph.D. in Industrial Engineering and Management, ETH Zurich M.Sc. in Chemical Engineering, ETH Zurich, Spain

Dr. Stefano Mariani

Associate Professor, Structural Mechanics, Department of Civil and Environmental Engineering, Ph.D., in Structural Engineering Polytechnic University of Milan Italy

Dr. Ciprian Lapusan

Ph. D in Mechanical Engineering Technical University of Cluj-Napoca Cluj-Napoca (Romania)

Dr. Francesco Tornabene

Ph.D. in Structural Mechanics, University of Bologna Professor Department of Civil, Chemical, Environmental and Materials Engineering University of Bologna, Italy

Dr. Kitipong Jaojaruek

B. Eng, M. Eng, D. Eng (Energy Technology, Asian Institute of Technology). Kasetsart University Kamphaeng Saen (KPS) Campus Energy Research Laboratory of Mechanical Engineering

Dr. Burcin Becerik-Gerber

University of Southern Californi Ph.D. in Civil Engineering Ddes, from Harvard University M.S. from University of California, Berkeley M.S. from Istanbul, Technical University

Hiroshi Sekimoto

Professor Emeritus Tokyo Institute of Technology Japan Ph.D., University of California Berkeley

Dr. Shaoping Xiao

BS, MS Ph.D. Mechanical Engineering, Northwestern University The University of Iowa, Department of Mechanical and Industrial Engineering Center for Computer-Aided Design

Dr. A. Stegou-Sagia

Ph.D., Mechanical Engineering, Environmental Engineering School of Mechanical Engineering, National Technical University of Athens, Greece

Diego Gonzalez-Aguilera

Ph.D. Dep. Cartographic and Land Engineering, University of Salamanca, Avilla, Spain

Dr. Maria Daniela

Ph.D in Aerospace Science and Technologies Second University of Naples, Research Fellow University of Naples Federico II, Italy

Dr. Omid Gohardani

Ph.D. Senior Aerospace/Mechanical/ Aeronautical, Engineering professional M.Sc. Mechanical Engineering, M.Sc. Aeronautical Engineering B.Sc. Vehicle Engineering Orange County, California, US

Dr. Paolo Veronesi

Ph.D., Materials Engineering, Institute of Electronics, Italy President of the master Degree in Materials Engineering Dept. of Engineering, Italy

Contents of the Issue

Global Journal of Researches in Engineering: A
Mechanical and Mechanics Engineering
Volume 22 Issue 2 Version 1.0 Year 2022
Type: Double Blind Peer Reviewed International Research Journal
Publisher: Global Journals
Online ISSN: 2249-4596 & Print ISSN: 0975-5861

Why Conventional Engineering Laws are *Irrational,* and a *Paradigm Shift* that Results in *Rational* Laws

By Eugene F. Adiutori

Abstract- Conventional engineering laws are irrational for three reasons: When the laws are applied to *nonlinear* behavior, they have *three* variables to describe how *two* variables are related; they are founded on Fourier's *erroneous* claims that dimensions *can rationally* be assigned to *numbers,* and dimensions *can rationally* be multiplied or divided. Until now, it has been globally accepted that parameter symbols in rational equations represent numerical value *and* dimension. The proposed paradigm shift *requires* that parameter symbols in equations represent *only* numerical value, *and* if an equation is *quantitative*, the dimension units that underlie parameter symbols *must* be specified in an accompanying nomenclature. The proposed paradigm shift results in laws and equations that are dimensionally homogeneous because they are *dimensionless*. The new laws are analogs of $y = f\{x\}$. The new laws state that the *numerical value* of parameter *y* is a function of the *numerical value* of parameter *x*, and the function may be proportional, linear, or nonlinear. The new laws are rational because they *always* have only *two* variables, they do *not* require that dimensions be assigned to numbers, and they do *not* require that parameter dimensions be multiplied or divided.

Keywords: dimensional homogeneity, dimensions, irrational equations, irrational laws, newton's laws, paradigm shift, parameters, proportions, rational equations, rational laws.

GJRE-A Classification: DDC Code: 512.74 LCC Code: QA241

Strictly as per the compliance and regulations of:

Why Conventional Engineering Laws are *Irrational,* and a *Paradigm Shift* that Results in *Rational* Laws

Eugene F. Adiutori

Abstract- Conventional engineering laws are irrational for three reasons: When the laws are applied to *nonlinear* behavior, they have *three* variables to describe how *two* variables are related; they are founded on Fourier's *erroneous* claims that dimensions *can rationally* be assigned to *numbers,* and dimensions *can rationally* be multiplied or divided. Until now, it has been globally accepted that parameter symbols in rational equations represent numerical value *and* dimension. The proposed paradigm shift *requires* that parameter symbols in equations represent *only* numerical value, *and* if an equation is *quantitative*, the dimension units that underlie parameter symbols *must* be specified in an accompanying nomenclature. The proposed paradigm shift results in laws and equations that are dimensionally homogeneous because they are *dimensionless*. The new laws are analogs of $y = f\{x\}$. The new laws state that the *numerical value* of parameter y is a function of the *numerical value* of parameter x, and the function may be proportional, linear, or nonlinear. The new laws are rational because they *always* have only *two* variables, they do *not* require that dimensions be assigned to numbers, and they do *not* require that parameter dimensions be multiplied or divided. The new laws make it *much simpler* to learn and apply engineering science because they *always* contain only *two* variables, and because *all* parameters (such as h and E) that were created by assigning dimensions to *numbers* are *abandoned*. They are *not* replaced because they are *not* necessary.

Keywords: *dimensional homogeneity, dimensions, irrational equations, irrational laws, newton's laws, paradigm shift, parameters, proportions, rational equations, rational laws.*

I. Introduction

Conventional engineering laws such as Eq. (1) are irrational because:

$$q = h\Delta T \tag{1}$$

- If q is a nonlinear function of ΔT (as in free convection, condensation, and boiling), h is a *variable*. Consequently Eq. (1) has *three* variables (q, h, and ΔT) to describe how *two* variables (q and ΔT) are related. It is *irrational* to use equations that have *three* variables to describe how *two* variables are related.
- The laws are based on Fourier's *erroneous* claims that dimensions *can* rationally be assigned to *numbers*, and parameter dimensions *can* rationally be multiplied or divided.

The proposed paradigm shift *requires* that parameter symbols in equations represent *only* numerical values, and if an equation is *quantitative*, the dimension units that underlie parameter symbols *must* be specified in an accompanying nomenclature. The proposed paradigm shift results in the replacement of laws that are analogs of Eq. (1) with laws that are analogs of Eq (2).

$$y = f\{x\} \tag{2}$$

Equation (2) states that the *numerical value* of parameter y is a function of the *numerical value* of parameter x, and the function may be proportional, linear, or nonlinear. The new laws make it *much simpler* to learn and apply engineering science because they *always* contain only *two* variables, and because *all* parameters (such as h and E) that were created by assigning dimensions to *numbers* are *abandoned*. They are *not* replaced because they are *not* necessary.

a) Dimensional Homogeneity until 1822

Until 1822, scientists and engineers such as Galileo and Newton agreed that:

- Parameter symbols in proportions and equations represent numerical value *and* dimension.
- Parameters *cannot* be multiplied or divided because parameter dimensions *cannot* be multiplied or divided.[1]
- Equations *cannot* describe how parameters are related because parameters *cannot* be multiplied or divided.
- Proportions need *not* be dimensionally homogeneous.
- Equations *must* be dimensionally homogeneous.

Because proportions need *not* be dimensionally homogeneous, and because proportions that relate two

Author: *Ventuno Press. e-mail: efadiutori@aol.com*

[1] However, a dimension *can* be divided by the *same* dimension. For example, meters *can* be divided by meters, and seconds *can* be divided by seconds, but meters *cannot* be divided by seconds. In the qualitative equations that result, all terms are dimensionless ratios. This methodology was used by Galileo.

parameters do *not* require that parameters be multiplied or divided, proportions are generally used instead of equations. That is why Hooke's [2] law is Proportion (3) instead of an equation, Newton's [3] law of cooling[2] is Proportion (4) instead of Eq. (5), and Newton's [4] second law of motion is Proportion (6) instead of Eq. (7).

$$\sigma \alpha \varepsilon \tag{3}$$

$$(dT_{body}/dt)\ \alpha \quad (T_{air} - T_{body}) \tag{4}$$

$$q = h\Delta T \tag{5}$$

$$a\ \alpha f \tag{6}$$

$$f = ma \tag{7}$$

b) Fourier's Heat Transfer Experiment, and the Proportion and Equation that Resulted

Fourier performed a heat transfer experiment in which a warm, solid body is cooled by the steady-state forced convection of ambient air. Fourier concluded that Proportion (8) and Eq. (9) correlate the data.

$$q\ \alpha\ \Delta T \tag{8}$$

$$q = c\Delta T \tag{9}$$

Newton and his colleagues would have been satisfied by Proportion (8), but it did *not* satisfy Fourier because he wanted an *equation*, and it *had* to be dimensionally homogeneous. Equation (9) did *not* satisfy Fourier because it is *not* dimensionally homogeneous.

c) Fourier's Revolutionary and Unproven View of Dimensional Homogeneity that Enabled him to Transform in Homogeneous Eq. (9) to Homogeneous Eq. (10)

Fourier recognized that Eq. (9) could be transformed to a dimensionally homogeneous equation *only* if it were rational to *assign* dimensions to *number c* in Eq. (9), *and* rational to *multiply and divide* parameter dimensions. Fourier [1] describes his *revolutionary* and *unproven* view of dimensional homogeneity in the following:

. . . every undetermined magnitude or constant has one dimension proper to itself, and the terms of one and the same equation could not be compared, if they had not the same exponent of dimension. . . this consideration is derived from primary notions on quantities; for which reason, in geometry and mechanics, it is the equivalent of the fundamental lemmas which the Greeks have left us ***without proof.***

It is important to note that, in Fourier's nearly 500 page treatise, *The Analytical Theory of Heat* [1], he made *no effort* to prove that his view of dimensional homogeneity is rational. He did *not* include the Greek lemmas, he did *not* cite a reference where the Greek lemmas could be found, and he did *not* include his own proof.

Fourier's *revolutionary* view of dimensional homogeneity includes the following *erroneous* claims:

- Dimensions *can* be assigned to *numbers*.
- Parameter *dimensions can* be multiplied or divided.

In accordance with his *erroneous* view of dimensional homogeneity, Fourier *assigned* the symbol h and the dimension of $q/\Delta T$ to *number c* in Eq. (9), then *multiplied* h and ΔT, resulting in dimensionally homogeneous Eq. (10).

$$q = h\Delta T \tag{10}$$

d) The Definition of h

American heat transfer texts generally do not define h. Nomenclatures in heat transfer texts generally state only that h is "heat transfer coefficient". However, rearranging Eq. (10) results in Eq. (11).

$$h = q/\Delta T \tag{11}$$

Equations (10) and (11) state that h and $q/\Delta T$ are *identical* and *interchangeable*. They also state that h is a symbol for the *dimensional group* $q/\Delta T$.

Combining Eqs. (10) and (11) results in Eq. (12). Note that Eqs. (10) and (12) are *identical* because h and $q/\Delta T$ are *identical* and *interchangeable*.

$$q = (q/\Delta T)\Delta T \tag{12}$$

The nomenclature in *every* conventional heat transfer text should state "h is a symbol for the dimensional group $q/\Delta T$—*i.e.* h and $q/\Delta T$ are *identical* and *interchangeable*".

e) What Eq. (10) meant in Most of the Nineteenth Century

In most of the nineteenth century, Eq. (10) was *always* a *proportional* equation, and h was *always* a proportionality *constant*. Fourier warned that Eq. (10) applies *only* if a solid, warm body is cooled by the *steady-state forced convection* of *ambient air*. He *emphasized* that Eq. (9) does *not* apply if a solid, warm body is cooled by the *natural convection* of ambient air because the coolant flow rate would *vary*, and consequently the relationship between q and ΔT would *not* be proportional.

[2] American heat transfer texts generally refer to Eq. (5) as "Newton's law of cooling", and claim that Newton created h. However, Eq. (5) *cannot* be Newton's law of cooling because cooling is a *transient* phenomenon, and Eq. (5) is a *steady-state* equation. Also because Eq. (5) *requires* that h and ΔT be multiplied, whereas in Newton's time, it was *irrational* to multiply parameters. Newton could *not* have created h because he could *not* rationally have multiplied h times another parameter.

f) What Eq. (10) has meant Since Sometime near the End of the Nineteenth Century

Sometime near the end of the nineteenth century, the heat transfer community decided to ignore Fourier's warning that Eq. (10) applies *only* if the heat transfer behavior is proportional. It decided to apply Eq. (10) even if the relationship between q and ΔT is *nonlinear*.

When Eq. (10) is applied to *nonlinear* heat transfer phenomena, it is *not* an equation because a *proportional* equation *cannot* describe *nonlinear* behavior. Even though Eq. (10) is a proportional equation, it *must now* be interpreted to mean that the relationship between q and ΔT *may* be proportional, linear, or nonlinear, and h *may* be a *constant* or a *variable*.

g) The Equation that should have Replaced Eq. (10) when it began to be Applied to Nonlinear Phenomena

When the decision was made to apply Eq. (10) to nonlinear phenomena, Eq. (10) *should* have been *abandoned* because it obviously *cannot* describe *nonlinear* behavior. Equation (10) should have been replaced by Eq. (13) because it correctly states that the relationship between q and ΔT may be *proportional, linear, or nonlinear*, and h may be a *constant* or a *variable*.

$$q = h\{\Delta T\}\Delta T \tag{13}$$

Note that Eqs. (13) and (13a) are *identical.* They *both* state that q is a function of ΔT, and the function may be proportional, linear, or nonlinear.

$$q = f\{\Delta T\} \tag{13a}$$

However, Eq. (13a) could *not* rationally have replaced Eq. (10) because, based on conventional parameter symbolism, Eq. (13a) is *not* dimensionally homogeneous.

h) Why Conventional Engineering Laws are Irrational

Substituting $q/\Delta T$ for h in Eq. (13) results in Eq. (14).

$$q = (q/\Delta T)\{\Delta T\}\Delta T \tag{14}$$

Equation (14) is a *rigorously correct* expression of the modern law of convective heat transfer. Note that Eq. (14) is an analog of Eq. (15), and $q/\Delta T$ (i.e. h) is an analog of $(y/x)\{x\}$.

$$y = (y/x)\{x\}x \tag{15}$$

In mathematics, if y is a *nonlinear* function of x, Eq. (15) is *never* used because $(y/x)\{x\}$ is a *third* variable, and it *greatly* complicates problem solutions. Equation (16) is *always* used because it *always* has only *two* variables, and therefore it *always* allows nonlinear problems to be solved in the simplest possible way—ie with y and x *separated* rather than *combined* in an analog of $(y/x)\{x\}$.

$$y = f\{x\} \tag{16}$$

Laws such as Eqs. (10), (12), (13), and (14) are *irrational* because, if q is a nonlinear function of ΔT, they have *three* variables (q, $q/\Delta T$, and ΔT) to describe how *two* variables (q and ΔT) are related. And similarly for *all proportional* engineering laws that are applied to *nonlinear* phenomena.

i) Proof that Fourier was Wrong. Dimensions cannot Rationally be Assigned to Numbers

Langhaar [5] explains why dimensions *cannot* rationally be assigned to numbers:

*Dimensions **must not** be assigned to numbers, for then any equation could be regarded as dimensionally homogeneous.*

j) Proof that Fourier was Wrong. Dimensions cannot Rationally be Multiplied or Divided

Conventional engineering laws and equations are based in part on Fourier's *unproven* claim that parameter *dimensions can* be multiplied or divided. Fourier was *wrong*. As demonstrated by the following, parameter dimensions *cannot* rationally be multiplied or divided.

"Multiply four times seven" means "add seven four times". Therefore "multiply meters times kilograms" *must* mean "add kilograms meters times". Because "add kilograms meters times" has *no meaning*, dimensions *cannot* be multiplied.

"Divide forty by five" means "how many fives are in forty". Therefore "divide meters by seconds" *must* mean "how many seconds are in meters". Because "how many seconds are in meters" has *no meaning*, dimensions *cannot* be divided.

k) Irrational Views in Conventional Engineering

The following are irrational views in conventional engineering.

- Hooke's law, Proportion (17), *and* Young's law, Eq. (18), are *identical*. They *both* state that stress equals a constant times strain. Therefore it is *irrational* to *require* Young's law to be dimensionally homogeneous, and *not* require Hooke's law to be dimensionally homogeneous.

$$\sigma \alpha \varepsilon \tag{17}$$

$$\sigma = E_{elastic}\varepsilon \tag{18}$$

- A chart of q vs ΔT is a picture of Eq. (19).

$$q = f\{\Delta T\} \tag{19}$$

It is *irrational* to *reject* Eq. (19) because it is *not* dimensionally homogeneous, and to *accept* a *chart* of Eq. (19) that is *not* dimensionally homogeneous.

- Charts are *dimensionless* because they describe how the *numerical value* of parameter *y* is related to the *numerical value* of parameter *x*. If a chart is *quantitative,* the dimension units that underlie parameters *x* and *y must* be specified on the chart, or in an accompanying nomenclature.

Because charts are pictures of equations, and because charts are *dimensionless*, it is *irrational* to *not* have equations in which parameter symbols are *dimensionless*.

The above *irrational* views have *no place* in the engineering science that results from the paradigm shift.

l) What Equations can Rationally describe about how Parameters are Related

Equations *can* rationally describe how the *numerical values* of parameters are related because dimensionless equations are *inherently* dimensionally homogeneous. If a dimensionless equation is *quantitative*, the dimension units that underlie parameter symbols (that are *not* in dimensionless groups) *must* be specified in an accompanying nomenclature.

m) The Proposed Paradigm Shift

The proposed paradigm shift *requires* that parameter symbols in equations represent *only* numerical value. If an equation is *quantitative*, the dimension units that underlie parameter symbols *must* be specified in an accompanying nomenclature.

n) The Engineering Science that Results from the Proposed Paradigm Shift

The engineering science that results from the proposed paradigm shift is described by:

- *All* proportions and equations are *dimensionless* because *all* parameter symbols represent *only* numerical value.
- *All* proportions and equations are *dimensionally homogeneous* because they are dimensionless.
- If an equation is *quantitative*, the dimension units that underlie parameter symbols are specified in an accompanying nomenclature (except for symbols in dimensionless groups).
- *All* engineering laws are replaced by analogs of Eq. (20) which states that the *numerical value* of parameter *y* is a function of the *numerical value* of parameter *x*, and the function may be proportional, linear, or nonlinear.

$$y = f\{x\} \tag{20}$$

- There are *no* parameters that were created by assigning dimensions to numbers.

o) How to Transform Conventional Texts to Texts based on the Proposed Paradigm Shift

To transform conventional engineering texts to texts based on the proposed paradigm shift:

- Replace laws with analogs of $y = f\{x\}$.
- In equations that include analogs of (y/x), replace analogs with y/x, then separate x and y.

For example, to transform Eq. (21) to a paradigm shift equation, replace h and k_{wall}/t_{wall} with $q/\Delta T$, then separate q and ΔT, resulting in Eq. (22).

$$U = (1/h_1 + t_{wall}/k_{wall} + 1/h_2)^{-1} \tag{21}$$

$$\Delta T_{total} = \Delta T_1\{q\} + \Delta T_{wall}\{q\} + \Delta T_2\{q\} \tag{22}$$

It is important to note that Eqs. (21) and (22) are *identical*. They mean *exactly the same thing*. Equation (21) is written in the *opaque* language of conventional engineering. Equation (22) is written in the *transparent* language of the proposed paradigm shift. (Convection heat transfer correlations are generally in the form $\Delta T\{q\}$ because that is the form required by Eq. (22).

Textbooks for other branches of engineering are transformed to paradigm shift texts in the same way heat transfer texts are transformed—i.e. by replacing conventional laws with laws that are analogs of Eq. (16), and transforming equations by *separating* x and y.

p) How Data are Correlated in Conventional Engineering, and in Engineering based on the Proposed Paradigm Shift

Experimenters *cannot* obtain h data or E data because there is *no such thing* as h *or* E. They are *symbols* for *dimensional groups* $q/\Delta T$ and Δ/Δ.

In conventional engineering, experimenters obtain q data and ΔT data, and use it to determine $q/\Delta T$ values and $(q/\Delta T)\{\Delta T\}$ correlations—ie to determine h values and $h\{\Delta T\}$ correlations.

In engineering based on the proposed paradigm shift, experimenters obtain q data and ΔT data, and use it to determine $\Delta T\{q\}$ correlations. And similarly for other engineering branches.

q) Correlation Transformations and Experiments

It is important to note that the proposed paradigm shift does *not* require that experiments that resulted in *conventional* correlations be *repeated*. It requires merely that conventional correlations be transformed by separating parameter x and parameter y as described in Section 16, or that the data that resulted in conventional correlations be used to determine correlations that are analogs of $y = f\{x\}$.

II. Conclusions

Conventional engineering science works well when applied to problems that concern *proportional* behavior because it is founded on laws that are *proportional* equations, and the coefficients in the laws (such as *h* and *E)* are *proportionality constants*. It does *not* work well when applied to problems that concern *nonlinear* behavior because the coefficients in the laws (such as *h* and *E*) are *extraneous variables*, and they *greatly* complicate problem solutions.

Engineering science should be founded on the proposed paradigm shift because it results in laws that work well with *all* forms of behavior—proportional, linear, and nonlinear. The new laws make it *much simpler* to learn and apply engineering science because they *always* have only *two* variables, and because *all* parameters (such as *h* and *E*) that were created by assigning dimensions to *numbers* are *abandoned*. They are *not* replaced because they are *not* necessary.

Nomenclature

a	acceleration
c	arbitrary constant
E	modulus
F	force
h	$q/\Delta T$
k	$q/(dT/dx)$
m	mass
q	heat flux
T	temperature
t	time or wall thickness
x	arbitrary variable
y	arbitrary variable
ε	strain
σ	stress

References Références Referencias

1. Fourier, J., 1822, *The Analytical Theory of Heat*, Article 160, Dover edition (1955) of the 1878 English translation.
2. Hooke, R., 1676, encoded in "A Description of Helioscopes" per *Robert Hooke's Contributions to Mechanics* by F. F. Centore, Martinus Nijhoff/The Hague, 1970.
3. Newton, I., "A Scale of the Degrees of Heat", *Phil Trans Royal Soc* (London), 1701, **22**, p. 824.
4. Newton, I., *The Principia*, 1726, 3rd edition, translation by Cohen, I. B. and Whitman, A. M., 1999, p 460, University of California Press.
5. Langhaar, H. L., 1951, *Dimensional Analysis and Theory of Models*, p. 13, John Wiley & Sons.

This page is intentionally left blank

Global Journal of Researches in Engineering: A
Mechanical and Mechanics Engineering
Volume 22 Issue 2 Version 1.0 Year 2022
Type: Double Blind Peer Reviewed International Research Journal
Publisher: Global Journals
Online ISSN: 2249-4596 & Print ISSN: 0975-5861

Numerical Analysis and Parametric Optimization of a Static Wavy Flag for Heat Transfer Enhancement

By Swadesh Suman & Sanjay Mahadev Gaikwad
Army Institute of Technology

Abstract- This work investigates the effect of different parameters of a static wavy flag vortex generator on the heat transfer in a rectangular channel using Computational Fluid Dynamics (CFD) analysis. This work encompasses optimizing several parameters of a flag such as flag height from the surface, position in the channel, number of triangular shapes in a flag, and rectangular surface area of the flag. Post analysis results exhibit encouraging results with average Nusselt number in flag height (FH) optimization exceeding that in no flag condition by 41.84%, 47.79%, 54.68% for Re 8236, 12354, and 18344, respectively whereas further position optimization of FH optimized flag exceeds average Nusselt number in no flag condition by 46.86%, 70.68% and 87.26% for the corresponding Re. With significantly less practical application of flags for heat transfer enhancement in industry, this work aims to establish flags as an effective heat transfer enhancement device and demonstrate that with the right optimized parameters, a significant increase of heat transfer in the channel can be achieved.

Keywords: *convective heat transfer, heat transfer enhancement, turbulence, vortex generator.*

GJRE-A Classification: *DDC Code: 621.4022 LCC Code: TJ260*

Strictly as per the compliance and regulations of:

Numerical Analysis and Parametric Optimization of a Static Wavy Flag for Heat Transfer Enhancement

Swadesh Suman [α] & Sanjay Mahadev Gaikwad [σ]

Abstract- This work investigates the effect of different parameters of a static wavy flag vortex generator on the heat transfer in a rectangular channel using Computational Fluid Dynamics (CFD) analysis. This work encompasses optimizing several parameters of a flag such as flag height from the surface, position in the channel, number of triangular shapes in a flag, and rectangular surface area of the flag. Post analysis results exhibit encouraging results with average Nusselt number in flag height (FH) optimization exceeding that in no flag condition by 41.84%, 47.79%, 54.68% for Re 8236, 12354, and 18344, respectively whereas further position optimization of FH optimized flag exceeds average Nusselt number in no flag condition by 46.86%, 70.68% and 87.26% for the corresponding Re. With significantly less practical application of flags for heat transfer enhancement in industry, this work aims to establish flags as an effective heat transfer enhancement device and demonstrate that with the right optimized parameters, a significant increase of heat transfer in the channel can be achieved.

Keywords: convective heat transfer, heat transfer enhancement, turbulence, vortex generator.

I. Introduction

Performance optimization of systems involving heat transfer through channels has always been the area of focus in the past decades. Numerous systems which employ heat transfer through channels like automotive, refrigeration and air-conditioning, electrical and electronic system are becoming compact gradually and with it, the demand for effective and efficient heat transfer is increasing. Correlations presented by Dittus and Boelter well relate the Nusselt number inside the channel with the Reynolds number and the Prandtl number of the fluid [1]. Modification of the Nusselt number is generally attained by altering the Reynolds number as varying the Prandtl number is rather challenging. Alteration of the Reynolds number is accomplished by introducing additional turbulences in the flow. One of the methods employed for introducing additional turbulences in the flow is the utilization of vortex generators.

Author α: Department of Mechanical Engineering, Army Institute of Technology, Pune, India. e-mail: swadesh.ni@gmail.com
Author σ: Assistant Professor, Department of Mechanical Engineering, Army Institute of Technology, Pune, Maharashtra, India.
e-mail: gaikwads.sanjay@gmail.com

Ralph Kristoffer B. Gallegos and Rajnish N Sharma [2] outlined the categories as well as the advantages and disadvantages of each category of vortex generators and presented a brief review on flags as vortex generators. The two categories of vortex generators are active and passive. Many reviews and studies on passive vortex generators like swirl flow devices and other approaches including bubble fin assistance, surface modifications, reduced weight fin configuration, etc. have been extensively reported [3-10]. The use of active vortex generators like piezo fans and magnetic fans for improvement of heat transfer is studied by Gilson GM et al. [11] and Ma HK et al. [12,13]. Jae Bok Lee et al. [14,15] explored the dynamics of the flag in symmetric as well as asymmetric configuration and the effects of various parameters such as bending rigidity, channel height, and Reynolds number on the overall thermal efficiency of the system. Zheng Li et al. [16] studied the effects of Youngs's modulus of the flapping vortex generator on its vorticity fields and heat transfer performances. Atul Kumar Soti et al. [17] used a fluid-structure interaction solver to show the flow-induced deformation as an effective heat transfer technique and examined the role of the Reynolds number, Prandtl number, and the material properties of the plate in the thermal improvement. Jaeha Ryu et al. [18] examined the flapping dynamics of the flag in terms of bending rigidity and Reynold number employing the immersed boundary method. Sung Goon Park et. al [19] with the help of immersed boundary method studied the various dynamic modes of the flag and the vortical structures produced in the wake region of the flag. F. Herrault et al. [20] and Hidalgo and Glezer [21,22] utilized oscillating reeds in the high aspect ratio rectangular microchannels and manifested significant improvements in the thermal performance of the system. Shoele and Mittal [23] studied the material properties of flexible reed on vibratory dynamics, and heat transfer, establishing that thermal performance depends more strongly on the reed inertia than its bending stiffness.

Some recent performance optimization of an engineering system is also based on constructal theory. According to the constructal theory by A. Bejan: "For a finite-size flow system to persist in time (to live) its configuration must change in time so that it provides greater and greater access to its currents" [24]. A review

Nomenclature

ρ_a	Density of fluid (air) (kg/m^3)	T_i	Initial average temperature of the fluid at the channel's inlet (K)
A_c	Cross section area of the channel (m^2)	T_d	Difference between the final and initial average temperature of the fluid (K)
V	Velocity of the fluid (air) (m/s)	T_w	Average temperature of the aluminium plate surface (K)
C_p	Specific heat capacity of air at constant pressure (J/kg K)	T_f	Average temperature of the fluid (K)
k	Thermal Conductivity of the medium (w/m-K)	T_a	Difference between the average temperature of the surface and fluid (K)
μ	Dynamic viscosity of the fluid (air) (Pa.s)	FH	Flag height
ρ_{al}	Density of aluminium (kg/m^3)	RS	Rectangular surface
A_s	Surface area of the aluminium plate (m^2)		FLAG GEOMETRIES
$C_{p(al)}$	Specific heat capacity of aluminium at constant pressure (J/kg K)	ROTF	Rectangular flag combined with one triangular flag
k_{al}	Thermal Conductivity of aluminium (w/m-K)	RTTF	Rectangular flag combined with two triangular flags
Q	Heat carried away by the fluid (w/m^2)	RTeTF	Rectangular flag combined with three triangular flags
D_h	Hydraulic diameter of the channel (m)	RFTF	Rectangular flag combined with four triangular flags
$\dot{M}$	Mass flow rate (kg/s)	RFiTF	Rectangular flag combined with five triangular flags
h	Average heat transfer coefficient (w/m^2 K)		
Nu	Average Nusselt number of the fluid		
Re	Reynolds number		
$\emptyset_q$	Heat flux (W/m^2)		
T	Temperature (K)		
T_o	Final average temperature of the fluid at the channel's outlet (K)		

of constructal theory and the ongoing research trends in this domain is presented by A. Bejan and S. Lorente in [25,26]. Chen LinGen [27,28] focuses on the emergence and expansion of constructal theory and its application in China over the past decade to solve engineering problems. Adrian Bejan [29] solved the fundamental problem of collection and channeling the heat generated volumetrically in a low conductivity volume of a given size to one point. Huijun Feng et al. [30] emphasized enhancing the heat transfer rates by just making a few design changes based on an optimized process of heat and mass transfer between the fluids and used constructal optimization for heat dissipation in "+" shaped high conductivity channels to increase the global heat conductivity performance of electronic device [31] and to reduce entransy dissipation rate of X-shaped vascular networks (XSNV) [32]. Chen LinGen et al. [33] have accomplished optimal constructs of the eight types of heat sinks with different constraints and carried out a comparison between them based on the different optimization objectives. Huijun Feng et al. [34] executed a triple optimization on an irreversible Kalina cycle system 34 (KCS-34) model with variable temperature heat reservoirs using finite-time-thermodynamics. H. J. Feng et al. [35] have adopted a Global optimization method to study the tree-shaped hot network over a rectangular area. Huijun Feng et al. [36] carried out the constructal design of a supercharged boiler (SB) superheater with optimization objectives as heat transfer rate and power consumption factors of SB superheater.

This work builds on the earlier work of Swadesh Suman et al. [37]. According to Swadesh suman et al. [37], the shape exhibiting the highest heat transfer is the

combination of rectangular and two triangular shapes (RTTF). This work utilizes RTTF for the further optimization process. The channel geometry, velocity conditions, boundary conditions, and fluid properties are identical to that used by Swadesh Suman et al. [37]. ANSYS 2014 is used for the numerical work. Geometry is modeled in ANSYS ICEM, analysis, and post-processing is carried out in ANSYS FLUENT and ANSYS CFD-POST, respectively.

II. Problem Description

a) Channel Geometry, Fluid Properties and Boundary Condition

The channel geometry, fluid properties, and boundary conditions are identical to that employed in the investigation carried out by Swadesh suman et al. [37]. The length, breadth, and height of the channel are 150 mm, 150 mm, and 110 mm respectively which set forth the hydraulic diameter of the channel as 126.9 mm. A heater of 20 w capacity, which provides a constant heat flux of 888.88 w/m^2, is installed in the identical fashion as that in the investigation of Swadesh [37]. The existing fluid in the channel is air. The air temperature at the inlet of the channel is between 25 and 30 degrees Celsius so the density, dynamic viscosity, thermal conductivity, and specific heat of air is taken as 1.174 kg/m^3, 18.605 μ Pa.s, 0.0256 w/m-k, 1006.43 j/kg-k respectively. At the channel's inlet velocity inlet boundary condition and at the channel's outlet pressure outlet boundary condition with outlet pressure as 1 atm is applied. No slip boundary condition is employed at the channel's walls and the flag surface. Three different velocity conditions i.e., 1.1 m/s, 1.65 m/s, and 2.45 m/s are used for the numerical investigation.

b) Governing Equations

Since the study involves both heat conduction and convection, it is one of the classical problems of conjugate heat transfer. The conduction in the aluminum plate is a three-dimensional steady state without a heat source within the plate. The equation shows 3-D steady state heat conduction equation without a heat source within the volume [1].

$$\frac{\partial}{\partial x}\left(\frac{\partial T}{\partial x}\right)+\frac{\partial}{\partial y}\left(\frac{\partial T}{\partial y}\right)+\frac{\partial}{\partial z}\left(\frac{\partial T}{\partial z}\right)=0 \quad (1)$$

Where T is the temperature.

Standard K - **ε** viscous model is used in Ansys Fluent for the analysis as the Reynolds number falls under the turbulent range. The standard K - **ε** model requires two additional equations to solve the additional unknown given by the Reynolds stress term in the RANS equation (Reynolds Average Navier Stokes) [38].

$$\rho\bar{u}_j\frac{\partial\bar{u}_i}{\partial x_j}=\rho\bar{f}_i+\frac{\partial}{\partial x_j}[-\bar{p}\delta_{ij}+\mu(\frac{\partial\bar{u}_i}{\partial x_j}+\frac{\partial\bar{u}_j}{\partial x_i})-\rho\overline{u'_i u'_j}] \quad (2)$$

Here,

u represents instantaneous velocity

$\bar{u}$ represents mean (time averaged) component of velocity

u' represents fluctuating component of velocity

ρ represents density

$\overline{f_i}$ is a vector representing external forces

μ represents dynamic viscosity of fluid

The additional equations of K - **ε** model are [32]

For turbulent kinetic energy K

$$\frac{\partial}{\partial t}(\rho k)+\frac{\partial}{\partial x_i}(\rho k u_i)=\frac{\partial}{\partial x_j}\left[\frac{\mu_t}{\sigma_k}\frac{\partial k}{\partial x_j}\right]+2\mu_t E_{ij}E_{ij}+\rho\epsilon \quad (3)$$

For dissipation Rate **ε**

$$\frac{\partial}{\partial t}(\rho\epsilon)+\frac{\partial}{\partial x_i}(\rho k u_i)=\frac{\partial}{\partial x_j}[u\frac{\mu_t}{\sigma_\epsilon})\frac{\partial\epsilon}{\partial x_j}]+C_{1\epsilon}\frac{\epsilon}{k}2\mu_t E_{ij}E_{ij}-C_{2\epsilon}\rho\frac{\epsilon^2}{k} \quad (4)$$

u_i represents velocity component in corresponding direction

E_{ij} represents component of rate of deformation

μ_t represent eddy viscosity

$$\mu_t=\rho C_\mu\frac{k^2}{\epsilon}$$

The equations also consist of some adjustable constants σ_k, σ_ϵ,$C_{1\epsilon}$,$C_\mu$and $C_{2\epsilon}$. The values of these constants have been arrived at by numerous iterations of data fitting for a wide range of turbulent flows [39]. These are as follows:

$\sigma_k = 1.00$
$\sigma_\epsilon = 1.30$
$C_\mu = 0.09$
$C_{1\epsilon} = 1.44$
$C_{2\epsilon} = 1.92$

c) Selection of Parameters

Various parameters related to the flag are the shape of the flag, the position of the flag in the channel, the height of the flag from the surface, the surface area of the flag, and the width of the flag. For the optimization based on the shape of a flag, the shape optimized flag established by Swadesh suman et al. [37] is selected. Two other parameters which can be selected from the shape optimized flag is the number of triangular shape and the relative area of the rectangular shape of the flag. This shape-optimized flag is used for further parametric optimization. Keeping the width of the flag constant, the various parameters to optimize are the height of the flag

from the surface, the position of the flag in the channel, the number of triangular shapes, and the relative area of the rectangular shape in the shape-optimized flag.

d) Grid Independence Study

To remove the influence of the grid size on the result, a grid independence study is performed by varying the Grade scale factor (GSF) of the meshing in Ansys ICEM. The geometry selected is the rectangular channel with no flag condition. The initial value of GSF is kept at 1 and was increased by 0.5 until the variation of the *Nu* is acceptable. The Reynolds number for this study is chosen as 12354 corresponding to the velocity of 1.65 m/s. Table 1 shows the total number of cells, nodes, and *Nu* variation at different values of GSF.

Table 1: Variation of *Nu* with GSF

GSF	Total number of cells	Total number of nodes	*Nu*	*Re*
1	302502	54225	256.7	12354
1.5	1025087	180077	247.4	12354
2	2430221	419890	249.2	12354
2.5	4709977	806414	247.7	12354
3	8193797	1398852	240.5	12354

The *Nu* value at GSF 1.5 showed a drop of 3.62% than the *Nu* value at GSF 1. Although this drop is within the permissible limit, to further reduce the error analysis is carried out at GSF 2. At GSF 2 the variation in the *Nu* value was just 0.72%. Further at GSF 2.5 and 3, it showed the variation of 0.61% and 2.9% respectively. So, based on the variation at different GSF values and time of computation, the ideal value of GSF is chosen 2 and further analysis is carried out at GSF 2.

III. Flag Height (FH) Optimization

a) Representation of FH and CFD Simulations

Figure 1 represents flag height (FH) which is varied to find the optimum height of RTTF from the plate. Shape-optimized RTTF and its arrangement in the channel by Swadesh Suman et al. [37] is used for FH optimization. The initial height of RTTF from the plate is 2.5 mm. FH is varied from 0.5 mm to 5 mm, increasing it by 0.5 mm from 0.5 mm to 3 mm and by 1 mm from 3 mm to 5 mm.

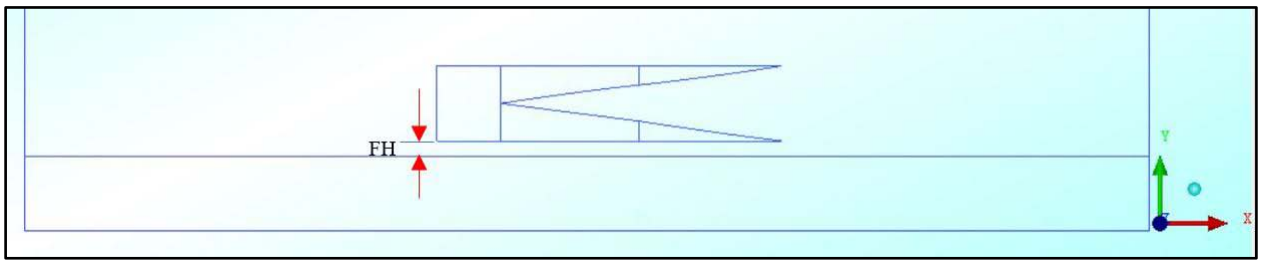

Figure 1: Representation of Flag Height (FH)

Figure 2a and 2b show the thermal boundary layer formed in the case of FH 1 mm and FH 2 mm. The temperature contour in each case shows the difference in temperature.

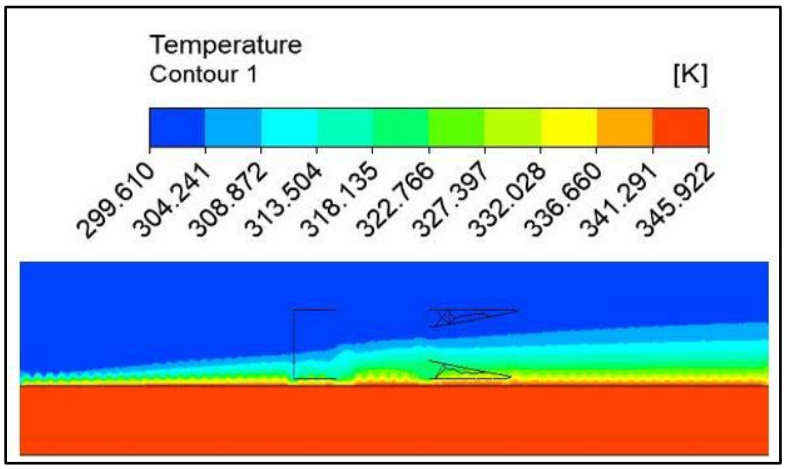

Figure 2a): FH = 1 mm

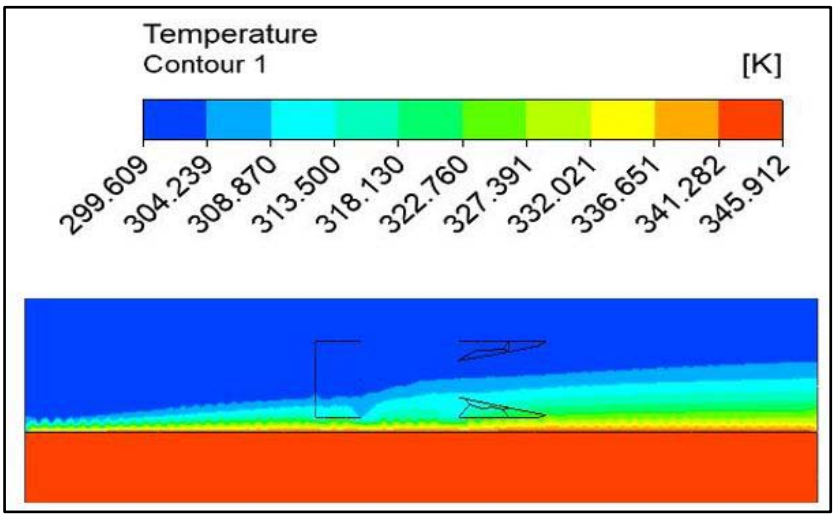

Figure 2b): FH = 2 mm

Figure 2: Thermal Boundary Layer at Different Flag Height

b) Procedure followed during Calculations

The procedure followed during the calculations is same as that used by Swadesh Suman et al. [37]. Fig 3 shows the lines plotted along the length of the channel and an average temperature is obtained for each line. The well distributed lines along the channel's height gives good idea of the average temperature of air at channel's outlet.

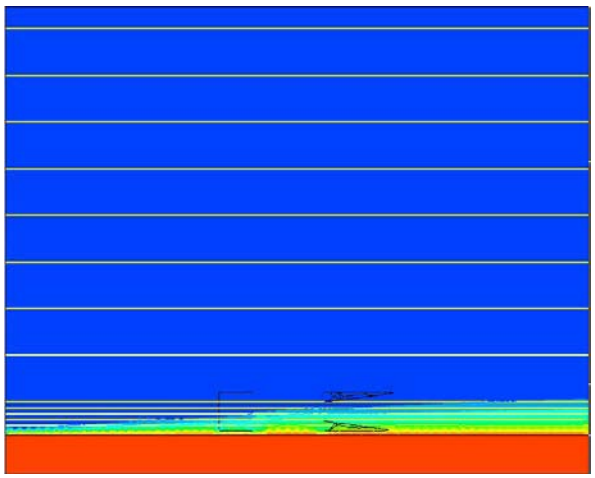

Figure 3: Lines Plotted along the Length of the Channel

Following procedure is then followed to find out the average Nusselt number in each case:-

Step 1: Mass flow rate $(\dot{M}) = \rho \times A_c \times V$ (5)

Step 2: Temperature change in fluid $(T_d) = T_o - T_i$ (6)

Step 3: Heat carried away by the fluid $(Q) = \dot{M} \times C_p \times T_d$ (7)

Step 4: Average temperature difference between surface and fluid $(T_a) = T_w - T_f$ (8)

Step 5: Average heat transfer coefficient $(h) = \frac{Q}{A_s \times T_a}$ (9)

Step 6: Nusselt no $(Nu) = \frac{h \times D_h}{k}$ (10)

Step 7: Reynolds no $(Re) = \frac{\rho \times V \times D_h}{\mu}$ (11)

c) Results and Discussion

Table 2 shows the Nusselt number for each flag height at different velocity conditions. The highest *Nu* is achieved at a flag height equal to 1 mm for each velocity condition and it increases significantly by 10.06%, 7.28%, and 7.55% when compared with *Nu* values for flag height of 1.5 mm and exceeds that in no flag condition by 41.84%, 47.79%, 54.68% for Re 8236, 12354 and 18344, respectively. *Nu* values at each different velocity condition shoot up with the decrease in

FH up to 1 mm. At FH 0.5 mm, *Nu* values diminishes significantly by 11.1%, 9.3%, and 8.5% than that of FH 1 mm for *Re* 8236, 12354, and 18344, respectively. The same has been depicted in fig 4 which presents the graph between *Nu* and *Re*.

Table 2: Nusselt Number at Different Flag Heights

Velocity (m/s)	*Nu*	*Re*
No flag condition		
1.1	239	8236
1.65	249	12354
2.45	267	18344
FH 0.5 mm		
1.1	301	8236
1.65	334	12354
2.45	380	18344
FH 1 mm		
1.1	339	8236
1.65	368	12354
2.45	413	18344
FH 1.5 mm		
1.1	308	8236
1.65	343	12354
2.45	384	18344
FH 2 mm		
1.1	299	8236
1.65	312	12354
2.45	348	18344
FH 2.5 mm		
1.1	288	8236
1.65	301	12354
2.45	324	18344
FH 3 mm		
1.1	278	8236
1.65	294	12354
2.45	322	18344
FH 4 mm		
1.1	274	8236
1.65	291	12354
2.45	319	18344
FH 5 mm		
1.1	272	8236
1.65	287	12354
2.45	314	18344

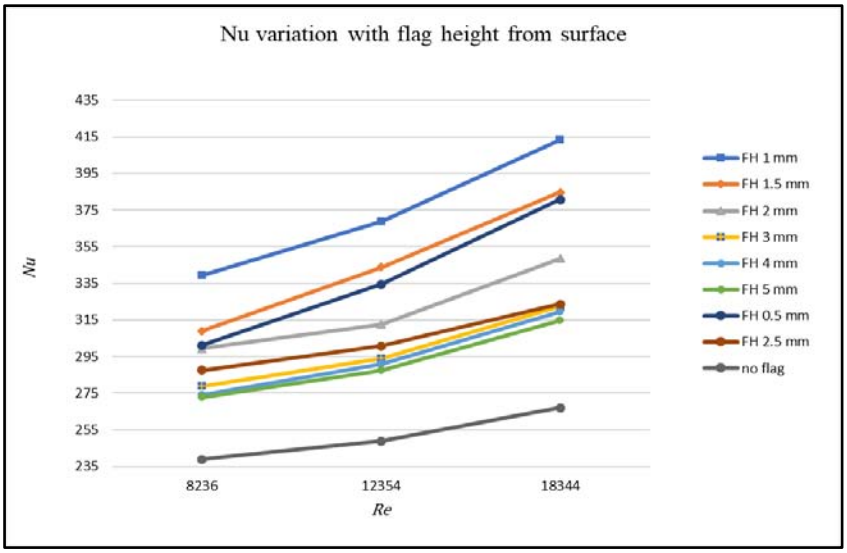

Figure 4: Average Nusselt Number vs Reynolds Number for Different Flag Heights

IV. Optimization of Position of Flag in Channel

a) Representation of Position of the Flag

RTTF with FH 1 mm is used for the optimization of the position of the flag. Figure 5 represents the position of the flag from the inlet which is varied to find the optimum position of RTTF from the inlet. The initial position of RTTF from the inlet is 55 mm. The position from the inlet is varied from 15 mm to 65 mm, increasing it by 10 mm in each step.

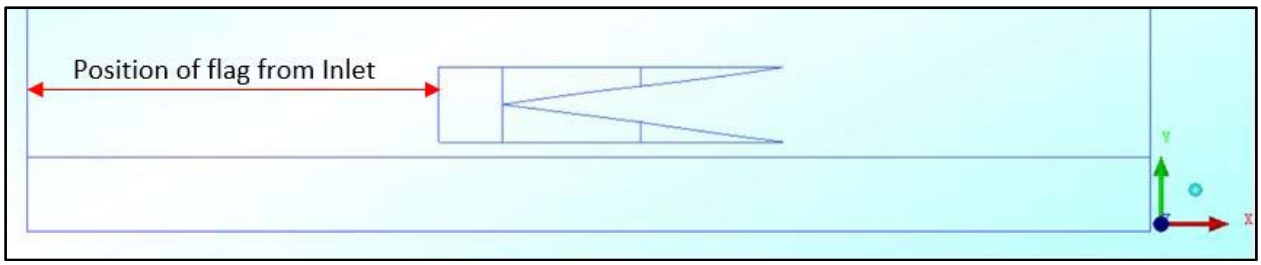

Figure 5: Representation of Position of Flag from inlet

b) Procedure followed during Calculations

The procedure followed for the calculation of *Nu* is the same as that of Flag height optimization.

c) Results and Discussion

Table 3 shows the Nusselt number for the position of the flag at different velocity conditions. The highest *Nu* is achieved at a flag position equal to 35 mm for each velocity condition. *Nu* at flag position 35 mm is greater than that at flag position 25 mm by 2.63%, 6.78%, 10.13%, and by 2.03%, 8.97%, 12.10% for *Re* 8236, 12354, 18344 respectively when compared with *Nu* values for flag position 45 mm. Whereas it exceeds *Nu* in no flag condition by 46.86%, 70.68%, and 87.26% for the corresponding Re. In each case, the percentage rise in *Nu* increases with an increase in the velocity of air in the channel. *Nu* values at each different velocity condition shoot up with the decrease in flag positions from 65 mm up to 35 mm and afterward, it diminishes till the flag position is 15 mm. The same has been depicted in fig 6 which presents the graph between *Nu* and *Re*.

Table 3: Nusselt number at different flag positions

Velocity (m/s)	*Nu*	*Re*
No flag condition		
1.1	239	8236
1.65	249	12354
2.45	267	18344
Position of flag = 15 mm		

1.1	340	8236
1.65	372	12354
2.45	438	18344
Position of flag = 25 mm		
1.1	342	8236
1.65	398	12354
2.45	454	18344
Position of flag = 35 mm		
1.1	351	8236
1.65	425	12354
2.45	500	18344
Position of flag = 45 mm		
1.1	344	8236
1.65	390	12354
2.45	446	18344
Position of flag = 55 mm		
1.1	339	8236
1.65	368	12354
2.45	413	18344
Position of flag = 65 mm		
1.1	268	8236
1.65	295	12354
2.45	319	18344

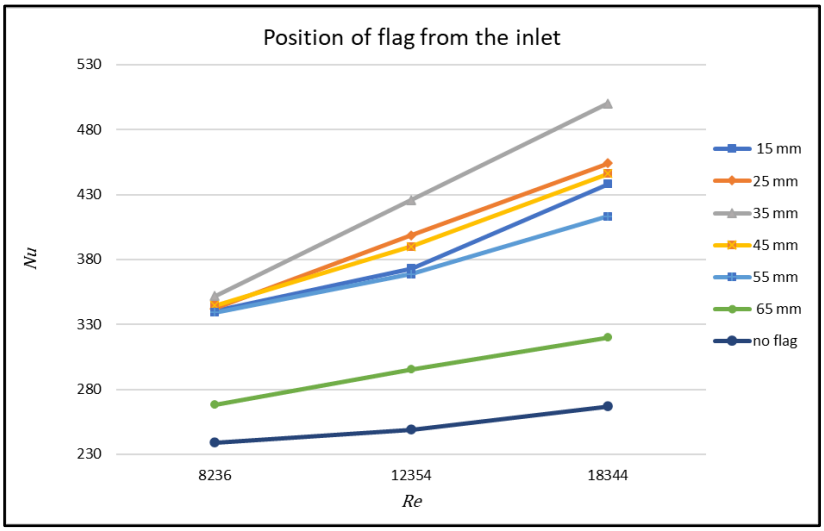

Figure 6: Average Nusselt number vs Reynolds number for different position of flag

V. Optimization of Number of Triangular Shape in RTTF

a) Flag Geometries

RTTF used for this stage has FH as 1 mm and position from the inlet as 35 mm. In the investigation by Swadesh suman et al. [37], RTTF showed higher heat transfer than ROTF. So, to check the dependency of heat transfer on the number of triangular shapes, the number of triangular shapes is varied. Fig. 7 shows all five flag geometries. The total surface area of the triangular part of RTTF is kept constant while varying the number of triangular shapes. Fig 7 also incorporates the symbolic representation allotted to each flag with the different number of triangular shapes.

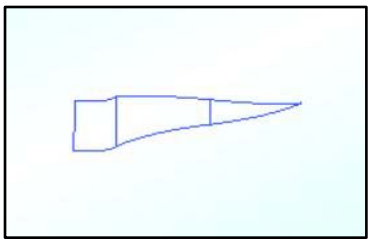

7a) Rectangular flag combined with one triangular flag (ROTF)

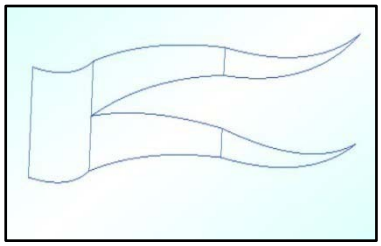

7b) Rectangular flag combined with two triangular flags (RTTF)

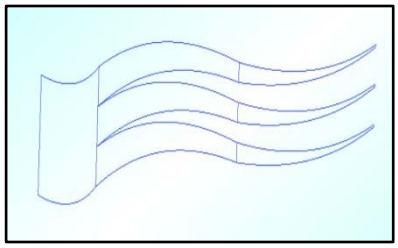

7c) Rectangular flag combined with three triangular flags (RTeTF)

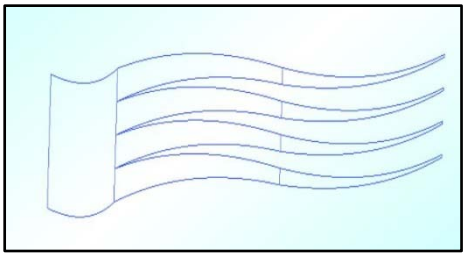

7d) Rectangular flag combined with four triangular flag (RFTF)

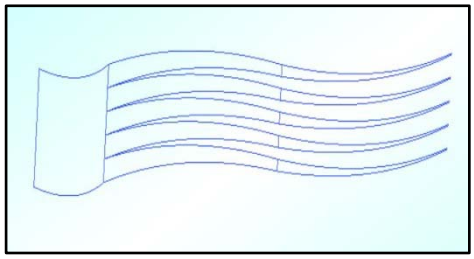

7e) Rectangular flag combined with five triangular flag (RFiTF)

Figure 7: Flag geometries

b) Procedure followed during Calculations

The procedure followed for the calculation of *Nu* is the same as that of Flag height optimization.

c) Results and Discussion

Table 4 shows the Nusselt number for flags with different triangular shapes at different velocity conditions. The highest *Nu* is achieved for RTTF at each velocity condition. *Nu* for RTTF is greater than RFiTF by 6.04%, 17.40%, 26.58% for *Re* 8236, 12354, 18344 respectively and by 8.33%, 18.71%, 31.57% for *Re* 8236, 12354, 18344 respectively when compared with *Nu* values for RFTF. The percentage rise in *Nu* of RTTF increases with an increase in velocity when compared to other flags. Fig 8 shows the graph between *Nu* and *Re* for each distinct flag.

Table 4: Nusselt Number for Flags with Different Number of Triangular shapes

Velocity (m/s)	*Nu*	*Re*
No flag condition		
1.1	239	8236
1.65	249	12354
2.45	267	18344
ROTF		
1.1	285	8236
1.65	308	12354
2.45	345	18344
RTTF		
1.1	351	8236
1.65	425	12354
2.45	500	18344
RTeTF		
1.1	281	8236
1.65	302	12354
2.45	341	18344

RFTF		
1.1	324	8236
1.65	358	12354
2.45	380	18344
RFiTF		
1.1	331	8236
1.65	362	12354
2.45	395	18344

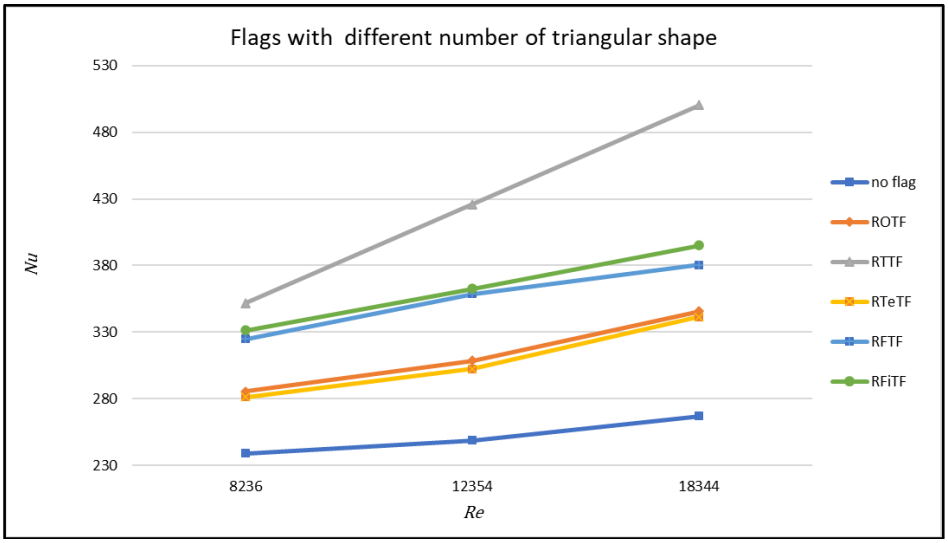

Figure 8: Average Nusselt number vs Reynolds number for different number of triangular shapes

VI. Optimization of the Rectangular Surface (RS) Area of Flag

a) *Problem Description*

RTTF has the highest heat transfer during the optimization process based on the number of triangular shapes. So, for the rectangular surface area optimization, RTTF is chosen. The surface area of the rectangular part in RTTF is 100 mm^2. This area is varied from 50 mm^2 to 150 mm^2 with a step of 25 mm^2.

b) *Procedure followed during Calculations*

The procedure followed for the calculation of *Nu* is the same as that of Flag height optimization.

c) *Results and Discussion*

Table 5 shows the Nusselt number for flags with different RS areas at distinct velocity conditions. The highest *Nu* is achieved for RTTF with RS area of 100 mm^2 at each velocity condition. *Nu* for RTTF with 100 mm^2 is greater than that with 125 mm^2 by 5.72%, 5.19%, 5.48% and that with150 mm^2 by 6.04%, 7.86%, 10.86% for *Re* 8236, 12354, 18344, respectively. Fig 9 shows the graph between *Nu* and *Re* for each distinct flag. Following fig 9, there is an increase in the *Nu* with the increase in RS area from 50 mm^2 to 100 mm^2. At the RS area of 100 mm^2, *Nu* is the highest and afterward, it diminishes with an increase in RS area from 100 mm^2 to 150 mm^2.

Table 5: Nusselt Number for Flags with Different Rectangular Area

Velocity (m/s)	*Nu*	*Re*
No flag condition		
1.1	239	8236
1.65	249	12354
2.45	267	18344
RS area = 50 mm²		
1.1	309	8236
1.65	352	12354
2.45	395	18344

RS area = 75 mm²		
1.1	312	8236
1.65	356	12354
2.45	413	18344
RS area = 100 mm²		
1.1	351	8236
1.65	425	12354
2.45	500	18344
RS area = 125 mm²		
1.1	332	8236
1.65	404	12354
2.45	474	18344
RS area = 150 mm²		
1.1	331	8236
1.65	394	12354
2.45	451	18344

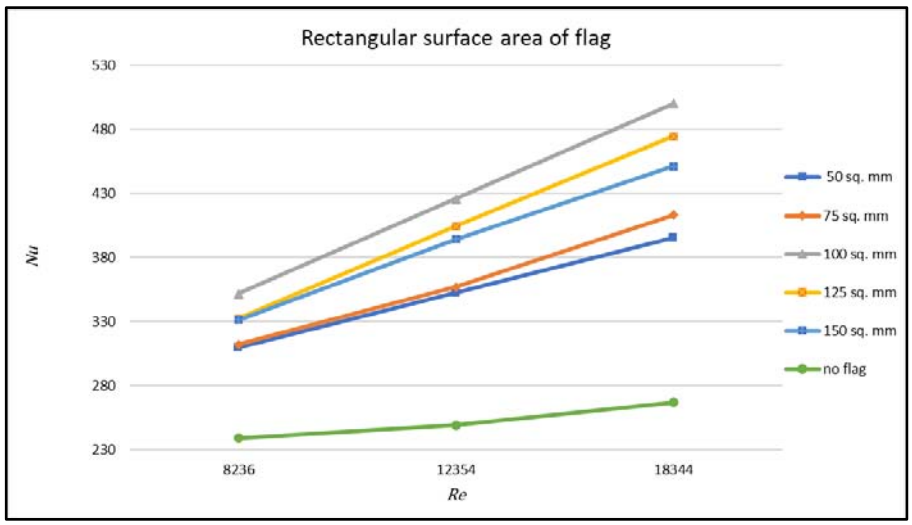

Figure 9: Average Nusselt Number vs Reynolds Number for Different Rectangular Surface Area of Flag

VII. Optimal Parameter Selection and Performance Oprimization

This study is the extension of the investigation carried out by Swadesh Suman et al, [37]. RTTF which is the shape optimized flag according to Swadesh [37] is chosen for the optimization based on new parameters. RTTF's position in the channel is 55 mm from the channel inlet and 2.5 mm from the surface. The position of the flag in the channel and flag height is chosen as the optimization parameters. Since RTTF is the combination of rectangular and two triangular shapes, therefore two other parameters namely the area of the rectangular part and the number of triangular shapes are also chosen as the optimization parameters. Similar to the method adopted by Swadesh [37], the overall optimization process is divided into four stages. For the first stage, RTTF of the shape optimization by Swadesh is considered and for the next stages, the optimized flag from the previous stage is considered.

Table 6 shows the value of *Nu* after each stage of parametric optimization. The % increase in *Nu* in each case shoots up with the increase in the velocity of air in the channel. This can be seen in column 4 of Table 6. The highest increase in *Nu* is observed during the optimization of the position of the flag in the channel.

Table 6: Performance Optimization

Performance optimization			
Velocity (m/s)	*Nu*	*Re*	% Increase in *Nu* wrt no flag
No flag condition			
1.1	239	8236	0
1.65	249	12354	0
2.45	267	18344	0
RTTF from Shape optimization (Swadesh [37])			
1.1	288	8236	20.50
1.65	301	12354	20.88
2.45	324	18344	21.35
After Flag height optimization			
1.1	339	8236	41.84
1.65	368	12354	47.79
2.45	413	18344	54.68
After Optimization of position of flag			
1.1	351	8236	46.86
1.65	425	12354	70.68
2.45	500	18344	87.26
After Optimization of number of triangular shapes			
1.1	351	8236	46.86
1.65	425	12354	70.68
2.45	500	18344	87.26
After Optimization of RS area			
1.1	351	8236	46.86
1.65	425	12354	70.68
2.45	500	18344	87.26

VIII. Conclusion

This present numerical investigation focuses on the effect of different parameters of a static wavy flag vortex generator on heat transfer. These parameters are flag height from the surface, position in the channel, number of triangular shapes in a flag, and rectangular surface area of the flag. The method adopted for numerical investigation is Computational Fluid Dynamics (CFD) and the software used is ANSYS 2014.The ideal value of GSF for the geometry is selected as 2. The overall optimization process is divided into four stages with the first stage being the flag height optimization, the second stage is the position in the channel, the third stage is the number of triangular shapes and the fourth stage is the rectangular surface area of the flag. For each stage, the optimized flag from the previous stage is considered and for the first stage, shape optimized RTTF by Swadesh suman et al. [37] is considered. For the first stage, the highest *Nu* is achieved at flag height equal to 1 mm for each velocity condition exceeding that in no flag condition by 41.84%, 47.79%, 54.68% for Re 8236, 12354, and 18344, respectively. For the decrease in FH from 5 mm to 1 mm, *Nu* values showed an upward trend but with a further decrease in FH to 0.5 mm it diminished. For the second stage, the highest *Nu* is achieved at the flag position equal to 35 mm and it exceeds that in no flag condition by 46.86%, 70.68%, and 87.26% for *Re* 8236, 12354, 18344, respectively. A similar trend as the first stage in *Nu* values is seen in the second one as well, it shoots up with the decrease in flag positions from 65 mm up to 35 mm and then decreases flag position to 15 mm. In the third stage, RTTF with a flag height of 1mm and flag position of 35 mm from the inlet has the highest *Nu* when compared with flags with a different number of triangular shapes. For the fourth and final stage, RTTF with a rectangular area of 100 mm^2 has the highest *Nu* among the flags with the different rectangular areas. The *Nu* increases with the increase in RS area from 50 mm^2 to 100 mm^2 and afterward, it diminishes with an increase in RS area from 100 mm^2 to 150 mm^2. Thus, from the results of this investigation, it can be deduced that with the right

optimized parameters, a significant increase in heat transfer in the channel can be achieved.

References Références Referencias

1. Bergman TL, Incropera FP. Fundamentals of heat and mass transfer, 7. Hoboken, N.J: John Wiley; 2011.
2. Ralph Kristoffer B. Gallegos, Rajnish N Sharma, "Flags as vortex generators for heat transfer enhancement: Gaps and challenges," in *Renewable and Sustainable energy reviews*, 76(2017) 950-962.
3. Sheikholeslami M, Gorji-Bandpy M, Ganji DD. Review of heat transfer enhancement methods: focus on passive methods using swirflow devices. Renew Sustain Energy Rev 2015; 49:444–69.
4. Ahmed HE, Mohammed HA, Yusoff MZ. An overview on heat transfer augmentation using vortex generators and nanofluids: approaches and applications. Renew Sustain Energy Rev 2012; 16:5951–93.
5. Alam T, Saini RP, Saini JS. Use of turbulators for heat transfer augmentation in an air duct – A review. Renew Energy 2014; 62:689–715.
6. Amar Raj Singh Suri, Anil Kumar & Rajesh Maithani (2017), "Convective Heat Transfer Enhancement Techniques of Heat Exchanger Tubes: A Review", in *International Journal of Ambient Energy*, DOI: 10.1080/01430750.2017.1324816.
7. M. Arulprakasajothi, U. Chandrasekhar, K. Elangovan & D. Yuvarajan, "Influence of conical strip inserts in heat transfer enhancement under transition flow", in *International Journal of Ambient Energy*, Volume 41, 2020 - DOI: 10.1080/01430750.2018.1472651.
8. M. Abeens, M. Meikandan, Jaffar Sheriff & R. Murunganadhan, "Experimental analysis of convective heat transfer on tubes using twisted tape inserts, louvered strip inserts and surface treated tube", in *International Journal of Ambient Energy,* Volume 41, 2020- DOI: 10.1080/01430750.2018.1476263.
9. K. Logesh, R. Arunraj, S. Govindan, M. Thangaraj & G. K. Yuvashree, "Numerical investigation on possibility of heat transfer enhancement using reduced weight fin configuration", in *International Journal of Ambient Energy,* Volume 41, 2020 - DOI: 10.1080/01430750.2018.1451382.
10. K. Subramani, K. Logesh, S. Kolappan & S. Karthik, "Experimental investigation on heat transfer characteristics of heat exchanger with bubble fin assistance", in *International Journal of Ambient Energy,* Volume 41, 2020- DOI: 10.1080/01430750.2018.1472654.
11. Gilson GM, Pickering SJ, Hann DB, Gerada C. Piezoelectric fan cooling: a novel high reliability electric machine thermal management solution. Ind Electron IEEE Trans 2013; 60:4841–51.
12. Ma HK, Liao SK, Li YT. Study of multiple magnetic vibrating fins with a piezoelectric actuator. Therm. Meas. Model. Manag. Symp. (SEMI-THERM), 2015 31st, IEEE, 2015, p. 309–13.
13. Ma HK, Tan LK, Li YT. Investigation of a multiple piezoelectric–magnetic fan system embedded in a heat sink. Int Commun Heat Mass Transf 2014; 59:166–73.
14. Jae Bok Lee, Sung Goon Park, Boyoung Kim, Jaeha Ryu, Hyung Jin Sung, "Heat transfer enhancement by flexible flags clamped vertically in a Poiseuille channel flow," in *International Journal of Heat and Mass Transfer,*107 (2017) 391–402.
15. Jae Bok Lee, Sung Goon Park, Hyung JinSung, "Heat transfer enhancement by asymmetrically clamped flexible flags clamped in a channel flow," in *International Journal of Heat and Mass Transfer,*116(2018) 1003-1015.
16. Zheng Li, Xianchen Xu, Kuojiang Li, Yangyang Chen, Guoliang, Huang , Chung-lung Chen, Chien-Hua Chen, "A flapping vortex generator for heat transfer enhancement in a rectangular airside fin,'' in *International Journal of Heat and Mass Transfer,*118 (2018) 1340–1356.
17. Atul Kumar Soti, Rajneesh Bhardwaj, John Sheridan, "Flow-induced deformation of a flexible thin structure as manifestation of heat transfer enhancement" in *International Journal of Heat and Mass Transfer,* 84 (2015) 1070–1081.
18. Jaeha Ryu, Sung Goon Park, Boyoung Kim, Hyung JinSung, "Flapping dynamics of an inverted flag in a uniform flow", in *Journal of fluid and structures* 57 (2015) 159-169.
19. Sung Goon Park, Boyoung Kim, Cheong Bong Chang, Jaeha Ryu, Hyung Jin Sung , "Enhancement of heat transfer by a self-oscillating inverted flag in a Poiseuille channel flow" in *International Journal of Heat and Mass Transfer,* 96 (2016) 360–370.
20. Herrault F, Hidalgo PA, Ji C-H, Glezer A, Allen MG, "Cooling performance of micromachined self-oscillating reed actuators in heat transfer channels with integrated diagnostics", in *Micro Electro Mech. Syst. (MEMS), 2012 IEEE In: Proceedings of the 25th International Conference, IEEE,* 2012, p. 1217–20.
21. Hidalgo P, Glezer A, "Direct actuation of small-scale motions for enhanced heat transfer in heated channels", in *ASME-JSME-KSME 2011 Jt. Fluids Eng. Conference, American Society of Mechanical Engineers,* 2011, p. 3123–9.
22. Hidalgo P, Glezer A, "Small-scale vorticity induced by a self-oscillating fluttering reed for heat transfer augmentation in air cooled heat sinks", in Inter PACK/*ICNMM2015, San Francisco, CA.* 2015.
23. Shoele K, Mittal R, "Computational study of flow-induced vibration of a reed in a channel and effect

on convective heat transfer", in *Phys Fluids* 2014;26:127103.
24. A. Bejan, Advanced Engineering Thermodynamics, 2nd edn, Wiley, New York, 1997.
25. A. Bejan, S. Lorente, "Design with Constructal Theory" New Jersey: Wiley, 2008.
26. Sylvie Lorente, Adrian Bejan, "Current trends in constructal law and evolutionary design" in *Heat Transfer-Asian Research*, 2019, 48(8): 357-389.
27. Chen LinGen, "Progress in study on constructal theory and its applications", in *Science China Technological Sciences* 2012, 10.1007/s11431-011-4701-9.
28. Lingen Chen, Huijun Feng, Zhihui Xie, Fengrui Sun, "Progress of constructal theory in China over the past decade", in *International Journal of Heat and Mass Transfer,* 130 (2019) 393-413.
29. Adrian Bejan, "Constructal-theory network of conducting paths for cooling a heat generating volume", in *International Journal of Heat and Mass Transfer,*0017 9310/97 S17.00- 0.00.
30. Huijun Feng, Lingen Chen, ZhihuiXie, "Multi-disciplinary, multi-objective and multi-scale constructal optimizations for heat and mass transfer processes performed in Naval University of Engineering, a review", in *International Journal of Heat and Mass Transfer*, 115 (2017) 86-98.
31. Huijun Feng, Lingen Chen, ZhihuiXie, "Constructal optimizations for ''+" shaped high conductivity channels based on entransy dissipation rate minimization", in *International Journal of Heat and Mass Transfer*, 119 (2018) 640-646.
32. Feng Huijun, Chen LinGen, XIE Zhihui, "Constructal entransy dissipation rate minimization for X-shaped vascular networks", in *Science China Technological Science*, 11431-018-9392-1.
33. Chen LinGen, Yang AiBo, Feng HuiJun, Ge YanLin, Xia ShaoJun, "Constructal design progress for eight types of heat sinks", in *Science China Technological Science*, 11431-019-1469-1.
34. Huijun Feng, Wanxu Qin, Lingen Chen, Cunguang Cai, Yanlin Gea, Shaojun Xia, "Power output, thermal efficiency and exergy-based ecological performance optimizations of an irreversible KCS-34 coupled to variable temperature heat reservoirs" in *Energy Conversation and Management*, 205 (2020) - 112424.
35. H.J. Feng, L.G. Chen, Z.H. Xie, F.R. Sun, "Constructal complex-objective optimization for tree-shaped hot water networks over a rectangular area using global optimization method", in *International Communications of Heat and Mass Transfer*, 87 (2017) 147-156.
36. Huijun Feng, ZhuojunXie, Lingen Chen, Zhixiang Wu, Shaojun Xia, "Constructal design for supercharged boiler superheater", in *Energy*, 2020, 191: 116484.
37. Swadesh suman, Vineeth Uppada, Swati Singh, Sanjay Mahadev Gaikwad, "Numerical investigation and experimental validation of Shape amd Position optimization of a static wavy flag for heat transfer enhancement", in *International Journal of Ambient Energy,* DOI: 10.1080/01430750.2020.1818120.
38. Hinze, J O., 1975, *Turbulence*, McGraw-Hill, New York.
39. Launder. B. E., Spalding D. B., 1974, "The Numerical Computation of Turbulent Flows," in *Computer Methods in Applied Mechanics and Engineering*, 3, pp. 269–289.

Global Journal of Researches in Engineering: A
Mechanical and Mechanics Engineering
Volume 22 Issue 2 Version 1.0 Year 2022
Type: Double Blind Peer Reviewed International Research Journal
Publisher: Global Journals
Online ISSN: 2249-4596 & Print ISSN: 0975-5861

Numerical Thermal Stress Analysis on Semiconductors with Nano-Fluid Coolant

By Luis Medina, Kevin Harvey, Cory Davison, Edgar Rubio, Morteza Mohssenzadeh, Hamidreza Ghasemi Bahraseman & Taha Ghaemi Bahraseman

Shahid Beheshti University

Abstract- During the course of normal operation, electrical components made from semiconducting materials undergo significant stress from heating. This causes parts to wear out more quickly or, in the more extreme cases, fail altogether. In order to maintain a stable operating temperature, many different types of cooling systems have been used. Our work investigates the best materials to use in these systems, carefully considering effectiveness, cost, and longevity in our assessment. Ansys simulation software was used to simulate the effects of different coolants on removing heat from a semiconductor. The coolants are air, water, and aluminum oxide. Though we didn't model the results of forced convection across these materials, the natural convection heat transfer results in finding the more efficient coolant. Considering liquid cooling methods for semiconductor-based devices, the kind of fluid plays a vital role in the transfer of energy.

Keywords: *thermal stress, nano-fluid aluminum oxide coolant, semiconductors.*

GJRE-A Classification: *DDC Code: 519.4 LCC Code: QA297*

Strictly as per the compliance and regulations of:

Numerical Thermal Stress Analysis on Semiconductors with Nano-Fluid Coolant

Luis Medina [α], Kevin Harvey [σ], Cory Davison [ρ], Edgar Rubio [ω], Morteza Mohssenzadeh [¥], Hamidreza Ghasemi Bahraseman [§] & Taha Ghaemi Bahraseman [χ]

Abstract- During the course of normal operation, electrical components made from semiconducting materials undergo significant stress from heating. This causes parts to wear out more quickly or, in the more extreme cases, fail altogether. In order to maintain a stable operating temperature, many different types of cooling systems have been used. Our work investigates the best materials to use in these systems, carefully considering effectiveness, cost, and longevity in our assessment. Ansys simulation software was used to simulate the effects of different coolants on removing heat from a semiconductor. The coolants are air, water, and aluminum oxide. Though we didn't model the results of forced convection across these materials, the natural convection heat transfer results in finding the more efficient coolant. Considering liquid cooling methods for semiconductor-based devices, the kind of fluid plays a vital role in the transfer of energy. The Aluminum Oxide was selected in a 2% solution and 40nm wide particles to simulate for our nanofluid as it is commonly used in the industry and data for it was readily available. The aluminum oxide nanofluid had the best cooling performance of the three tested materials.

Keywords: thermal stress, nano-fluid aluminum oxide coolant, semiconductors.

I. Introduction

Because many of these components can only work properly within a relatively narrow temperature range, an entire industry has materialized that is dedicated to keeping them cool[1]. Consequently, a great deal of time and money has been spent researching the best materials for transferring energy from the delicate components and releasing it into another medium[2]. We entered this project with the goal of finding the most suitable materials for cooling semiconductor-based electrical components like CPUs. The two types of cooling methods examined are the use of heat sinks and pumped liquid cooling.

First, we examine cooling systems using heat sinks. Heat sinks transfer heat from the component via conduction and release that heat in the surrounding air through both convection and radiation. The primary factor in determining the effectiveness of a material for this process is its thermal conductivity, though thermal diffusivity is also a major factor[3]. The former determines the material's ability to transfer heat away from the source while the latter speaks to its ability to move the energy throughout itself, as well as radiate it away. Usually, heat sinks are used in a forced convection system with air being moved across the heat sink fin[4]. We examined several materials for this section and have arranged them within Table_1.

Table 1: Comparison of Suitable Heat Sink Materials [5, 6]

Metals:	Aluminum	Copper	CarbAl
Density	2.7 g/cm ^ 3	8.96 g/cm ^ 3	1.75 g/cm ^ 3
Thermal Conductivity	205 W/mK	401 W/mK	400 W/mK
Thermal Diffusivity	0.84 cm ^ 2/s	1.12 cm ^ 2/s	2.78 cm ^ 2/s
Comments:	Lightweight, decent conductivity, lackluster diffusivity	Excellent Thermal Conductivity, decent thermal diffusivity, relatively heavy	Very lightweight, Excellent Thermal conductivity, Excellent Thermal diffusivity

Though we didn't model the results of forced convection across these materials, from the data present the best material for transferring energy from a component is clearly CarbAl. With a low density reminiscent of aluminum and a thermal conductivity comparable to the much heavier copper, CarbAl provides the best attributes of both materials. Its thermal diffusivity is also significantly higher than the others, allowing for better energy flux throughout itself. This material was designed in 2008 by Applied Nanotech Inc. and remains a superior material for many applications, including heat sinks for high end applications.

Author α σ ρ ω ¥ §: Department of Physical Science, Engineering Program, San Diego Mesa Community College, San Diego, California, USA. e-mail: hghasemi@sdccd.edu

Author χ: Mechanical Engineering Department, Shahid Beheshti University, Tehran, Iran.

II. Nanofluid Simulation

With regards to liquid cooling systems for semiconductor-based devices, the type of fluid plays a significant role in the transfer of energy. We selected Aluminum Oxide in a 2% solution and 40nm wide particles to simulate for our nanofluid as it is commonly used in the industry and data for it was readily available [7] [8]. The properties of the Materials used (simulated) in this study are provided in tables 2, 3 and 4. Boron-doped silicon and phosphorus-doped silicon, Air, Water, Aluminum oxide nanoparticles for nanofluid.

Table 2: Properties of Materials Common to Liquid Cooling Systems [9]

Fluids	Air	Water	Al_3O_2 Nanofluid
Density	1.225 kg/m^3	998.2 kg/m^3	3.95 g/cm ^ 3
Thermal Conductivity	0.0242 W/mK	0.6 W/mK	30 W/mK
Specific Heat	1006.43 J/kg-K	4182 J/kg-K	541-955 J/kg-K
Convection Heat Transfer Coefficient	1000 W/(m^2-K)	3001 W/(m^2-K)	9000 W/(m^2-K)

Table 3: Properties of Semiconductor [4]

Density	2.33 g/cm^3
Specific heat	0.168 Cal/g-K
Thermal Conductivity	149 W/m-K
Thermal Expansion	2.6 μm/m-K
Young's Modulus	51-80 GPa
Poisson's Ratio	0.064-0.28

Table 4: Nanoparticles Properties

Aluminum Oxide Al_2O_3 99+% purity, 80 nm radius [9]	
Crystallographic Structure	Rhombohedral
Density	3.97 g/cm^3
Thermal Conductivity	18 W/ mol-K
Specific Heat	880 J/kg-K
Price	$55 / 100 gram
Tin Oxide SnO_2 99.9% purity, 50-70 nm radius [10]	
Crystallographic Structure	Tetragonal
Density	6.95 g/cm^3
Thermal Conductivity	40 W/ mol-K
Specific Heat	44.3 J/mol-K
Price	$110 / 100 gram
Silicon Oxide SiO_2 99.9% purity, 800 nm radius [11]	
Crystallographic Structure	Amorphous
Density	2.65 g/cm^3
Thermal Conductivity	1.1-1.4 W/ mol-K
Specific Heat	1.01 J/g-K
Price	$98 / 100 gram

III. ANSYS Analysis Setup & Methodology

Simulation was done using convection to transfer heat from SM to cooling fluid. Convective heat transfer coefficient (h_c) was used the principal property of fluid for simulation.

We found that this coefficient depended type of medium such as gas or liquid, flow properties such as velocity, viscosity and other flow and temperature dependent properties [8].

Many of the research papers we found used other values and coefficients that are the norm in the field of thermodynamics. Nusselt, Rayleigh, and Reynolds numbers were discussed in these papers, however, since these are out of the scope of this class, we decided to use convection [12-14]. The terms stated above do depend on convection so it's not as to completely ignore the experimental results from researchers; convection allowed us to simplify our model.

Main purpose was to compare the cooling capabilities of air, water, and nanofluids by forced convection. Finding comparable values for the heat transfer coefficients (HTC) of each of these values was a problem, mainly because it was difficult to find experimental results that had been performed under the same conditions [12-15]. However, we were able to find papers that contained the information for water and aluminum oxide nanofluids although there were calculations needed as well as estimating values from graphs demonstrating results. These papers contained the needed coefficients for water and Al-Ox under similar conditions such as mass flow (1.5 liters per minute) and temperature (40℃) therefore we could use comparable values for their respective HTCs [7, 8].

A simplified geometry was used in the simulation. The actual geometry of a transistor (our example for semiconductor) was convoluted. In addition, the electronic components had to be omitted from the modeling because the focus was on thermal impact and because it was simpler to declare one region of the geometry as the heat source. Another simplification had to do with energy bands, to understand and model such concept, an understanding of Fermi function, Fermi-Dirac distribution, Boltzmann approximation, and electron concentration under different temperature conditions [12-15].

What we expected to see in the ANSYS Fluent heat maps was the heat dissipated from the source out through the boundaries making contact with the fluid. However, this was not the case the first few times that we ran the simulation. This was due to the geometry of our model; we had placed one geometry meant to represent the fluid above the geometry representing the semiconductor. There was an issue with the boundary where the surfaces met and thus, we decided to change our approach by convection.

Once we read up on how convection worked, we could set up our model an analogous fashion [5]. This resulted in a simpler model where only a single geometry was needed which was meant to represent the semiconductor.

Using ANSYS Fluent, the mesh was imported and given three different boundaries. The bottom edge along with both vertical edges were all labeled “outlet boundary” meaning these edges were to make contact with our test fluids (air, water, nanofluid). The top edge was the heat source; it was meant to be analogous to the conduction band on a transistor although in reality the situation is complex [15]. The surface of the body was the third boundary and this is where the properties of a semiconductor were applied to.

IV. Results

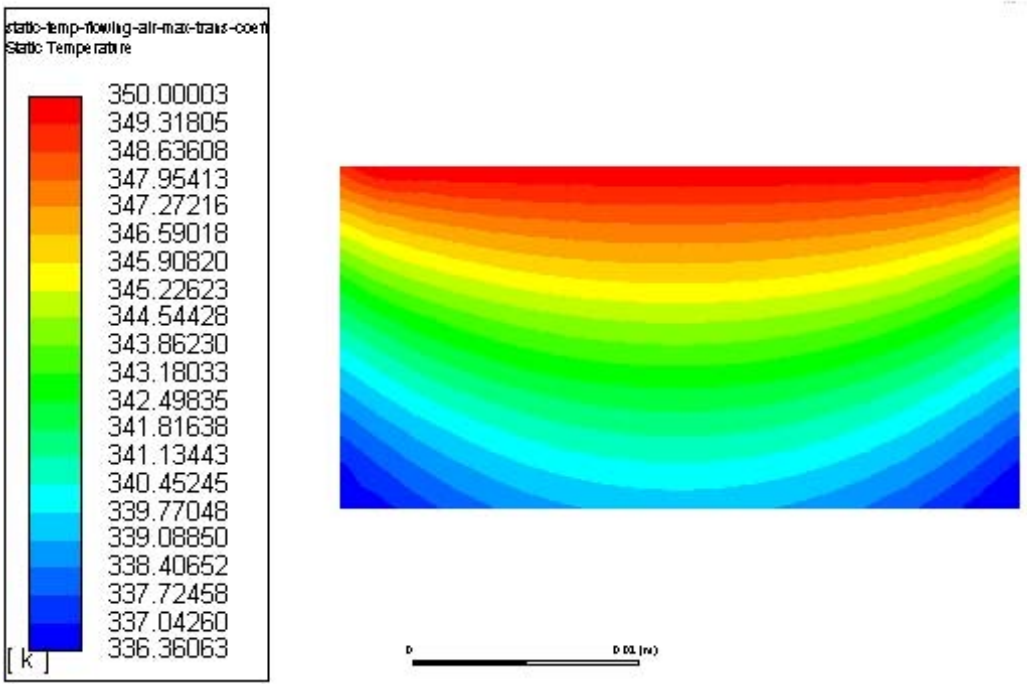

Figure 1: Static Temperature Contour for air with heat transfer coefficient of 1000 W/m^2-K

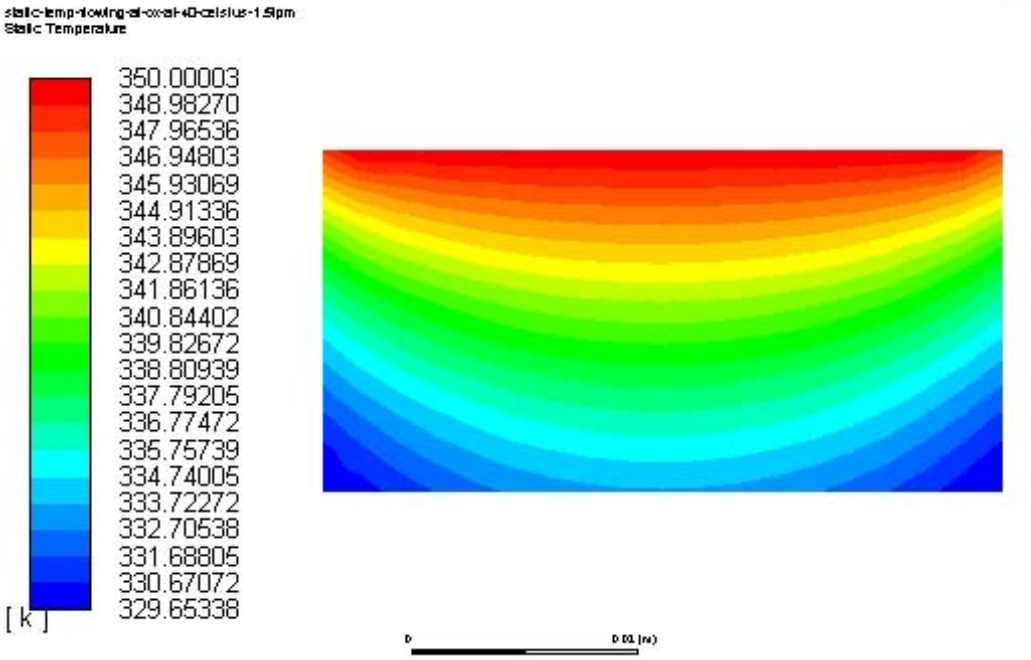

Figure 2: Static Temperature Contour for Water with heat transfer coefficient of 3000 W/m ^ 2-K

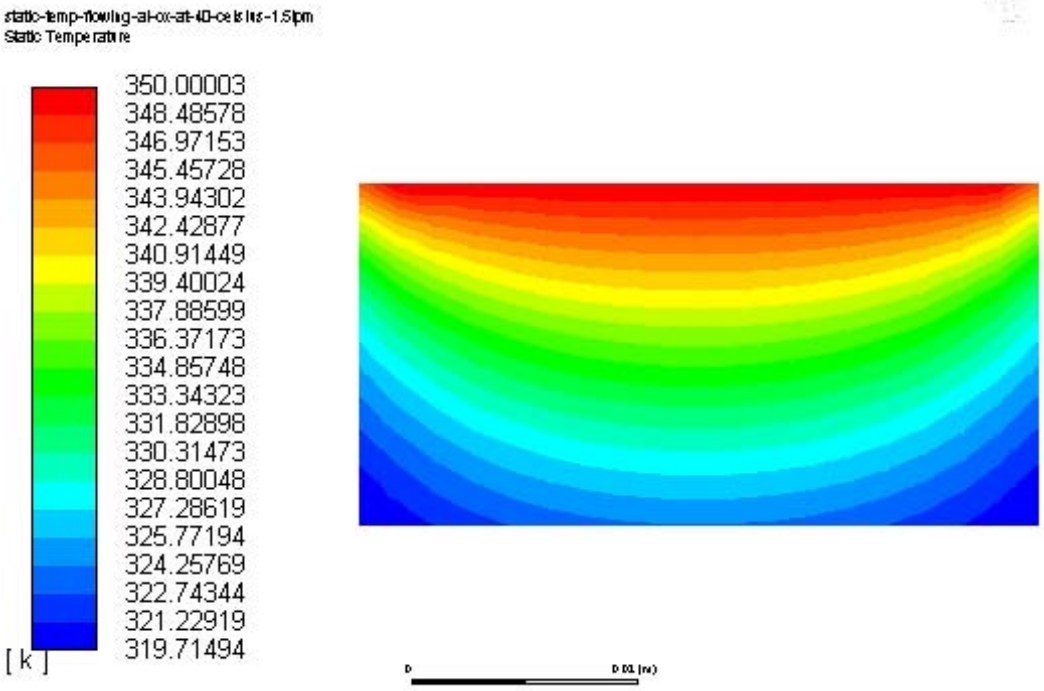

Figure 3: Static Temperature for Al-Ox Nanofluid with heat transfer coefficient of 9000 W/m ^ 2-K

A nanofluid composed of 98% water and 2% aluminum oxide (of particle size 40nm) showed significant improvement (Figure 3) in the rate of heat transfer over water (Figure 2) and air (Figure 1). Faiza Nazir's results showed a 200% improvement over water's rate of heat transfer [7].

V. Discussion

According to a handful of the research papers and experimental reports, the principal variables that accounted for the nanofluid's superior performance included: intensification of turbulence or eddy, suppression or interruption of the boundary layer as well as dispersion or back mixing of the suspended

nanoparticles, in addition to the nanoparticles' thermal conductivity and heat capacity [12].

VI. Conclusion

The Al_3O_2 (40nm @ 2% volume) nanofluid had the best cooling performance of the three tested materials.

References Références Referencias

1. National Advisory Committee for Aeronautics Report 1170: *Behavior of Materials Under Conditions of Thermal Stress*. S.S. Manson. https://ntrs.nasa.gov/search.jsp?R=19930092197.
2. Calculation of Semiconductor Failure Rates by William J. Vigrass: http://docplayer.net/29883772-Calculation-of-semiconductor-failure-rates.html.
3. ISSI Semiconductor Reliability http://www.issi.com/WW/pdf/semiconductor-reliability.pdf.
4. SONY Semiconductor Device Failure Analysis https://www.sony-semicon.co.jp/products_en/quality/pdf/qr_chap3e_201604.pdf.
5. Thermal Conductivity of common Materials and Gases. (n.d.). Retrieved from https://www.engineeringtoolbox.com/thermal-conductivity-d_429.html.
6. http://nebula.wsimg.com/64df31e4e255fda9996382f790bb04a9?AccessKeyId=D6756B5639AB3254C10B&disposition=0&alloworigin=1.
7. F. M. Nasir et al., "Heat Transfer of Aluminium-Oxide Nanofluids in a Compact Heat Exchanger", Applied Mechanics and Materials, Vols. 465-466, pp. 622-628, 2014.
8. Xuan, Yimin & Li, Qiang. (2003). Investigation on Convective Heat Transfer and Flow Features of Nanofluids. Journal of Heat Transfer-transactions of The Asme - J HEAT TRANSFER. 125. 10.1115/1.1532008.
9. US Research Nanomaterials Inc, Aluminum Oxide Nanopowder https://www.us-nano.com/inc/sdetail/208?gclid=Cj0KCQiA1IXfBRCpARIsAKvManzhB9eagV9bde3Hx9mvYV2zLZqs6W-SZcaBCPnCiY1FacLXvQq8kyQaAnQOEALw_wcB.
10. SkySpring Nanomaterials Tin Oxide Nanoparticles https://ssnano.com/inc/sdetail/tin_oxide_nanoparticles/235?gclid=Cj0KCQiA1IXfBRCpARIsAKvManxFGgLMk0Mac00qbatkytqkWYI7qnUya1yVQTFDe-LwstqnGGHDUrgaAozYEALw_wcB.
11. US Research Nanomaterials, Inc Silicon Oxide Spherical Powder https://www.usnano.com/inc/sdetail/46881?gclid=Cj0KCQiA1IXfBRCpARIsAKvMany0m1-f4aOhSU5fVZkOtjGKpuWl6eRWZdOVh3WhrkM3gE0LzQOikT0aArMREALw_wcB.
12. Aghayari, R., Maddah, H., Sharifnezhad, Z., Hakiminejad, A., Sarli, S. (2015). Aluminum Oxide Nanofluid Energy Transfer. *Transp Phenom Nano Micro Scales*, 3(1), 54-61. doi: 10.7508/tpnms.2015.01.006.
13. K. Viswanatha Sharma and N. Hisham B Hamid (eds.), Engineering Applications of Nanotechnology, Topics in Mining, Metallurgy and Materials Engineering, DOI 10.1007/978-3-319-29761-3_2.
14. Adnan, M. Husein and R. A., Bakar and K., Kadirgama and K. V., Sharma (2013) *Experimental Measurements of Nanofluids Thermal Properties*. International Journal of Automotive and Mechanical Engineering (IJAME), 7. pp. 850-863. ISSN 1985-9325(Print); 2180-1606 (Online).
15. https://people.eecs.berkeley.edu/~hu/Chenming-Hu_ch1.pdf Journal of Applied Physics 91, 5079 (2002); https://doi.org/10.1063/1.1458057.

This page is intentionally left blank

Global Journal of Researches in Engineering: A
Mechanical and Mechanics Engineering
Volume 22 Issue 2 Version 1.0 Year 2022
Type: Double Blind Peer Reviewed International Research Journal
Publisher: Global Journals
Online ISSN: 2249-4596 & Print ISSN: 0975-5861

Passive Sensing Jaw for Grasping and Orienting

By Alessandro Luchetti, Mariolino De Cecco, Matteo Perotto, Paolo Bosetti, Daniele Fontanelli, Luigi Palopoli, Fabiano Zenatti, Matteo Zanetti, Luca Maule & Mattia Tavernini

University of Trento

Abstract- The goal of this work is to present an innovative design for a smart robotic gripper, which is able to grasp different randomly deployed prismatic and cylindrical packages and orient them through a mechanically passive alignment system with sensing capability. It consists in a new concept of end-effector combined with an ad-hoc path planning for aligning residual worst cases. The system uses gravity and an angular sensor embedded into the gripper to detect the object orientation and, if necessary, formulate a control strategy to align it before the release phase. An initial screening experiment was executed to find the parameters that most influence the alignment angle and execution time. Two worst-case pack ages were tested in different working conditions. The results show that the percentage of success of the system is high even in the worst operating conditions.

GJRE-A Classification: FOR Code: 091399

Strictly as per the compliance and regulations of:

Passive Sensing Jaw for Grasping and Orienting

Alessandro Luchetti [α], Mariolino De Cecco [σ], Matteo Perotto [ρ], Paolo Bosetti [ω], Daniele Fontanelli [¥], Luigi Palopoli [§], Fabiano Zenatti [χ], Matteo Zanetti [ν], Luca Maule [Θ] & Mattia Tavernini [ζ]

Abstract- **The goal of this work is to present an innovative design for a smart robotic gripper, which is able to grasp different randomly deployed prismatic and cylindrical packages and orient them through a mechanically passive alignment system with sensing capability. It consists in a new concept of end-effector combined with an ad-hoc path planning for aligning residual worst cases. The system uses gravity and an angular sensor embedded into the gripper to detect the object orientation and, if necessary, formulate a control strategy to align it before the release phase. An initial screening experiment was executed to find the parameters that most influence the alignment angle and execution time. Two worst-case pack ages were tested in different working conditions. The results show that the percentage of success of the system is high even in the worst operating conditions.**

I. Introduction

Picking, aligning, and placing objects of different shapes and sizes is a very common task in the automation industry. The most commonly used interfaces for picking involve vacuum force obtained via suction cups and sponges or mechanical friction provided by soft and rigid jaws [1], which have the higher capability to grip objects of different shapes, volumes, and masses without changing the jaw shapes. The jaws can be designed in different configurations and actuated either by pneumatic systems, which are noisy and expensive as they require a vacuum line, or by mechanical systems.

Author α: PhD Student, Department of Mechanical Engineering, University of Trento, Trento, Italy. e-mail: alessandro.luchetti@unitn.it
Author σ: Professor, Department of Mechanical Engineering, University of Trento, Trento, Italy. e-mail: mariolino.dececco@unitn.it
Author ρ: Graduate Student, Department of Mechanical Engineering, University of Trento, Trento, Italy.
e-mail: matteo.perotto@alumni.unitn.it
Author ω: Professor, Department of Mechanical Engineering, University of Trento, Trento, Italy. e-mail: paolo.bosetti@unitn.it
Author ¥: Professor, Department of Information Engineering and Computer Science, University of Trento, Trento, Italy.
e-mail: daniele.fontanelli@unitn.it
Author §: Professor, Department of Information Engineering and Computer Science, University of Trento, Trento, Italy.
e-mail: luigi.palopoli@unitn.it
Author χ: Engineer, Dolomiti Robotics Srl, Trento, Italy.
e-mail: fabiano.zenatti@dolomitirobotics.it
Author ν: Postdoctoral researcher, Department of Mechanical Engineering, University of Trento, Trento, Italy.
e-mail: matteo.zanetti@unitn.it
Author Θ: Engineer, Postdoc Robosense Srl, Trento, Italy.
e-mail: l.maule@robosense.it
Author ζ: Engineer, Postdoc Robosense Srl, Trento, Italy.
e-mail: m.tavernini@robosense.it

Parallel configuration is the most commonly used for picking objects of standard geometries, since higher dexterity configurations require a complex and expensive adaptive control strategy. One example of high dexterity configuration is the dexterous hand presented in [2], [3] and [4]. Examples of the complexity of the control strategy for this kind of solutions are reported in [5] for rolling approach, in [6] for sliding approach and [7] for gaiting approach. The choice of using a parallel gripper is justified in the manufacturing field by Bracken [8], who proposed a geometrical classification of parts to be gripped into six shape categories (i.e., spherical, rectangular, cylindrical, triangular, holed and flexible) and stated that the gripper able to deal with most shapes is the parallel two-jaw gripper.

Assuming that a robotic system is composed of a robot and a mechanical parallel gripper, it is possible to solve the alignment problem with two strategies: using a high degree of-freedom manipulator equipped with a gripper that has no alignment capability or performing the alignment by using the gripper rather than robot kinematics. Holladay et al. [9] demonstrated that the task can be solved in a shorter time and with a smaller work space using the second approach.

The orientation problem using only the gripper can be solved in several ways, but the most commonly used is pivoting [10]. It consists in closing the gripper jaws in such a way that the object can rotate around the axis passing through the contact points. Rao et al. [11] demonstrated the effectiveness of this orienting technique by making four degree of freedom robot to move a polyhedral part in space (along all the object's degrees of freedom). This approach takes advantage of gravity to complete the alignment so that the alignment system can be defined as passive. It also introduces a constraint on the gripping distance from the object's center of mass. Making the realignment system to be active allows to get rid of this constraint and to control the alignment angle, but the introduction of additional hardware decreases reliability while increasing costs.

In this paper, we propose and validate a new design with a passive realignment system to be integrated into parallel mechanical grippers. In addition, in pick and place operations it can be necessary to choose if the object has to be realigned or not, a problem that is addressed using a passive mechanical system integrating an angular sensor monitoring in real-

time the inclination of the object and synthesising an appropriate control strategy based on planned actions.

II. Related Works

An example of a passive system is given by [12], where each jaw has a vertical V-groove cavity with a small hard contact point attached to an elastic strip that orthogonally crosses the groove. When the gripping force is low, the rotation is obtained by pivoting the object around the axis created by hard contact points that are free to rotate. When the force increases, the strip goes into the groove, thus constraining the object. The interesting feature is that the type of contact between the object and the jaw is a function of the gripping force. Although not suitable for cubic objects, this solution can be retrofitted to different parallel jaws. Another possible detrimental effect is that the point-like contact may damage the object surface, which is also subject to wear, and requires high accuracy in sensing the object to grasp and in planning for the proper gripping point. Additionally, the proper grip ping force is another feature to be defined, which requires precise knowledge of the gripper-object friction coefficient.

Two other interesting examples are available in the literature, both based on pneumatic actuation. The one presented in [13] solves the problem of the correct gripping force choice by introducing an active rubber diaphragm between the jaw body and the fingertip. A bearing allows the fingertip to freely rotate when the diaphragm is not inflated, then the inflation allows it to stop quickly at a given angle. This design has the advantages of being fast and independent on the object geometry and grasping force. Additionally, it is equipped with a rotary magnetic encoder that allows for feedback control. The main limitation is the need for a pneumatic system.

The other solution presented in [14] uses an inflatable membrane to change the shape of the contact interface: when the pressure is high, the fingers have a prismatic shape and contact is restricted to a small area (ideally two points); when the pressure is low, the shape smoothly becomes a V-groove cavity, where cylindrical objects are held. The advantage of this design is that it is independent of the object geometry although it is only suitable to align cylindrical shapes and, again, it needs to be actuated by a pneumatic system.

The solution here presented is purely mechanical and passive, and integrates a sensing system. It can work with a wide range of object shapes while avoiding the use of a pneumatic system. It allows for a simpler, more reliable, and more cost-effective jaw design. The encoder also performs quick fault diagnosis, increasing robustness.

III. The Passive-Sensing Jaws

The jaws of the parallel gripper were designed with an innovative passive auto-alignment capability. Each of the two jaws has a different design and accomplishes different functions in the alignment operation. The one in Fig. 1 only works as a pivot to align the object, the other in Fig. 2 has three additional features:

1. a v-groove cavity;
2. a counterweight at an offset to the rotation axis;
3. a rotation sensor.

The v-shape, provided with an elastic film, is made to better secure cylindrical objects, the surrounding planar surface is instead used to improve contact with prismatic pack

Fig. 1: Detail of the jaw provided of polymeric disc pad

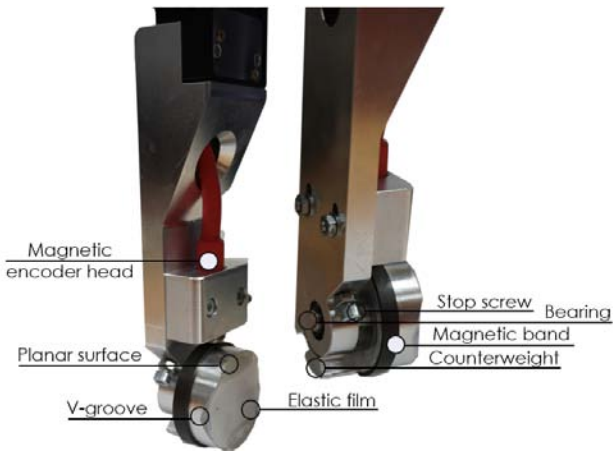

Fig. 2: Detail of the jaw provided of balancing mass and magnetic encoder

ages. The counterweight, on the other hand, has different functions: when the object is not grasped it makes the v shaped cavity parallel to the ground, allowing reliable grasping of cylindrical objects that lie with their axis parallel to the ground. The direction of the object's rotation depends on which side of the center of gravity it is grasped. On one side of the center of gravity, Fig. 3 (Extension 1), the object is not aligned because the rotation imposed by the gravity makes the counterweight motion in the direction of its end-stroke already reached. On the other side, Fig. 4 (Extension 1), the counterweight rotates in the other direction, making the package free to rotate in the same direction and reach its vertical position determined with the contact

with a stop screw. The reason why screws are used as mechanical stoppers is that the final angle can be tuned by tightening them. The tuning interval is [-6,20] degrees around vertical position. The rotation of the contact surfaces is obtained for both jaws using SKF 628/6-2Z deep groove ball bearings. The material used for both jaws is aluminum 7075 with an interchange able polyoxymethylene pad in the free rotating gripper disc to change the friction value.

The second jaw, Fig. 2, has a support for the reading head of a magnetic encoder used to read the angle value. The sensor used is the LIKA SMB5 magnetic sensor together with LIKA MT50 tape. The angular resolution after wrap

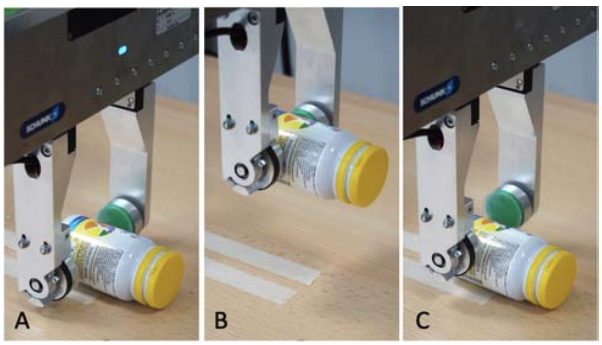

Fig. 3: Main sequence for moving a cylindrical object without alignment: (A) gripping with v-shaped cavity parallel to the ground, (B) lifting with fixed object, (C) releasing without movement of the jaw disks

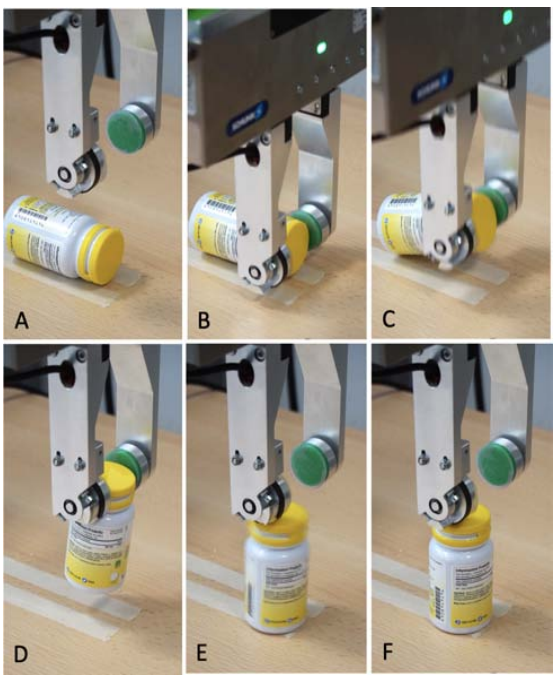

Fig. 4: Main sequence for moving a cylindrical object with alignment: (A-B) gripping with v-shaped cavity parallel to the ground, (C) lifting with the object rotation until the end of the counterweight stroke (D), (E-F) releasing with the counterweight and v-shaped cavity moving parallel to the ground

ping the magnetic strip on a 32 mm diameter cylinder be comes 1.15°, maximum speed is 16 m s^{-1}(100 rad s^{-1}). The encoder is equipped with the external LIKA IF40 converter that performs interpolation and provides digital output. The angle sensor is added also with the purpose of making the system able to detect faults and misalignment. It enables the robot controller to move the end-effector so that the object can be aligned in the best possible way, in terms of time and final angle with respect to the vertical direction, before re leasing the package. In case of fault the system could drop the object and run again an alignment process.

IV. Experimental Analysis on Pharmaceutical Packaging

The application fields of the developed system are many. In this work it has been tested for the alignment of packages for pharmaceutical use. In particular, their shape can be both prismatic and cylindrical with the geometric requirements of Fig. 5. As shown in Fig. 5, the average percentage (AVG) of cylindrical packages out of the overall worldwide packages depends on the country. Their weight is less than 800 g.

The packages has to be placed in a position of maximum-stability: the cylindrical have to be placed in vertical position; the prismatic maximizing the contact surface.

V. System Design

This section describes the important features of the hard ware components and the developed software used for statistical experiments.

a) Hardware Components

Fig. 6 shows the components used for testing.

Robot: The robot is the HS-4345 4-axis SCARA robot designed by Denso robotics. It has four links connected with three revolute and one prismatic joints.

Controller: The RC8 controller is the interface between the robot and the PC. From a software point-of-view, the ORiN middleware is used to build the client application to communicate with the controller. In this work the coded client application requests a service sending a packet over TCP stream using b-CAP communication protocol. Server assigns commands and responds to the client to confirm the service execution is completed.

Laser: Keyence LK-G157 laser displacement was used to set the position of the object's center of mass with respect to the object's main axis. The repeatability of the instrument is 0.5 μm.

Parallel gripper: The Shunk WSG 50 parallel gripper is used to actuate prototype jaws. It is equipped with force and position sensors and controlled sending commands via TCP/IP protocol.

b) Software Description

A state machine was designed to control the whole alignment process, whose main states, summarised in Fig. 7, are:

Idle: In Idle state the system is waiting to receive the object information about its shape, dimensions, mass, position and orientation, and if it has to be placed in maximum stability condition or only its location has to be changed. For the test application presented in this paper, all these information in were provided manually as input, while, in actual operative conditions, a dedicated vision system connected to a database will be used.

Positioning: In positioning state, the robot moves to the gripping point specified with a final end-effector position in the operational space and following an optimal planned path.

Gripping: Here the gripper grabs the object and uses its force sensors to detect the presence of the object: in case the object is lost, an error is returned and the system goes back to Idle state.

Lifting: The robot lifts the object and, depending on the gripping point, the object will be aligned or not. The height at which the object is lifted depends on object dimension and on the gripping point. When package alignment is needed, the lifting and pivoting phases show a dumped second order dynamic with different characteristics for different medicine packages, as shown by the encoder signals time evolution in Fig. 8 obtained with a sampling frequency of 100 Hz.

Robot Moving: The robot moves the object to the release point. During this phase the gripper, with its alignment axis, must always be orthogonal to the tangent of the trajectory. The direction of the robot's motion is selected such that the inertial force caused by the robot's acceleration adds an alignment torque to the package (i.e. it pushes the object to the mechanical stroke limit). In this way, if the object is already at the end of its stroke, the lateral acceleration acts on a constrained degree of freedom and does not affect the final angle.

Object Release: This final phase is crucial for the success of the orientation process and only depends on the final angle at the end of the motion phase. Fig. 9 shows the geometric condition for correctly releasing the cylinder in its stable configuration (cone stability).

The critical value of β, β_{cr}, is found making the ratio between the position of the object center of mass (*CM*) and the object diameter at the bottom surface.

Perception Loop: In the Perception loop the smart end effector perceives and combines information such as the current gripper position P_0, the final desired one P_p, the current object angle (θ_t), the gripping distance (h) w.r.t. the center of mass (*CM*), the object diameter (D) and its height (H), to plan the trajectory. Those information are used to realign the package using a reference alignment vertical plate if the object needs to be further aligned before release.

In particular, by the perceived information, the robot moves the gripper to the plate at a distance based on the radius of the cylindrical envelope of the package increased by a safety factor (d_t). A parametric arc movement forces the gripper to be parallel to the vertical plate, Fig. 10. The path chosen in this way guarantees the packages to be tangential to the wall at the final point P_p.

In this phase, the value of the object inclination (θ_t) is constantly checked along the planned gripper trajectory to determine when the object can be correctly released.

In Fig. 11 it is shown the sampled signal (100 Hz sampling frequency) of the rotary sensor during a full

	ITALY		EUROPE		AUSTRALIA		OTHER		ALL	
	No. of pharm.: 25 Items: 82.852 Packs: 283.348		No. of pharm.: 10 Items: 25.897 Packs: 64.941		No. of pharm.: 10 Items: 13.589 Packs: 67.696		No. of pharm.: 9 Items: 15.992 Packs: 167.229		No. of pharm.: 54 Items: 138.327 Packs: 583.214	
Dimensioni confezioni	MAX	MIN	MAX	MIN	MAX	MIN	MAX	MIN	MAX	MIN
Width	176 mm	19 mm	170 mm	19 mm	169 mm	20 mm	174 mm	20 mm	176 mm	19 mm
Lenght	265 mm	29 mm	286 mm	37 mm	283 mm	28 mm	258 mm	31 mm	286 mm	28 mm
Height	109 mm	12 mm	113 mm	12 mm	118 mm	10 mm	108 mm	13 mm	118 mm	10 mm
3D Diagonal	315 mm	61 mm	307 mm	62 mm	335 mm	65 mm	266 mm	64 mm	335 mm	61 mm
Diam. cylinders	123 mm	29 mm	138 mm	31 mm	105 mm	24 mm	135 mm	34 mm	138 mm	24 mm
Height cylinders	101 mm	24 mm	111 mm	18 mm	118 mm	21 mm	97 mm	18 mm	118 mm	18 mm
% cylinders	0,12%	0,00%	3,48%	0,07%	33,95%	14,52%	3,19%	0,00%	33,95%	0,00%
AVG % cylinders	0,01%		0,92%		20,45%		0,71%		4,08%	

Fig. 5: Size of drug packages worldwide

Fig. 6: System Architecture

alignment cycle and the effect of the different phases of the alignment cycle on the angle, described in the Perception Loop phase. In particular, at 3.5 s the object is gripped and lifted, reaching a final angle of approximately 40°. The robot forward acceleration makes the angle to stabilize around 55° at 5.5s, but this is not sufficient for having a successful release because the critical angle for this particular package equals 68°. As a consequence, the robot moves towards the vertical plate, that makes the final angle to be around 90 degrees allowing a safe release.

The code to manage the finite state machine for picking, positioning, aligning and releasing operations is written in C language on Microsoft Windows operating system. A multi-thread application was coded to simultaneously control the SCARA robot, the gripper and read the angle value, Fig. 12.

VI. Design of the Experiments

In this section we carry out a statistical analysis to validate the system design and present the obtained results. The design validation should verify the following hypothesis: system is able to pick up, perform pivoting and aligning of packages of different shapes and weights, in a reduced amount of time and with a low error percentage.

A first factorial screening experiment is performed in order to identify factors that have stronger influence on the pivoting capability. The response surface is then obtained and used to find the factors combination that leads to the worst final angle and the largest settling time. In other terms, this first experiment allows to obtain the worst operating condition for pivoting success. In this condition the complete pick align-place operation is performed to check the robustness of the system with real drug packages. In this final study, the effectiveness of the system is assessed through the percentage of successfully completed alignment operations.

All the statistical analysis was performed in RStudio, an integrated development environment for R programming language.

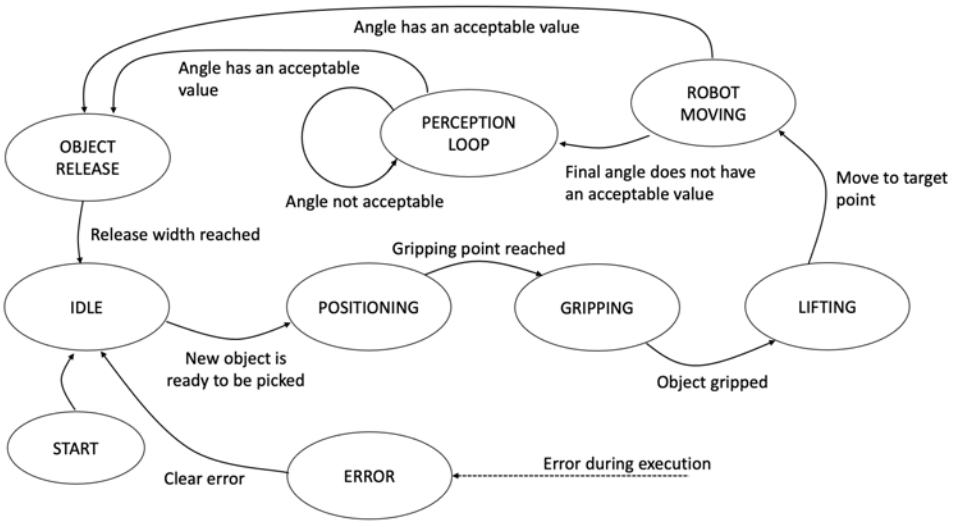

Fig. 7: State Machine with transition conditions

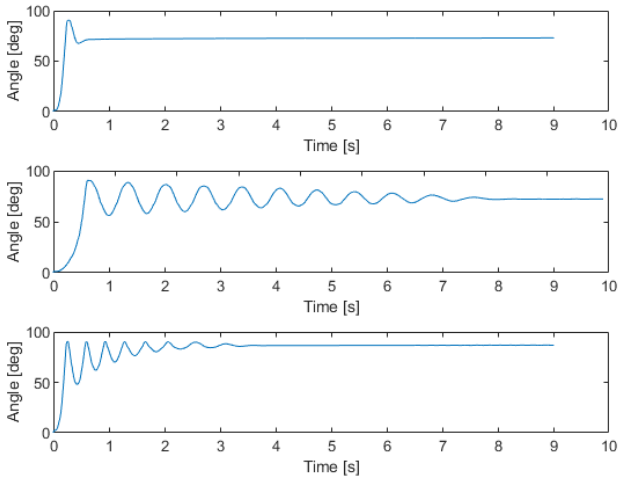

Fig. 8: Three signals sampled during the lifting and pivoting phase for different packages: The upper plot refers to large diameter, high package filled with homogeneous material. The middle one refers to large diameter, low height package filled with homogeneous material and the bottom one refers to small diameter, high package filled with non-homogeneous material

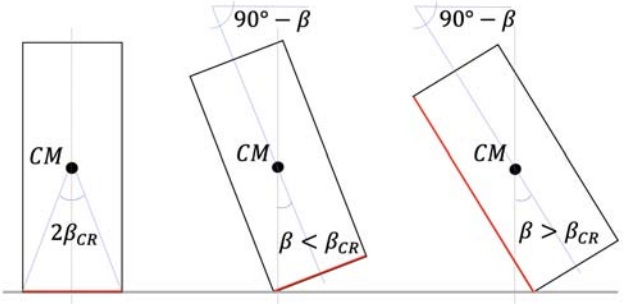

Fig. 9: Geometric condition for alignment success (cone of stability) with β the package's angle with the vertical plane and β_{cr} the threshold angle for stability. In red the final stability side of the package after release

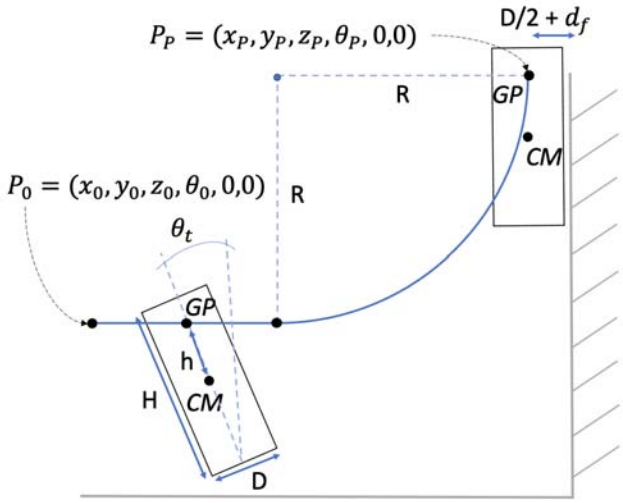

Fig. 10: Parametric arc curve from initial object's position P_0 to its final position P_p

a) Screening Experiment

The factorial experiment is the most efficient type of experiment for screening. After obtaining the factors significance, the objective is to obtain the response surface. The factorial design is augmented with several observations at the center to fit a model linear in all factors but one, which is quadratic. If the ANOVA shows that the quadratic term is significative, then we need to augment the factorial plan to a 3^n Central Composite Design, if not, a linear 2^n model is a reliable approximation. Blocking is used to perform sequential experimentation and augment the factorial design only if the second-order model is needed [15].

The choice of factors levels comes from prior and actual knowledge of the process and is made to fit the real operating conditions of the process when performing the central composite design. The design factors chosen for the factorial experiment with their low (*L*), center (*C*) and high (*H*) levels are reported below.

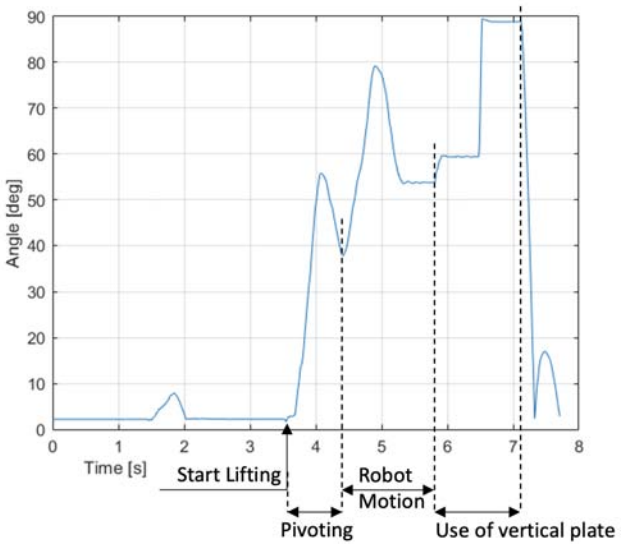

Fig. 11: Angle signal sampled during a full alignment cycle

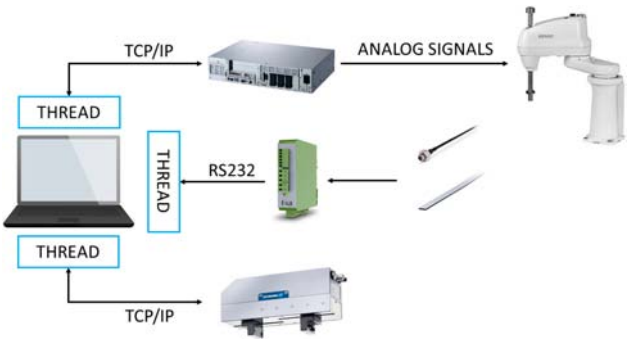

Fig. 12: Communication protocols overview

A. Distance percentage w.r.t. the geometrical center of mass, Fig. 13(b); *L*: 10% - *C*: 50% - *H*: 90%.
B. Object diameter; *L*: 35*mm* - *C*: 52.5*mm* - *H*: 70*mm*. C. Object height; *L*: 60*mm* - *C*: 90*mm* - *H*: 120*mm*.

D. Distance percentage of the inner material center of mass w.r.t. the container center of mass, Fig. 13(a)); *L*: 0% - *C* : 50% - *H* : 100%.
E. Robot vertical acceleration (percentage of the maximum allowed for the package mass); *L*: 20% - *C*: 40% - *H*: 60%.
F. Friction coefficient at gripping interface; *L*: standard interface - *C*: elastic film on V-shaped cavity - *H*: elastic film on both interfaces.
G. Gripping force; *L*: 10*N* - *C*: 19*N* - *H*: 28*N*.

All the other controllable factors affecting the alignment operation are held constant. The most relevant assumptions made during factors selection are presented hereafter.

Assuming that the gripper always makes the pivoting axis orthogonal to the cylinders longitudinal axis, the only gripper degree of freedom that is varied is the position along grip ping axis, all the others are held constant. Also the vertical distance of the grip from the plane is assumed fixed because, even if there is an error in estimating the diameter of the object, the V shape helps to center the grip.

When gripping an object, the gripping force rises from zero to its nominal value with a dynamics that depends on equivalent stiffness and damping at gripping interface. Here the transient is considered negligible and the force is assumed to ideally go from zero to its nominal value before gripping starts.

Mass, volume, inertia moment, diameter, height and gripping distance are not independent factors, so it is not possible to design an experiment taking all of them as factors.

Volume *V*, inertia moment, gripping distance *d* and material type are substituted with two factors: the relative distance of gripping point from the geometrical center of mass (A) and the relative distance of the center of mass of the inner material from the geometrical center of mass of the container (D). This is non zero when the material is non-homogeneous, while it is zero otherwise. For non-homogeneous materials, we refer to the unconstrained material contained within the package, e.g., pills or powders. On the other hand, for homogeneous material we refer to uniformly constrained materials such as fully filled liquid jars or thick creams.

The response variables of particular interest to characterize the alignment process are the final angle and the settling time. The first quantifies the alignment in steady state condition, when oscillations are completely damped, the second instead takes into account the alignment dynamics.

To satisfy the statistical requirements of the independence of observations, the matrix for the final design was generated randomizing the experiment order. A set of different 3D printed cylindrical objects is used to create all combinations of geometrical factors, shown in Fig. 14. They are filled with materials of different densities in order to obtain the same mass value. In Fig. 14, the orange and the black objects are filled with homogeneous and non-homogeneous material, respectively. In the latter case, the ratio between the position of the material center of mass w.r.t. the cylinder and the cylinder height is constant.

i. *Results*

The analysis of variance is performed on the factorial design added with central points. The fitted model for angle response variable is $Angle \sim A * B * C * D * E * F * G + A^2$, the one for time variable is $Time \sim A*B*C*D*E*F*G+ A^2$. The F values and p-values of the factors are reported in Tab. 1 and Tab. 2. The quadratic term is added to check if the 2^n factorial plan has to be augmented to a 3^n Central Composite Design. The high p-value of the quadratic term in both models proves that the linear model is sufficient to describe the system behaviour.

The analysis of variance response surfaces are then obtained fitting a first order model to the factorial data added to central points. Finally, the steepest descent path is determined to obtain the combination of factors that led to the worst condition for final angle and aligning time. A visual interpretation is given here reporting the values of factors when moving down the steepest descent path at 0.5 distance from the center point and at the factors high level (distance 1 from the center point). Results are reported in Tab. 3 and Tab. 4.

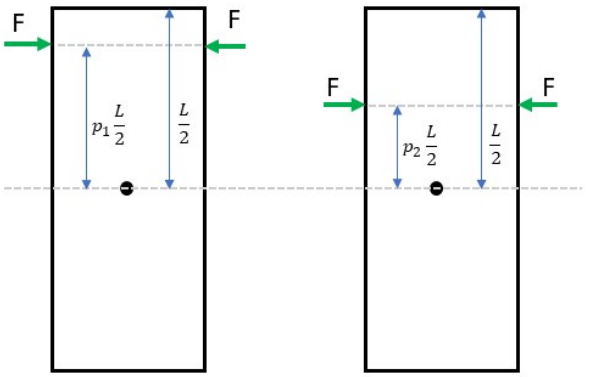

(a) Factor A measurement

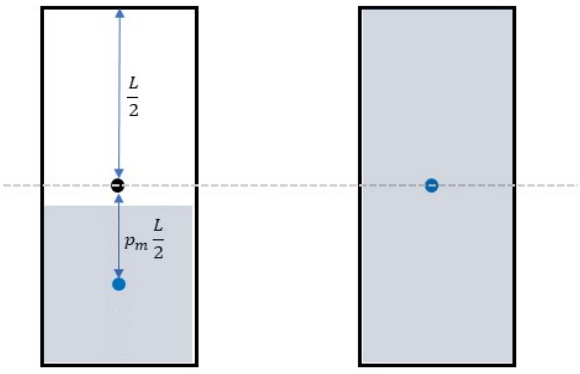

(b) Factor D measurement

Fig. 13: Relative definition for factors

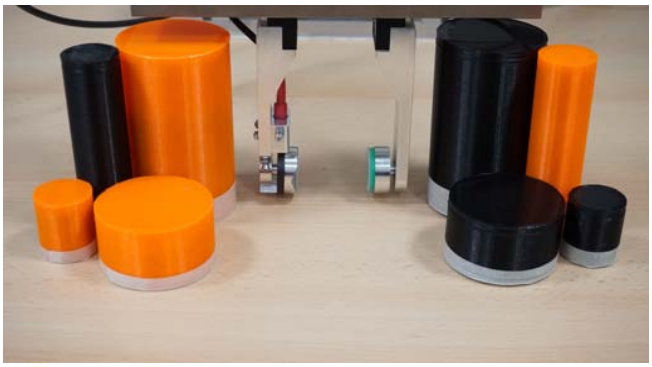

Fig. 14: Cylindrical 3D printed objects representing different factors combinations

The worst case for the final angle in the chosen range of operating conditions occurs when pivoting is performed with:

A: low gripping distance percentage
B: high diameter

Table 1: ANOVA results for angle variable

Factor	F value	p-value
(A) Gripping distance	341.46	4.84e-13
(B) Diameter	1448.04	< 2.2e-16
(C) Height	996.87	<2.2e-16
(D) Material	37.57	9.521e-09
(E) Vertical acceleration	5.547	0.02
(F) Friction coefficient	14.14	2.54e-4
(G) Gripping force	0.38	0.54
A^2	0.60	0.44

Table 2: ANOVA results for time variable

Factor	F value	p-value
(A) Gripping distance	3157.99	< 2.2e-16
(B) Diameter	280.32	< 2.2e-16
(C) Height	232.70	< 2.2e-16
(D) Material	15.73	1.193-4
(E) Vertical acceleration	11.31	1e-3
(F) Friction coefficient	10.71	1.36e-3
(G) Gripping force	142.88	< 2.2e-16
A^2	2.43	0.12

Table 3: Factors value on the steepest descent path for angle surface

Dist.	A	B	C	D	E	F	G
0	0.00	0.00	0.00	0.00	0.00	0.00	0.00
0.5	-0.20	0.33	-0.29	0.12	-0.02	0.02	0.01
1	-0.42	0.59	-0.60	0.32	-0.09	0.04	0.02

The worst case for the aligning time in the chosen range of operating conditions occurs when pivoting is performed with:

A: high gripping distance percentage
B: high diameter
C: high height
D: non-constrained material
E: high vertical acceleration
F: low friction coefficient
G: low gripping force

Table 4: Factors value on the steepest descent path for time surface

Dist.	A	B	C	D	E	F	G
0	0.00	0.00	0.00	0.00	0.00	0.00	0.00
0.5	0.23	0.28	0.27	-0.09	0.00	-0.06	-0.19
1	0.47	0.55	0.54	-0.21	0.05	-0.13	-0.35

These results are in accordance with the physics of the problem. The system can be modeled as a damped physical pendulum with additional energy loss caused by the bump against the stop screw. The amount of energy dissipated during the bump depends on the restitution factor. For what concerns the final angle, its value depends on the final balance between the torque of the gravity force that acts on the package center of mass and the unbalancing mass one. A short gripping distance implies a short lever arm for the gravity torque, resulting in a lower angle value. The unconstrained material moves to the bottom of the

(a) Package 1: 520x44 *mm* 52 *gr* (b) Package 2: 90x35 *mm* 175 *gr*

Fig. 15: Worst package for release (a) and for pivoting (b)

container, making the aligning torque after transient to be larger than the constrained case. It follows that the worst case is represented by the constrained material case. A high gripping force can prevent the bearings from correctly rotate and a low acceleration does not help in the aligning operation.

Analyzing the time variable, the high gripping distance con tribute to have a larger torque, while the non-constrained material adds an aligning torque to the system when the package starts to rotate. The large diameter and large height condition makes the inertia moment, and consequently the kinetic energy, to be higher. The kinetic energy is also increased by the large vertical acceleration. Since a larger kinetic energy implies to have more bumps and a longer transient, the final aligning time results to be longer.

The time needed for the entire aligning operation depends on several factors, one of the most relevant being the package initial and final position and orientation. Moreover, the aligning angle and time are highly depending on the robot lateral dynamics. By assuming that the robot will be operated to minimize the time of the process, next experiments to validate the gripper in the whole robotic system are performed fixing only the geometric conditions at their worst for the aligning angle:

B: larger diameter
C: short height
D: homogeneous material

b) Testing: Pick-align-place

The worst-case drug package characteristics found for pivoting in Section 5.1 are not the same as those for the re lease operation. The latter case is influenced only by pure geometric considerations from the values of the position of the center of mass and the diameter of the object at the bottom surface as seen in section 4.1. In contrast with the diameter, the position of the center of mass is affected by uncertainty, especially if the material contained in the package is not homogeneous. We can assume that the center of mass in the geometric center of gravity is a good approximation and conservative. In fact, even though pharmaceutical packages contain heterogeneous material, due to the effect of gravity during rotations, the inside material would go to the lower part and this would lower the center of mass increasing the critical angle for stability. To have a small height and small diameter implies a lower critical angle, so another package of drugs was selected to take into account the worst case for release, which is reported in Fig. 15(b).

In order to provide a complete analysis of the system, two test campaigns were carried out to validate the robustness of final design on both worst cases with packages of Fig. 15. The centres of mass of both packages correspond to the geometric centres due to the homogeneity of the material contained inside.

In order to take into account the most critical source of uncertainty related to the identification of the object position and therefore its center of mass estimation, both the previously defined drug packages are tested randomly varying the gripping point between 10% and 90% of their half eighth (Fig. 16). In both cases, 200 gripping positions are generated from a uniform distribution, and the releasing success is tested for both packages after pivoting only and also with the robot moving on a trajectory.

i. *Results*

The results of these experiments are presented in Tab. 5 and Tab. 6. All the incorrect alignments occurs when the gripping distance is near 10%.

VII. Conclusion

In this paper, we have presented an innovative design for a smart robotic gripper able to grasp objects of cylindrical and prismatic shapes and then orient them through a mechanically passive alignment system. The gripper is endowed with sensors to detect object misalignment and, if necessary, uses an external vertical plate for re-orientation. The statistical performance analysis shows that the worst condition for the pivoting operation is represented by small height, large diameter packages filled with homogeneous material. Moreover, geometrical considerations on object stability are made to find the worst packages characteristics for release success: small height, small diameter, filled with homogeneous material.

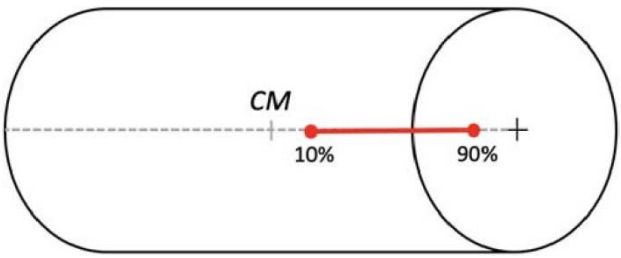

Fig. 16: Gripping interval between 10% and 90% of the cylindrical package half height

Table 5: Percentage of alignment success for package 1

Success rate for the worst package for pivoting		
After pivoting	After motion	After aligning loop
84.5 %	97.5 %	98.5 %

Table 6: Percentage of alignment success for package 2

Success rate for the worst package for release		
After pivoting	After motion	After aligning loop
87.5 %	96.5 %	99 %

Two commercial packages representing the two worst cases are tested in different working conditions. When both packages are released after the vertical motion of the robot, considering also the robot lateral motion and using an additional vertical plate as backup solution to complete the alignment operation, the success rate considering also the worst cases is around 99%.

The cases in which the alignment is not successful are those in which the gripping point is close to the center of gravity. The probability of success consistently increase with a vision system that can reliably estimate the position of the centre of mass. The results shows that the percentage of success of the system is high even in the worst operating conditions, see Extension 1.

Acknowledgements

The authors thank GPI SpA[1] for providing the main requirements and hardware used for testing. Further thanks go to Lika[2] for the encoder components.

References Références Referencias

1. Lundstrom, G., 1974. "Industrial robot grippers". *Industrial Robot: An International Journal*.
2. Salisbury, J., 1982. Kinematics and force analysis of articulated hands, phd thesis.
3. Dafle, N. C., Rodriguez, A., Paolini, R., Tang, B., Srinivasa, S. S., Erdmann, M., Mason, M. T., Lundberg, I., Staab, H., and Fuhlbrigge, T., 2014. "Extrinsic dexterity: In-hand manipulation with external forces". In 2014 IEEE International Conference on Robotics and Automation (ICRA), IEEE, pp. 1578–1585.
4. Mason, M. T., Salisbury, J. K., and Parker, J. K., 1989. *Robot hands and the mechanics of manipulation*.
5. Bicchi, A., and Sorrentino, R., 1995. "Dexterous manipulation through rolling". In Proceedings of 1995 IEEE International Conference on Robotics and Automation, Vol. 1, IEEE, pp. 452–457.
6. Cherif, M., and Gupta, K. K., 1999. "Planning quasi-static fingertip manipulations for reconfiguring objects". *IEEE Transactions on Robotics and Automation,* **15**(5), pp. 837–848.
7. Xu, J., Koo, T. J., and Li, Z., 2007. "Finger gaits planning for multifingered manipulation". In 2007 IEEE/RSJ International Conference on Intelligent Robots and Systems, IEEE, pp. 2932–2937.
8. Bracken, F. L., Insolia, G. E., and Zimmers, E. W., 1989. *The Interrelationship of Parts Classification and Gripper Design for Automated Assembly*. Springer Berlin Heidelberg, Berlin, Heidelberg, pp. 54–58.
9. Holladay, A., Paolini, R., and Mason, M. T., 2015. "A general framework for open-loop pivoting". In 2015 IEEE International Conference on Robotics and Automation (ICRA), pp. 3675–3681.
10. Hou, Y., Jia, Z., and Mason, M. T., 2019. Reorienting objects in 3d space using pivoting.
11. Rao, A., Kriegman, D. J., and Goldberg, K. Y., 1996. "Complete algorithms for feeding polyhedral parts us ing pivot grasps". *IEEE Transactions on Robotics and Automation,* **12**(2), pp. 331–342.
12. Chavan-Dafle, N., Mason, M. T., Staab, H., Rossano, G., and Rodriguez, A., 2015. "A two-phase gripper to reorient and grasp". In 2015 IEEE International Conference on Automation Science and Engineering (CASE), pp. 1249–1255.
13. Taylor, I. H., Chavan-Dafle, N., Li, G., Doshi, N., and Rodriguez, A., 2020. "Pnugrip: An active two-phase gripper for dexterous manipulation". In 2020 IEEE/RSJ International Conference on Intelligent Robots and Systems (IROS), IEEE, pp. 9144–9150.
14. Chavan-Dafle, N., Lee, K., and Rodriguez, A., 2018. "Pneumatic shape-shifting fingers to reorient and grasp". In 2018 IEEE 14th International Conference on Automation Science and Engineering (CASE), pp. 988–993.
15. Montgomery, D. C., 2017. *Design and analysis of experiments*. John wiley & sons.

[1] https://www.gpi.it
[2] https://www.lika.it

Global Journal of Researches in Engineering: A Mechanical and Mechanics Engineering
Volume 22 Issue 2 Version 1.0 Year 2022
Type: Double Blind Peer Reviewed International Research Journal
Publisher: Global Journals
Online ISSN: 2249-4596 & Print ISSN: 0975-5861

Determination of the Influence of Factors on the Properties of Aerated Concrete Obtained on the Basis of Floating Ash Cenospheres and Analysis of the Results of the Experimental Study by the Method of Mathematical Modeling

By Shaikhslam Takibayuly, Kuandyk Cakanov, Askar Kurmanov & Gulnar Jukenova

Mongolian University of Science and Technology

Annotation- The article discusses the results of a study by the method of mathematical modeling and the influence of various factors on the properties of aerated concrete obtained on the basis of floating ash cenospheres. The use of the cenosphere of floating ash from thermal power plants for the production of aerated concrete and other materials is very important for solving many issues, including saving natural resources, reducing the cost of thermal energy, reducing the cost of building materials and environmental pollution from ash waste, etc. These studies pay great attention to devoted to the analysis and confirmation of the results of the experiment based on the methods of mathematical modeling.

Keywords: floating ash, cenosphere, mathematical modeling, factors, properties of aerated concrete.

GJRE-A Classification: DDC Code: 330.028 LCC Code: HB139

Strictly as per the compliance and regulations of:

Determination of the Influence of Factors on the Properties of Aerated Concrete Obtained on the Basis of Floating Ash Cenospheres and Analysis of the Results of the Experimental Study by the Method of Mathematical Modeling

Shaikhslam Takibayuly [α], Kuandyk Cakanov [σ], Askar Kurmanov [ρ] & Gulnar Jukenova [ω]

Faculty of Engineering, NAO Toraigyrov University. city Pavlodar, 140008, Kazakhstan.
e-mail: takibai@mail.ru

Annotation- **The article discusses the results of a study by the method of mathematical modeling and the influence of various factors on the properties of aerated concrete obtained on the basis of floating ash cenospheres. The use of the cenosphere of floating ash from thermal power plants for the production of aerated concrete and other materials is very important for solving many issues, including saving natural resources, reducing the cost of thermal energy, reducing the cost of building materials and environmental pollution from ash waste, etc. These studies pay great attention to devoted to the analysis and confirmation of the results of the experiment based on the methods of mathematical modeling. In the same mathematical way, conclusions were drawn on the correspondence between the results of preliminary and recent tests.**

Keywords: floating ash, cenosphere, mathematical modeling, factors, properties of aerated concrete.

I. Introduction and Research Method

The cenosphere is an aluminosilicate microsphere composed of aluminosilicate cenospheres or fly ash cenospheres (FAC). It is emitted together with fly ash during the combustion of pulverized coal particles. Volatile and floating are synonymous with the lightest part of the ash, and floating ash is a special light particle that floats and accumulates on the surface of the ash storage water. Cenospheres, which belong to the group of fly ash microspheres, are currently widely used as fillers for artificial materials and other products [1-3]. Large volumes of fly ash are discharged into the natural lakes of the ash storage facilities of the Ekibastuz GRES-1 and GRES-2 in the Pavlodar region of Kazakhstan, most of which accumulates along the coast of the lakes. Therefore, they are called floating ash.

Author α σ: Faculty of Engineering, NAO Toraigyrov University ORCIDiD., city Pavlodar, Kazakhstan. e-mails: takibai@mail.ru, kuan_altei@mail.ru
Author ρ: Mongolian University of Science and Technology, city Ulan-Bator, Mongolia. e-mail: sunjidmaa@must.edu.mn

The main objective of the study is to use the cenosphere of fly ash from Ekibastuz GRES-1 and GRES-2 of Kazakhstan as part of aerated concrete, and it is planned to test the effect of the cenosphere of ash components in the concrete mix and other factors on the properties of aerated concrete. Tests and confirmation for compliance with the results of the preliminary and main tests were carried out by the method of mathematical modeling.

Currently, the use of fundamental and applied scientific methods to determine the optimal research regime is increasing. The survey data will be processed mathematically and statistically to determine the average values of the numerical indicators of the studies, change their values in a certain space to obtain a mathematical model of the study, and then analyze the model to obtain the most effective study option using optimization methods. Mathematical modeling is the representation of the number of research experiments, factors and their relationship to each other in the form of tables, graphs and equations.

Mathematical modeling research refers to the relationship between the characteristics of influencing factors, production technology and product characteristics. The mathematical notation of the general form of the mathematical model is as follows:

$$Y = A\{X\}$$

Here: Y- is the output parameter of the study. It represents the main characteristics of the product, which are variously called objective functions or optimization parameters. A-input parameter is an operator that defines the mathematical operation of the transition to the output factor, i.e. the mathematical model. X- is the input factor. It is often called arguments. To obtain a mathematical model of research work, when a combination of theoretical and experimental methods is achieved, in this case the best results are achieved. Here, the theoretical method is used to analyze the

structural properties of the object of study and the product to obtain a general form of the equation (model), however, to determine the numerical values of the coefficients of the calculated part or equation and verify the theoretical conclusions, the experimental method should be used. If the result of the study of indicators is a random number, but in which the input parameter has a fixed value, and not random, then the mathematical model is called a regression model.

The experiment planning matrix is a numerical table showing the change in the values of factors in various sequences of experiments. Planning in which all factors change simultaneously is called experimental multi-factor planning. If the resulting equation for representing the object of study in the form of a mathematical model is non-linear, a second-order mathematical model is constructed [4,6,7].

II. The Purpose of The Study and The Main Part

The purpose of the study is to experimentally determine and establish the influence of constituent components and other factors on the physical and mechanical properties of aerated concrete. The correspondence between the results of the preliminary and main experiments is confirmed by mathematical modeling. For mathematical planning of the experiment, the compressive strength and average density of aerated concrete were taken as the main parameters (output parameters), the amount of ash-X_1, the amount of lime-X_2 and the water temperature-X_3 were chosen as influencing factors. On this basis, the planning matrix (table 1.) and the test matrix (table 2.) were compiled. The total number of experiments in the three-factor matrix is N = 20. Here, the number of repeated experiments at the main point (n0 = 8), the number of experiments at the hot point (ng = 6), the number of tests at the remote point (ny = 6) and the values of the remote point of the lines (a = (-) (+) 1.682). The purpose of the study and the main part. When planning an experiment of mathematical modeling, changes in the amount of ash, lime and water temperature are based on the results of previous experiments on the influence of factors on the properties of aerated concrete with a floating ash mixture at Ekibastuz GRES. In the composition of aerated concrete, Portland cement was chosen as the main binder, sand was used as an aggregate, and aluminum powder was used as a blowing agent. For testing, standard samples of cubes 10 × 10 × 10 cm in size were made, which were removed from the mold after being kept in a heat-moist treatment chamber at a temperature of 80°C for 14 hours. Based on the test, data on compressive strength and bulk density after hardening were obtained. within 28 days under normal conditions.

Table 1: Experiment planning matrix (initial data)

Influencing factors (code)	Unit measurements	Level of influencing factors					Intermediate value, J_i
		$-x$ remote -1,682	x_i lower (-1)	x_{i0} (0)	x_i upper (+1)	$+x$ remote 1,682	
Number of ash cenospheres.,(X_1)	%	14,7	25	40	55	65,2	15
Amount of lime, (X_2)	%	1,6	5	10	15	18,4	5
Water temperature, (X_3)	^{0}C	53,2	60	70	80	96,8	10

Table 2: Trial Matrix and Results

n	N	Coded factor values			Actual values of factors			Outgoing indicators (MPa), test repetition				$\sigma_N^2(Y)$	$\overline{Y}_R$ (МПа)	$\overline{Y}_{\rho(V)}$ (кг/м^3)
		x_1	x_2	x_3	X_1	X_2	X_3	Y_1	Y_2	Y_3	$\overline{Y}$			
n_h	1	+	+	+	55	15	80	1,40	1,33	1,28	1,34	0.0073	1,73	790
	2	+	+	-	55	15	60	1,28	1,31	1,36	1,31	0,0017	1,73	810
	3	+	-	+	55	5	80	1,79	1,72	1,81	1,77	0,0021	2,08	880
	4	+	-	-	55	5	60	1,66	1,60	1,83	1,70	0,0142	2,08	861
	5	-	+	+	25	15	80	2,65	2,59	2,67	2,63	0,0016	2,61	844
	6	-	+	-	25	15	60	2,58	2,54	2,65	2,59	0,0031	2,61	835
	7	-	-	+	25	5	80	2,80	2,83	2,87	2,83	0,0012	2,72	877
	8	-	-	-	25	5	60	2,78	2,82	2,84	2,81	0,009	2,72	872
n_r	9	-1,682	0	0	14,7	10	70	2,92	2,97	2,90	2,93	0,0013	3,17	932
	10	+1,682	0	0	65,2	10	70	2,68	2,60	2,61	2,63	0.0019	1,90	783
	11	0	-	0	40	1,6	70	2,62	2,53	2,50	2,55	0,0039	2,39	840

			1,682											
	12	0	+1,682	0	40	18,4	70	2,40	2,37	2,36	2,34	0,0014	2,00	857
	13	0	0	-1,682	40	10	53,2	2,30	2,31	2,31	2,31	0,0001	2,14	819
	14	0	0	+1,682	40	10	96,8	2,45	2,54	2,44	2,47	0,0031	2,14	805
n_0	15	0	0	0	40	10	70	2,40	2,49	2,40	2,43	0,0027	2,41	831
	16	0	0	0	40	10	70	2,40	2,35	2,42	2,39	0,0013	2,41	826
	17	0	0	0	40	10	70	2,37	2,39	2,41	2,39	0,0005	2,41	833
	18	0	0	0	40	10	70	2,35	2,48	2,43	2,42	0,0043	2,41	834
	19	0	0	0	40	10	70	2,36	2,40	2,35	2,37	0,0007	2,41	828
	20	0	0	0	40	10	70	2,40	2,43	2,41	2,41	0,0002	2,41	833
											46,62	0,0534		16791

Based on the results of three-factor matrix experiments, a mathematical regression model was developed for three second-order factors of type 2^3, representing changes in the strength and average density of aerated concrete, and the results of the study were determined. Next, the values of the influencing factors were determined, the values were changed in a certain space to obtain a mathematical model of the technological operation by experimental planning, and the output parameters of the model were optimized by the objective function formulas and by the graphical composition central planning method [5].

III. Experiment Results

Based on the results of the experiments, the three-factor matrix of the multifactor mathematical regression model representing the change in the strength of aerated concrete is written as follows

$$Y_R = 2{,}41 - 0{,}38x_1 - 0{,}1166x_2 + 0{,}031x_3 - 0{,}05x_1x_2 + 0{,}045x_1^2 - \\ - 0{,}0734x_2^2 - 0{,}093x_3^2$$

As a result of the experiment, the three-factor mathematical regression model for expressing the change in the volumetric mass of concrete is written as follows

$$Y_\rho = 830 - 24{,}71x_1 - 13{,}28x_2 - 8{,}87x_1x_2 - 4{,}37x_2x_3 + 11{,}28x_1^2 + \\ + 8{,}06x_2^2 - 4{,}87x_3^2$$

When analyzing mathematical models, the following was revealed: the ash content (x_1) and water temperature (x_3) more effectively affect the strength parameters, and the ash content (x_1) and lime (x_2) effectively affect the bulk mass parameters. To optimize the values of mathematical models representing the results of the experiment, the analytical method of the multifactorial objective function and the graphical method of central composition planning were used.

IV. Conclusion

When optimizing the analytical method of the multivariate objective function of the value of the output parameters of the three-factor mathematical regression model that expresses the properties of aerated concrete, the parameters found cover the indicated values in previous studies, with a minimum compressive strength of aerated concrete at a fixed point YR = 2.41 and a maximum average density Yρ = 916.

The graphical method for optimizing the values of mathematical models is based on central compositional planning. For optimizations by a graphical method, we obtain an equation based on experimental results to plot the relationship between compressive strength and bulk density of concrete. Therefore, the steady state reflection function is curved and relatively well expressed as a second order polynomial. Since 6 parallel experiments were performed at the zero level of testing, the results of which allow us to evaluate the model. On the test graph, the red lines show the central test points, the yellow lines show the main test points, and the green lines show the remote test points.

a) *Characterizing the equations of the output parameters of the compressive strength and graphs of the surface of the reflection function depending on the value of the influencing factors*

$$Y_R = 3.057 + 0.09X_1 + 0.33X_2 + 0.0015X_1^2 + 0.0004X_2^2 - 0.044X_1X_2$$

$X_3=60$ $X_3=70$ $X_3=80$

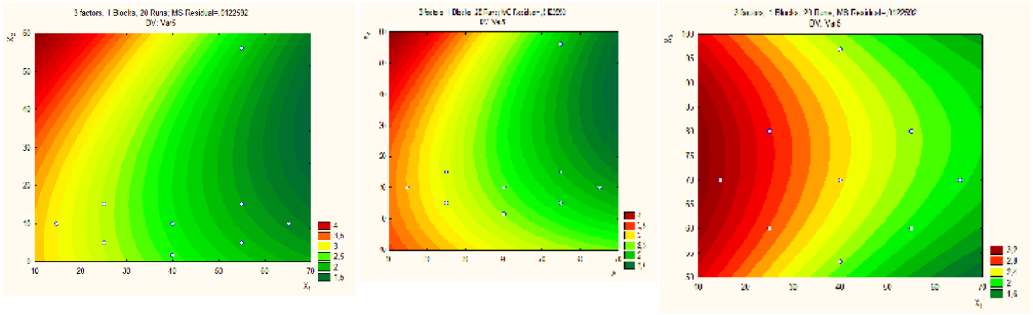

Figure 1: Graphs of synonymous lines on the reflection surface of the function Y_R depending on the values of the influencing factor X_3

$$Y_R = 0.04X_1 + 10.09X_2 + 0.00015X_1^2 - 0.006X_2^2 + 0.19$$

$X_2=5$ $X_2=10$ $X_2=15$

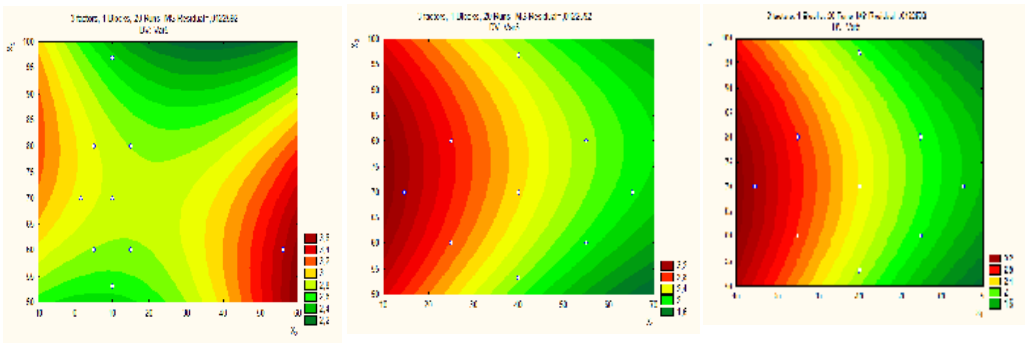

Figure 2: Graphs of synonymous lines on the reflection surface of the function Y_R depending on the values of the influencing factor X_2

$$Y_R = 0.03X_1 + 0.09X_2 + 0.0004X_1^2 - 0.0006X_2^2 - 1.68$$

$X_1=25$ $X_1=40$ $X_1=55$

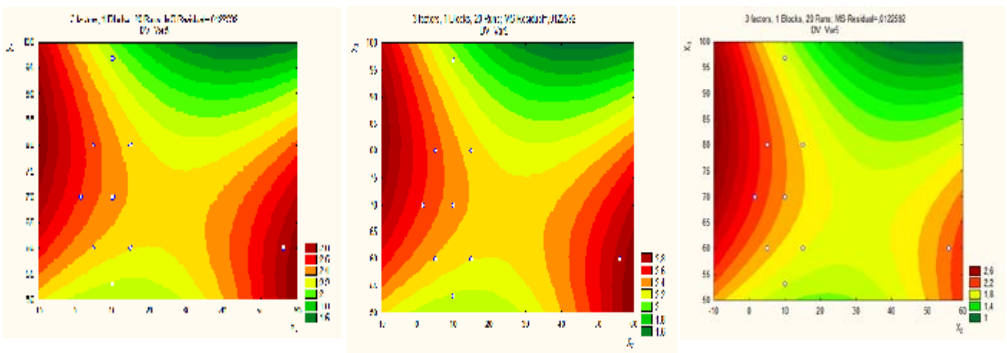

Figure 3: Graphs of synonymous lines on the reflection surface of the function Y_R depending on the values of the influencing factor X_1

b) *Characterizing equations for the output density parameter and graphs of the surface of the reflection function depending on the value of the influencing factors*

$$Y_\rho = 0.41X_1 + 8.18X_2 + 871.5$$

$X_3 = 60$ $X_3 = 70$ $X_3 = 80$

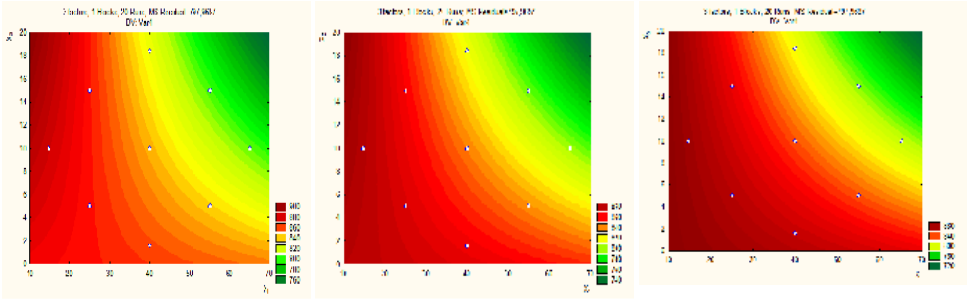

Figure 4: Graphs of synonymous lines on the reflection surface of the function Yρ depending on the values of the influencing factor X_3

$$Y_\rho = 1.12X_1 + 8.18X_2 + 816.7$$

X1=25 $X_1 = 40$ $X_1 = 55$

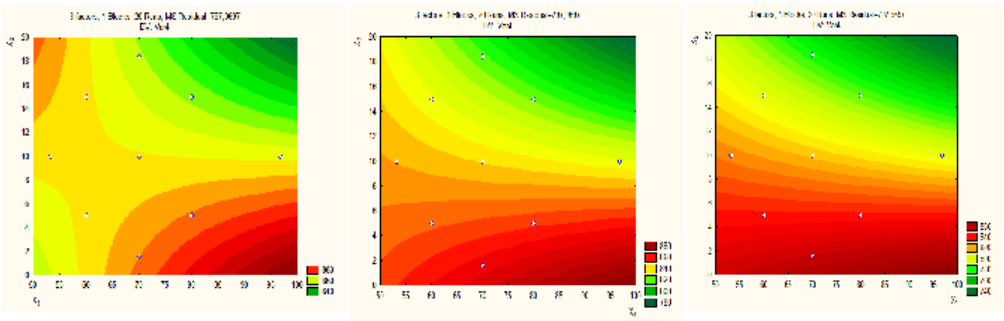

Figure 5: Graphs of synonymous lines on the reflection surface of the function Yρ depending on the values of the influencing factor X_1

$$Y_\rho = 1.12X_1 + 0.4X_2 + 846.9$$

$X_2 = 5$ $X_2 = 10$ $X_2 = 15$

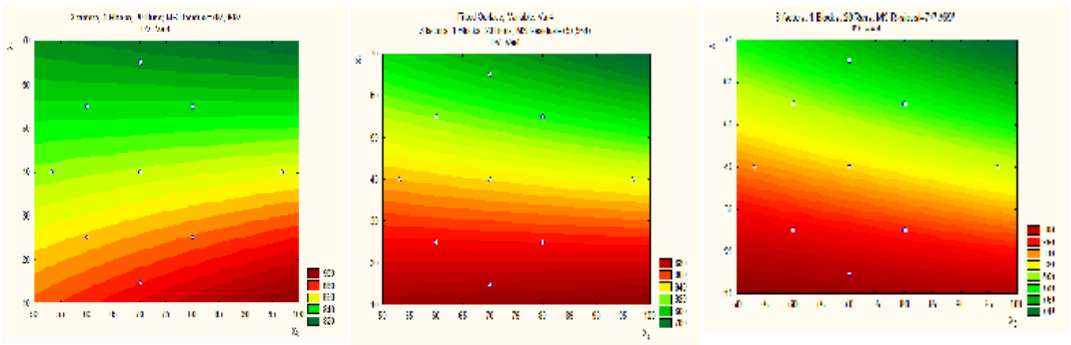

Figure 6: Graphs of synonymous lines on the reflection surface of the function Yρ depending on the values of the influencing factor X_2

As a result of graphical optimization for the outgoing strength indicators, the values of the points of the dependence graphs are 2.50; 2.40; 2.40 at the level of influencing factors X3 = 80, X1 = 40, X2 = 10 are close or correspond to the values of the central and main points of the experiment 2.61; 2.41; 2.40. According to the outgoing density indicators, their values correspond to 800;820;800 at the level of

influencing factors X3 = 80, X1 = 40, X2 = 10, which are close or correspond to the values of the central and main points of the experiment 844; 819; 805.

The fly ash cenosphere used in the study was relatively coarse-grained, consisted of up to 90% mullite crystals and a low content of calcium oxide and quartz, which weakened the reactivity and did not contribute to the achievement of high concrete strength.

References Références Referencias

1. James Hannan. Chemical Makeup of Fly and Bottom Ash Varies Significantly; Must Be Analyzed Before Recycled. Thermo Fisher Scientific (February 6, 2015). Retrieved May 29, 2018.
2. T. Shaixlam, D. Sunjidmaa, G. Batdemberel. A study of Ferrospheres in the Coal Fly Ash Open Journal of Applied Sciences, 2019,9,10-16 http://www.scirp.org/journal/ojapps ISSN Online: 2165-3925 ISSN Print: 2165-3917.
3. E. V. Fomenko, N. N. Anshits, N. G. Vasil'eva, E. S. Rogovenko, O. A. Mikhailova, E. V. Mazurova, L. A. Soloviev, and A. G. Anshits. The composition and structure of the shell of aluminosilicate microspheres of fly ash formed from the combustion of Ekibastuz coal. Siberian Federal University "Institute of Chemistry and Chemical Technology" - Krasnoyarsk, 2016.
4. Avdai Ch., Enkhtuyaa D. Technique of performance (static processing, modeling, diagnostics) of research works. - Ulaanbaatar, 2015. - 288 p.
5. Namzhildorzh B., Sunzhidmaa D., Olziyburen B. Barilgyn materials baigal orchind eeltey tekhnologin undesuud. Ulaanbaatar, 2015 he.253 h.
6. Adler Yu. P. Planning an experiment in the search for optimal conditions. - M.: Nauka, 1976. - 279 p.
7. Himmelblau D. Analysis of processes by static methods. Translation from English. M., 1988.357 p.

Global Journal of Researches in Engineering: A
Mechanical and Mechanics Engineering
Volume 22 Issue 2 Version 1.0 Year 2022
Type: Double Blind Peer Reviewed International Research Journal
Publisher: Global Journals
Online ISSN: 2249-4596 & Print ISSN: 0975-5861

Establishment of an Analytical Model for Determining Leakage Surfaces in an External Tooth Spur Gear

By Choupo Wankam Gervé & Tchotang Théodore
University of Yaounde I

Abstract- In gear power transmission systems, the lubricant helps reduce friction, wear of parts in contact, cooling of surfaces, reduction of operating noise, protection of components against corrosion, etc. In spite of that, the lubricant entrapment in the gears inter-tooth space generates substantial energy losses at very high rotational speeds. The best optimization of these energy losses requires the preliminary knowledge of the behavior of leakage surfaces of trapped lubricant during the gears rotation. The aim of this work is to develop a purely analytical model enabling to calculate the exact values of the axial and radial leakage surfaces of the lubricant in the inter-tooth space of external spur gears as well as the volumes of the pockets. From the modeling of the tooth profile and the parametric equations relating to external spur gears, we have developed a purely analytical model of the lubricant leakage surfaces in the inter-tooth space as a function of the angle of rotation.

Keywords: *gear, power transmission, energy losses, trapping, leakage surfaces, pocket volumes, inter-tooth.*

GJRE-A Classification: *FOR Code: 050599*

Strictly as per the compliance and regulations of:

Establishment of an Analytical Model for Determining Leakage Surfaces in an External Tooth Spur Gear

Choupo Wankam Gervé [α] & Tchotang Théodore [σ]

Abstract- In gear power transmission systems, the lubricant helps reduce friction, wear of parts in contact, cooling of surfaces, reduction of operating noise, protection of components against corrosion, etc. In spite of that, the lubricant entrapment in the gears inter-tooth space generates substantial energy losses at very high rotational speeds. The best optimization of these energy losses requires the preliminary knowledge of the behavior of leakage surfaces of trapped lubricant during the gears rotation. The aim of this work is to develop a purely analytical model enabling to calculate the exact values of the axial and radial leakage surfaces of the lubricant in the inter-tooth space of external spur gears as well as the volumes of the pockets. From the modeling of the tooth profile and the parametric equations relating to external spur gears, we have developed a purely analytical model of the lubricant leakage surfaces in the inter-tooth space as a function of the angle of rotation. Validation of the model was carried out via a comparative study between our results and those resulting from the work of Abdelilah LASRI and al and Diab Y. and al. Curves from our model and those of the reference articles merge after superposition and the relative differences are less than 10^{-2}. This work is therefore the first step in the calculation of the power lost by the lubricant trapping in the gears inter-tooth. It will be of great importance in minimizing power losses.

Keywords: gear, power transmission, energy losses, trapping, leakage surfaces, pocket volumes, inter-tooth.

I. Introduction

Due to their compactness and their ability to transmit high loads at high speeds, gears are widely used in automotive and aerospace applications through speed reducers, power transmissions in wind turbines, etc. In gear drives energy efficiency improving may require reducing power losses. Power losses in gears (gearboxes, reducers, etc.) can be grouped into two categories: power losses depending on the transmitted load (friction at the contact areas between the teeth and friction in the bearings, etc.) and those independent of the transmitted load (losses due to the trapping of the lubricant, the ventilation of the mobiles, etc.). Several researchers have been interested in load-dependent losses and enough models exist. The oil trapping in the inter-tooth space and the ventilation of the spindles are the two main sources of power dissipation in the case of losses independent of the loads. Very few studies and models exist on the loss of power by lubricant trapping and by consequent on the modeling of lubricant leakage surfaces. The vast majority of studies concerning the modeling of lubricant trapping in the inter-tooth space are empirical, numerical, and semi-analytical and based on approximations and estimations.

The first experimental studies on this subject permitted to make a difference between load-depending and load-independing losses. Devin R. and Hilty B.[1], made experimental investigations of load-independent losses caused by planetary gear sets and conclude that for high speeds (≥ 6000 r pm) the losses independent of the load become the major contributor. These experimental works allowed to develop and validate empirical, numerical and semi-analytical models.

Using NASA research center test rig, Anderson and al. [2], Krantz [3], Rohn and Handschuh [4] have developed several empirical formulas. Empirical formulations for the particular case of trapping losses in gears are based on the gears geometric parameters and include those of Terekhov [5], Wolfan Mauz [6], Butsch M. [7] and Maurer J. [8]. The empirical models developed provided global formulas for the estimation of pressing torque or power loss. It is necessary to point out that these formulas are only valid for external gearing and remain linked to the sensitivity and precision of the equipment used for the tests. Generally they are of very low precision with quite important deviations. As an example we can quote the model of Mauz[6], which indicates an uncertainty between 5 and 15% if the resisting torque is higher than 5 Nm and an uncertainty up to 50% for lower torque values. It is therefore necessary to set up another quite precise model. Many researchers have developed numerical models to understand the behavior of inter-tooth spaces during movement in order to estimate the power lost by trapping. Pechersky and Wittbrodt [9] used an approximation of the tooth profile expression to calculate the leakage surfaces. Diab Y. and al [10-11] have numerically evaluated the radial leakage surfaces (considered here as minimum distances between the tip corner of the gear and the profile) and they obtained the axial leakage surfaces by

Author α σ: University of Yaounde I, Yaounde, Cameroon. National Advanced School of Engineering, Civil and Mechanical Engineering Laboratory. e-mails: tchoupogerve@yahoo.fr, tchotang@yahoo.com

numerical integration. Abdelilah Lasri and al [12-14] used a numerical approximation to evaluate the radial surfaces (considered here as the minimum distance between the tooth profiles) and they obtained the axial leakage surfaces by numerical integration. David C. Talbot [15] calculates the power lost by trapping in planetary gears by discretizing in time and space the Conservation of Mass, Momentum and Energy equations. The leakage surfaces are obtained by numerical approximation through the surfaces meshing. Seetharaman and Kahraman [16] were inspired by the work of Pechersky and Wittbrodt [9] to establish a semi-analytical formulation for calculating leakage surfaces. However, several approximations are made there, namely a Taylor approximation of order 1 of the involute profileequation, the cancellation of certain portions of the surface, the use of approximate values of certain distances, etc. From the vectors ray approach, Massimo Rundo[17] established an analytical formula for trapped volume in crescent pumps. It is necessary to note that in this approach the length variation of the vector ray for an infinitesimal rotation is neglected. In addition, this formula is limited only to the portion where teeth profiles are in contact. For an efficient contribution to the power losses by the lubricant trapping of as well as the wear of the elements with a view to improve the energy performances in gears transmissions, it is essential to completely lift the veil on the inter-tooth zone during meshing. From the work of Seetharaman and Kahraman [16], we will establish a purely analytical model of the evolution of the radial and axial leakage surfaces as a function of the angle of rotation in a spur gear. This work has as particularity the use of the exact expression of the tooth profile in the calculations and the authenticity of the analytical expressions of the developed surfaces.

This work is divided into three main parts. The first part is devoted to the modeling of the tooth profile and the associated parametric equations. The second part deals with the calculations of the leakage surfaces from the tooth profile equations, with the radial leakage surface being considered as the minimum distance between the tooth profiles. The last part focuses on the results interpretation and the model validation. The model validation consist of a superposition of our results with those of A. Lasri and al [13] and Diab and al [10].

II. Material

a) Trapping Phenomenon

The lubricant used in gear transmissions to reduce corrosion, friction, cool the elements, etc., is trapped in the inter-tooth space during movement and becomes the seat of energy losses. Lubricant trapping is the jamming of the lubricant in the inter-tooth space during the meshing phase. The fraction of lubricant trapped in the inter-tooth space (in yellow in figure 1) is expelled under pressure radially toward the neighbouring pockets and or axially toward the outside of the gear during this phenomenon. The opposite phenomenon is reproduced during the unmeshing phase.

The geometry of the inter-tooth space relates to the type of tooth (straight, helical, hypoid, etc.) which constitutes the gear's wheels. In the particular case of spur gears, the axial leakage area remains constant over the tooth width. However, in the case of helical gear, the axial leakage area is variable over the tooth width.

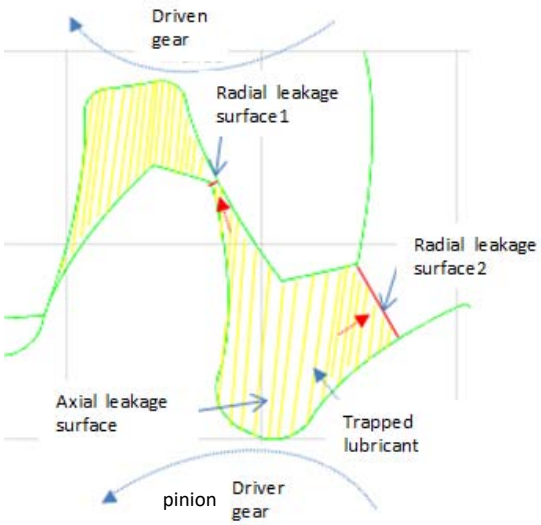

Figure 1: Inter-tooth space and trapped lubricant

b) Evolution of Radial and Axial Leakage Surfaces

The radial and axial leakage surfaces vary according to the angle of rotation. The further away from the initial position, the surfaces increase. Here, the initial position is the meeting point between the two pitch circles. The Figure 2 below illustrates the behavior of the leakage surfaces as a function of the angle of rotation from a) to h).

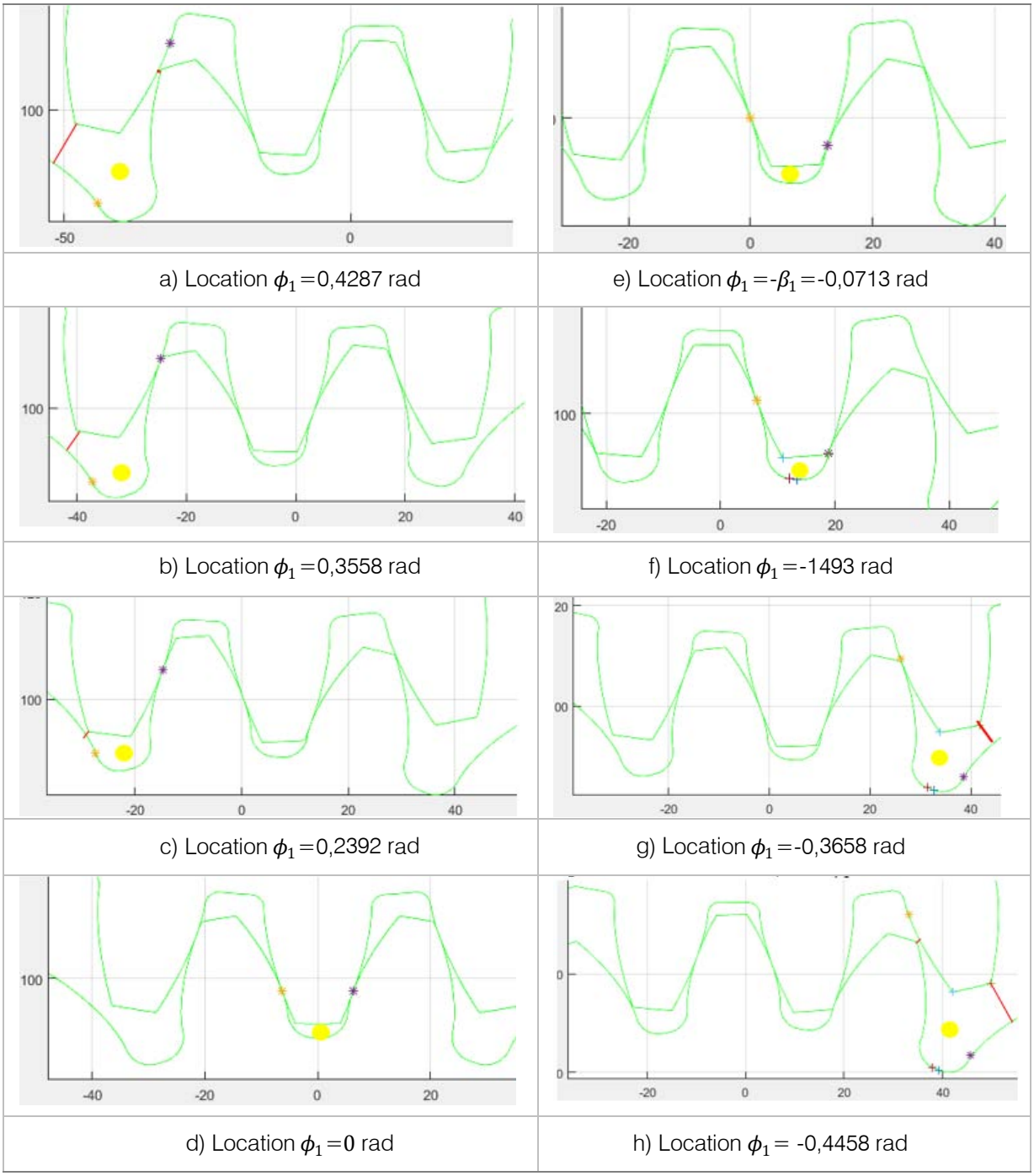

Figure 2: Evolution of the leakage surfaces as a function of the rotation angle

c) Coordinate System Linked to Gears

The pinion (driver) is associated to a fixed reference (O_f, x_f, y_f, z_f) and mobile reference (O_1, x_1, y_1, z_1), which revolves around (O_f, z_f) by an angle ϕ_1. Similarly, the gear (driven) is associated to fixed reference (O_p, x_p, y_p, z_p) and mobile reference (O_2, x_2, y_2, z_2), which revolves around (O_p, z_p) by an angle ϕ_2. Such as $\phi_2 = -(\rho_1/\rho_2)\ \phi_1 = -(r_1/r_2)\ \phi_1 = -(r_{s1}/r_{s2})\ \phi_1$. Figure 3 below illustrates all these different references.

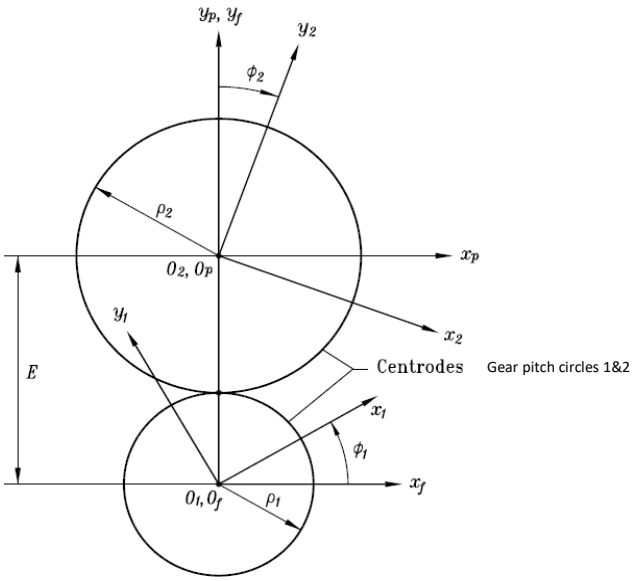

Figure 3: Tracking of gear system

In our calculations, the initial position is the position where the tooth profiles of the driving and driven gears meet at point I (the contact point between the pitch circles).

d) Geometry of a Spur Gear Tooth

The tooth shapes of spur gears are relative to the number of teeth. Generally, for a tooth, there will be the involute zone and the circular zone. Figure 4 below shows the detailed geometry of a 25-tooth gear.

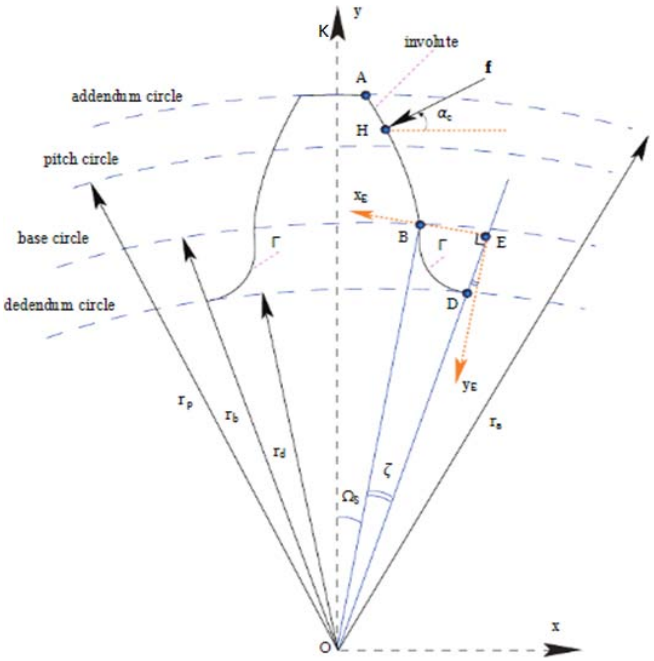

Figure 4: Geometry of an external spur gear

e) Leakage Surface and Border Points at a given Location

In a specific interval of the rotation angle, the profiles of the teeth meet, and consequently the radial leakage surfaces remain zero. Figure 5 below is a particular case. On this figure, C1 and C2 are the two contact points of the tooth profiles.

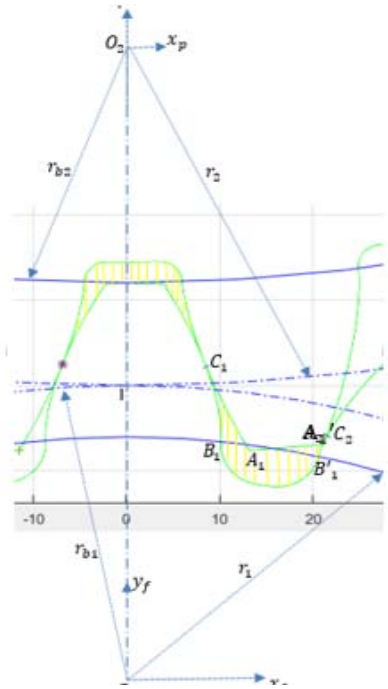

Figure 5: Leakage surface at a location where profiles are in contact

When the profiles are not in contact, the radial leakage surfaces are non-zero and, consequently the axial leakage surface has as its boundary the tooth profiles and the minimum distances between the adjacent profiles. The figure 6 below is an illustration of this situation.

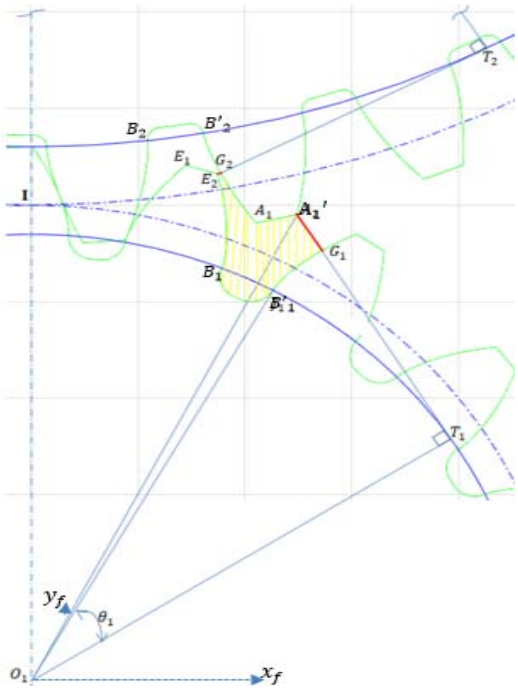

Figure 6: Radial and axial leakage Surfaces at a location where profiles are not in contact

f) Information Technology Tools

The simulation of the equations and the model obtained was carried out with the MATLAB R2016A application installed in an HP computer, AMD A6-3400 APU HD Graphics 1.40 GHz; 6 GB of RAM.

III. Method

a) Hypothesis

Our study was carried out under the following assumptions:

- The portion of tooth between the addendum circle and the base circle is in involute.
- The shape of the tooth portion after the base circle varies depending on the tooth number.
- Radial distances are minimum distances between adjacent profiles.
- The direction of rotation of positive angles is the trigonometric direction and, the direction of rotation of negative angles is the anti-trigonometric direction.
- In our calculations, the initial position (ϕ_i =0) is the position where the two adjacent profiles meet at the common point of the pitch circles. However, for the presentation and the comparative study of the results, we bring the initial position back to the position where (O_1O_2) passes simultaneously through the midpoints of the gear top land and the pinion root.

b) Calculation Algorithm

From the geometric parameters of a gear tooth, the parametric equations of the half tooth profile are established. The complete gear tooth is obtained by axial symmetry of this half tooth, followed by N-1 successive rotations of the primary tooth with respect to the axis of the gear and respective angles 2*π*k/N, 1≤k≤N-1. Where N is the number of teeth.

From the initial position, the coordinates of the boundary points of the leakage surfaces are calculated as a function of the rotation angle. From the properties of the involute of a circle, we calculate the radial distances as a function of the rotation angle and by surface integration, we obtain the radial surfaces. The figure 7 below is the algorithm that succinctly presents our working methodology.

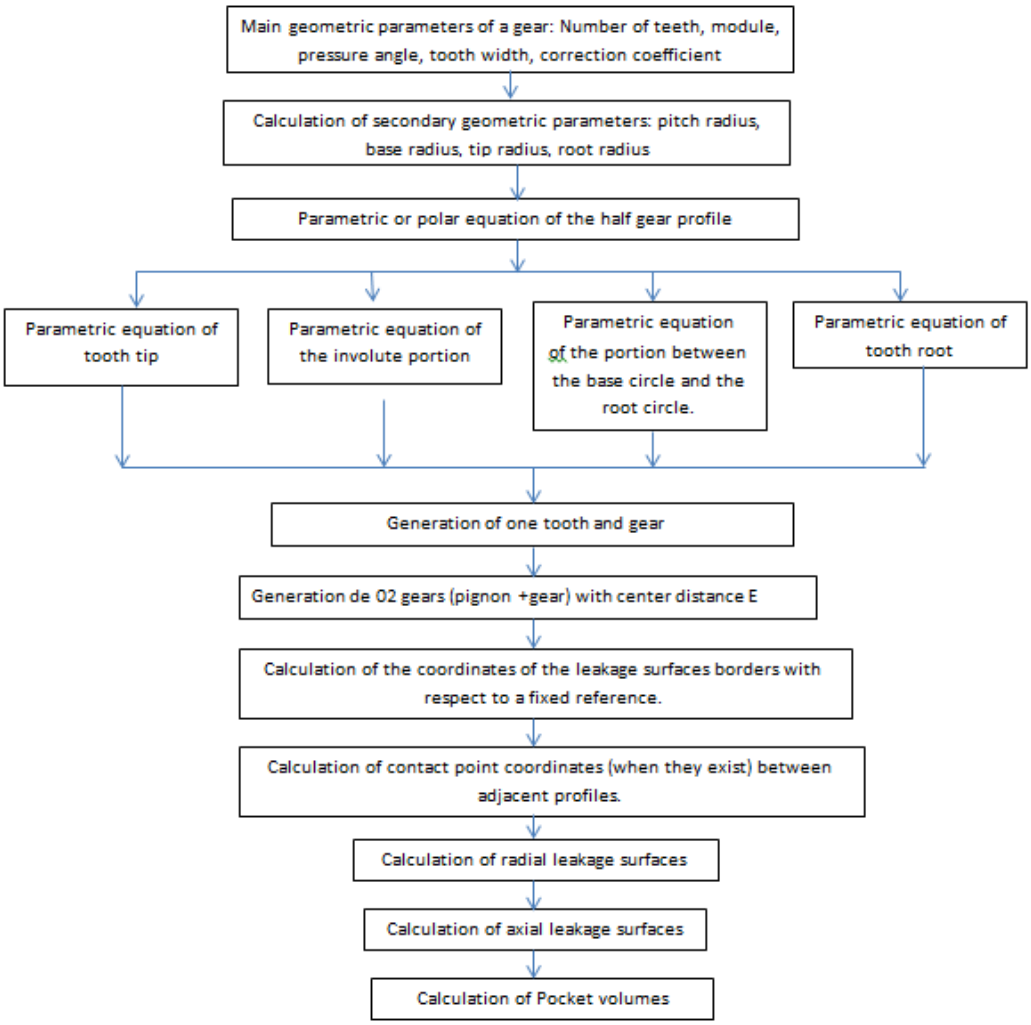

Figure 7: A calculation algorithm

c) Half Tooth Modeling

This modeling is carried out based on of the tooth profile shown in Figure 4.

1) *Tooth tip equation*

The tooth tip is a fraction of the tip circle (see figure 4). By applying the parametric equation of a circle with radius r_a (tip radius) centered in the point O_1, the parametric equation of the half of the geartooth tip is given in the coordinate system (o, x, y) by the relation (1) below:

$$\begin{cases} x(q) = r_a * \sin(q) \\ y(q) = r_a * \cos(q) \end{cases} \quad (1)$$

With $q_{min} \leq q \leq q_{max}$, q_{min} = mes ($\vec{\imath}$, $\overrightarrow{OA}$) and $q_{max} = \frac{\pi}{2}$

2) *Equations of the involute portion (AB)*

By applying the properties of the involute of the circle, the parametric equations of the portion (AB) in the fixed frame (O,x,y) are given by the relation (2) below:

$$\begin{cases} x(\theta) = -r_b\,(\sin(\theta) - \theta\cos(\theta)) \\ y(\theta) = r_b\,(\cos(\theta) + r_b\theta\sin(\theta)) \end{cases} \quad (2)$$

with $0 \leq \theta \leq [\frac{r_a^2}{r_b^2} - 1]^{1/2}$

3) *Equations of the portion between the base circle and the root circle*

On the figure 6,

$$0 \leq \zeta \leq \zeta_{max} \quad (3)$$

with $\zeta_{max} = \frac{\pi}{N} - \Omega_s$.

By application of the geometric construction properties (see[20]) ζ=arccos(2rb*rp/($rb^2 + rp^2$)).

In the cas of gears with pressure angle $\alpha = 20°$, when $\zeta_{max} \leq$ arccos(2rb*rp/ ($rb^2 + rp^2$)) then we take ζ=k*((π/N)-Ω_s); 0<k≤ 1.

In summary, in the portion between the base circle and the root circle 03 possible profiles shapes emerge depending on the number of teeth:

- If $r_b \leq r_p$: The circular portion does not exist. Our tooth will consist only of the involute part and the tooth top.
- If $r_b > r_p$: Two possibilities emerge.

- If arccos($2r_b{}^*r_p/(r_b{}^2 + r_p{}^2)$) ≤ ζ_{max} : In this case, this portion will consist of two (02) types of profiles, namely the arc of a circle BD followed by the root circle.
- If ζ_{max} <arccos($2r_b{}^*r_p/(r_b{}^2 + r_p{}^2)$): In this case, this portion is broken down into segment [BC] and arc of circle CD followed by the part of the root circle.

i. Case where arccos($2r_b{}^*r_p/(r_b{}^2 + r_p{}^2)$) ≤ ζ_{max}

Equation of segment [BC] in (o, x, y)

As a reminder, segment [BC] only exists when N<25 teeth. This segment equation requires knowledge of the coordinates of points B and C.

According to figure 5, the coordinates of point B are given by the relation (4) below:

$$\begin{cases} xB = rb\sin(\Omega_s) \\ yB = rb\cos(\Omega_s) \end{cases} \quad (4)$$

With $\Omega_s = \text{inv}(\alpha_0) + \beta_1$ and ξ=k*((π/N)-Ω_s); 0<k≤ 1

β_i is the angle between axis (O_1O_2) and (O_i, y_i) with axis (O_i, y_i) dividing the tooth of gear i in two equal parts.

$\beta_i = \frac{t_{si}}{2r_i}$ with $t_{si} = \frac{\pi m}{2}$ + 2*e*tan(α). t_{si}: tooth thickness at the standard pitch circle,

α: pressure angle, m: module, e: profile shift, -0.5≤e/m≤ 1.

The coordinates of point D are given by relation (5) below:

$$\begin{cases} xD = rp * \sin(\Omega_s + \zeta) \\ yD = rp * \cos(\Omega_s + \zeta) \end{cases} \quad (5)$$

Let K be the contact point between the tangent to $\overset{\frown}{CD}$ in D and the tangent to the involute in B. Then the coordinates of K are given by relation (6) below:

$$\begin{cases} xK = (rp * \tan(\Omega_s))/(\cos(\Omega_s + \zeta) + (\sin(\Omega_s + \zeta)) * \tan(\Omega_s)) \\ yk = xk/\tan(\Omega_s) \end{cases} \quad (6)$$

Let's posed1=sqrt(((xD-xk) ^ 2)+((yD-yk) ^ 2)) and d2=sqrt((xk) ^ 2 +(yk) ^ 2).

The coordinates of point C are given by relation (7) below:

$$\begin{cases} xC = (d1 + d2) * \sin(\Omega_s) \\ yC = (d1 + d2) * \cos(\Omega_s) \end{cases} \quad (7)$$

The following relation (8) is the parametric equation of the segment [BC] in (o, x, y):

$$\begin{cases} x = d \\ y = a * d \end{cases} \quad (8)$$

With xC ≤d ≤ xB et a=yB/xB = yC/xC;

The following relation (9) gives us the coordinates of the center of curvature E of the arc$\overset{\frown}{CD}$:

$$\begin{cases} xE = (rp + rc1) * \sin(\Omega_s + \zeta) \\ yE = (rp + rc1) * \cos(\Omega_s + \zeta) \end{cases} \quad (9)$$

With rc1=d1*tan((pi/4)+(ζ/2)). rc1 is the radius of curvature of the arc$\overset{\frown}{CD}$

Equation of arc $\overset{\frown}{CD}$ in the reference (o, x, y)

The Equation of the arc $\overset{\frown}{CD}$ in the reference (o, x, y) is given by the relation (10) below:

$$\begin{cases} x(q) = xE + rc1 * \sin(q) \\ y(q) = yE + rc1 * \cos(q) \end{cases} \quad (10)$$

With q_{min} ≤ q ≤ q_{max} , q_{min} = mes ($\vec{i}$, $\overrightarrow{EC}$) and q_{max} = mes ($\vec{i}$, $\overrightarrow{ED}$)

Equation of the circular portion between D and the tip circle in (o, x, y)

This portion is a fraction of the root circle. Its equation is given by relation (11) below:

$$\begin{cases} x(q) = rp * \sin(q) \\ y(q) = rp * \cos(q) \end{cases} \quad (11)$$

with qmin ≤ q ≤qmax; qmin = $\frac{\pi}{2}$ - $\frac{\pi}{N}$ and qmax= mes ($\vec{i}$, $\overrightarrow{OD}$)

ii. Case where arccos(2rb*rp/($rb^2 + rp^2$)) ≤ ζ_{max} : the segment [BC] does not exist

In this case, the center of curvature is given by the relation (12) below:

$$\begin{cases} xE = rb * \tan(\Omega_s + \zeta)/(\cos((\Omega_s) + \sin(\Omega_s) * \tan(\Omega_s + \zeta)) \\ yE = rb/(\cos((\Omega_s) + \sin(\Omega_s) * \tan(\Omega_s + \zeta)) \end{cases} \quad (12)$$

Where ζ=arccos(2rb*rp/($rb^2 + rp^2$))

The equation of the arc $\overset{\frown}{CD}$ in the reference (o, x, y) is given by the relation (10) below, with the curvature radius rc1 = ED=EB.

d) Gear Generating

For the generation of a complete gear wheel, the following methodology has been adopted:

- Codification on Matlab of the equations developed above (half of a tooth).
- Application of symmetry with respect to (O, $\vec{j}$) to get a whole tooth.
- Generating of N-1 others teeth by N-1 successive rotations of the initial tooth of respective angles (2*π/N)*i, with 1≤ i ≤N-1.

e) Calculation of Radial and Axial Leakage Surfaces

i. *Calculation of the border points coordinates at a given position (see figures 5 and 6).*

At a rotation angle ϕ_i around O_i with respect to the initial position, the coordinates of points A1, A1', E1, E1', B1, and B1' (see figures 5 and 6) in (O_f,x_f,y_f) are given by equations below:

The coordinates of the tooth tip corner of gear in (O_f, x_f, y_f) are given by relations (14) and (15) below:

$$\begin{cases} xA_1 = \text{ra2} * \sin(\text{inv}(\phi_{ra2}) - \text{inv}(\alpha_0) + \phi_2) \\ yA_1 = \text{E} - \text{ra2} * \cos(\text{inv}(\phi_{ra2}) - \text{inv}(\alpha_0) + \phi_2) \end{cases} \quad (13)$$

with ϕ_{rai} = arccos(rbi/rai), i=1,2 and $\text{inv}(\alpha_0)$ =tan(α_0) - α_0

$$\begin{cases} xA_1' = \text{ra2} * \sin(-\text{inv}(\phi_{ra2}) + \text{inv}(\alpha_0) + 2 * \beta_2 + \phi_2) \\ yA_1' = \text{E} - \text{ra2} * \cos(-\text{inv}(\phi_{ra2}) + \text{inv}(\alpha_0) + 2 * \beta_2 + \phi_2) \end{cases} \quad (14)$$

With ϕ_{rai} =arccos(rbi/rai), i=1,2

Equations (16) and (17) below are the coordinates of the pinion tooth tip corner in (O_f, x_f, y_f)

$$\begin{cases} xE_1 = \text{ra1} * \sin(-\text{inv}(\phi_{ra1}) + \text{inv}(\alpha_0) - 2\theta_{ra1} - \phi_1) \\ yE_1 = \text{ra1} * \cos(-\text{inv}(\phi_{ra1}) + \text{inv}(\alpha_0) - 2\theta_{ra1} - \phi_1) \end{cases} \quad (15)$$

θ_{rai} =β_i + $\text{inv}(\alpha_0)$- $\text{inv}(\phi_{rai})$, i=1,2

$$\begin{cases} xE_1' = \text{ra1} * \sin(-\text{inv}(\phi_{ra1}) + \text{inv}(\alpha_0) - \phi_1) \\ yE_1' = \text{ra1} * \sin(-\text{inv}(\phi_{ra1}) + \text{inv}(\alpha_0) - \phi_1) \end{cases} \quad (16)$$

θ_{rai} =β_i + $\text{inv}(\alpha_0)$- $\text{inv}(\phi_{rai})$, i=1,2

The coordinates of B'_1 and B_2 in (Of, xf, yf) are given by relations (18) and (19) below:

$$\begin{cases} xB'_1 = \text{rb1} * \sin(\Omega_s + \beta_1 + \phi_1) \\ yB'_1 = \text{rb1} * \cos(\Omega_s + \beta_1 + \phi_1) \end{cases} \quad (17)$$

$$\begin{cases} xB_2 = \text{rb2} * \sin(-inv(\alpha_0) + \pi - 2\beta_2 - \phi_2) \\ yB_2 = \text{E} + \text{rb2} * \cos(-inv(\alpha_0) + \pi - 2\beta_2 - \phi_2) \end{cases} \quad (18)$$

When $r_b \leq r_p$, the Coordinates of the contact points between the tooth profile and the root circle are given by the equation (19) below:

$$\begin{cases} xp_1 = \text{rp1} * \sin(\Omega_s - \tan(\text{ay}) + \text{ay} - \beta_1 - \phi_1) \\ yp_1 = \text{rp1} * \cos(\Omega_s - \tan(\text{ay}) + \text{ay} - \beta_1 - \phi_1) \end{cases} \quad (19)$$

With ay=Arccos(rb1/rp1);

Coordinates of contacts points (C_1 and C_2 of the pinion and gear (see figure 5).

Existence condition of C_1 and C_2

C_1 exists if and only if:

$$\tan(\alpha_0) - \sqrt{(\frac{r_{a1}}{r_{b1}})^2 - 1} \leq \phi_1 \leq -\frac{r_{s2}}{r_{s1}}(\tan(\alpha_0) - \sqrt{(\frac{r_{a2}}{r_{b2}})^2 - 1}) \quad (20)$$

In this case, the radial surface 1 is zero: $S_{r1} = 0$

C_2 exists if and only if:

$$(-\frac{r_{s2}}{r_{s1}})(-\tan(\alpha_0) - 2\beta_2 + \sqrt{(\frac{r_{a2}}{r_{b2}})^2 - 1}) \leq \phi_1 \leq -\tan(\alpha_0) + 2\beta_1 + \sqrt{(\frac{r_{a1}}{r_{b1}})^2 - 1} \quad (21)$$

In this case, the radial distance 2 is zero: $S_{r2} = 0$.

At the initial condition, C_1 is confused with I.

By applying the line of contact between the two conjugate surfaces, we obtain the coordinates of points C_i rotation angle ϕ_i around O_i with respect to the initial position in (O_f, x_f, y_f):

Then the coordinates of C_1 in (O_f, x_f, y_f) are given by the relation (22) below:

$$\begin{cases} xC_1 = \text{rb1} * (\sqrt{1 + {\theta_{C1}}^2}) \sin(\text{Arctan}(\theta_{C1}) - \theta_{C1} + \text{inv}(\alpha_0) - \phi_1) \\ yC_1 = \text{rb1} * (\sqrt{1 + {\theta_{C1}}^2}) \cos(\text{Arctan}(\theta_{C1}) - \theta_{C1} + \text{inv}(\alpha_0) - \phi_1) \end{cases} \quad (22)$$

with θ_{C1}=tan(α_0)-ϕ_1;

The coordinates of C_2 in (O_f, x_f, y_f) are given by the relation (23) below:

$$\begin{cases} xC_2 = \text{rb1} * (\sqrt{1+\theta_{C2}{}^2}) \sin(-\text{Arctan}(\theta_{C2}) + \theta_{C2} - \text{inv}(\alpha_0) + 2\beta_1 - \phi_1) \\ yC_2 = \text{rb1} * (\sqrt{1+\theta_{C2}{}^2}) \cos(-\text{Arctan}(\theta_{C2}) + \theta_{C2} - \text{inv}(\alpha_0) + 2\beta_1 - \phi_1) \end{cases} \quad (23)$$

with θ_{C2}=tan(α_0)- $2\beta_1+\phi_1$;

In (O_p, x_p, y_p), the coordinates of C_1 are given by the relation (24) below:

$$\begin{cases} xC_1 = \text{rb2} * (\sqrt{1+\theta'_{C1}{}^2}) \sin(\text{Arctan}(\theta'_{C1}) - \theta'_{C1} + \text{inv}(\alpha_0) - \pi - \phi_2) \\ yC_1 = \text{rb2} * (\sqrt{1+\theta'_{C1}{}^2}) \cos(\text{Arctan}(\theta'_{C1}) - \theta'_{C1} + \text{inv}(\alpha_0) - \pi - \phi_2) \end{cases} \quad (24)$$

with θ'_{C1}=tan(α_0)-ϕ_2;

In (Op, xp, yp), the coordinates of C_2 are given by the relation (25) below:

$$\begin{cases} xC_2 = \text{rb2} * (\sqrt{1+\theta'_{C2}{}^2}) \sin(-\text{Arctan}(\theta'_{C2}) + \theta'_{C2} - \text{inv}(\alpha_0) + \pi - 2\beta_2 - \phi_2) \\ yC_2 = \text{rb2} * (\sqrt{1+\theta'_{C2}{}^2}) \cos(-\text{Arctan}(\theta'_{C2}) + \theta'_{C2} - \text{inv}(\alpha_0) + \pi - 2\beta_2 - \phi_2) \end{cases} \quad (25)$$

with θ'_{C2}=tan(α_0)+ $2\beta_2+\phi_2$;

$$O_1C_2 = \text{rb1} * (\sqrt{1+\theta_{C2}{}^2});\ O_2C_2 = \text{rb2} * (\sqrt{1+\theta'_{C2}{}^2}),\ O_1C_1 = \text{rb1} * (\sqrt{1+\theta_{C1}{}^2});\quad O_2C_1 = \text{rb2} * (\sqrt{1+\theta'_{C1}{}^2})$$

ii. *Calculation of Radial Leakage Surfaces*

The radial leakage surfaces vary in function of the rotation angle of gear. For the calculation of the radial leakage surfaces we will distinguish 05 possibilities:

- When C_1 and C_2 exists, i.e., when the profiles touch each other simultaneously. In this case the surfaces S_{r1} and S_{r2} are simultaneously zero.
- When we are at the left of the initial position, and only C_2 exists (S_{r1}>0 and S_{r2}=0),
- When we are at the left of the initial position with C_1 and C_2 does not exist (S_{r1}>0 and S_{r2}>0),
- When we are at the right of the initial position and only C_2 exists (S_{r1}=0 and S_{r2}>0),
- When we are at the right of the initial position with C_1 and C_2 does not exist (S_{r1}>0 and S_{r2}>0),

The relations below give the expressions of the radial leakage surfaces in each of these cases cited above.

At the right of the initial position

- Case where S_{r1} =0 and S_{r2}> 0:

$$(\tan(\alpha_0) - \sqrt{(\frac{r_{a1}}{r_{b1}})^2 - 1} < \phi_1 < (-\frac{r_{s2}}{r_{s1}})(-\tan(\alpha_0) - 2\beta_2 + \sqrt{(\frac{r_{a2}}{r_{b2}})^2 - 1}))$$

According to figure 5,

$$S_{r2} = b * A_2G_1 \quad (26)$$

where b is the face of the tooth width.

$$A_2G_1 = A_2T_1 - G_1T_1 \quad (27)$$

with $A_2T_1 = \sqrt{O_1A_2{}^2 - rb_1{}^2}$, $G_1T_1 = rb_1\theta_1$,

$$\theta_1 = \text{mes}(\overrightarrow{O_1A_2}, \overrightarrow{O_1T_1}) - \text{mes}(\overrightarrow{O_1A_2}, \overrightarrow{O_1B'_1}) \text{ and } \text{mes}(\overrightarrow{O_1A_2}, \overrightarrow{O_1T_1}) = \arccos(\frac{rb_1}{O_1A_2})$$

$$\text{mes}(\overrightarrow{O_1A_2}, \overrightarrow{O_1B'_1}) = \text{mes}(\vec{i}, \overrightarrow{O_1A_2}) - \text{mes}(\vec{i}, \overrightarrow{O_1B'_1}) \quad (28)$$

with $\text{mes}(\vec{i}, \overrightarrow{O_1A_2}) = \arccos(((xA_2\text{-}0)(1\text{-}0))/O_1A_2)$ and $\text{mes}(\vec{i}, \overrightarrow{O_1B'_1}) = \arccos(((xB'_1\text{-}0)(1\text{-}0))/O_1B'_1)$.

- Case where $S_{r1}>0$ and $S_{r2}>0$: ($\phi_1 < \tan(\alpha_0)-\sqrt{(\frac{r_{a1}}{r_{b1}})^2-1}$)

According to figure 6,

$$S_{r1} = b * E_2G_2 \quad (29)$$

$$E_2G_2 = E_2T_2 - G_2T_2 \quad (30)$$

$$E_2T_2=\sqrt{{O_2E_2}^2-{rb_2}^2}\ , G_2T_2=rb_2\theta_2,\ \theta_2=\text{mes}(\overrightarrow{O_2E_2},\overrightarrow{O_2T_2}) - \text{mes}(\overrightarrow{O_2E_2},\overrightarrow{O_2J_2})$$

with $\text{mes}(\overrightarrow{O_2E_2},\overrightarrow{O_2T_2}) = \text{Arccos}(\frac{rb_2}{O_2E_2})$.

$$\text{mes}(\overrightarrow{O_2E_2},\overrightarrow{O_2J_2}) = \text{mes}(\vec{\imath}, \overrightarrow{O_2E_2}) - \text{mes}(\vec{\imath}, \overrightarrow{O_2J_2}) \quad (31)$$

$\text{mes}(\vec{\imath}, \overrightarrow{O_2E_2})$= arccos(((x$E_2$-0)(1-0))/ O_2E_2) and $\text{mes}(\vec{\imath}, \overrightarrow{O_2J_2})$= arccos(((x$J_2$-0)(1-0)) /$O_2J_2$) Sr1 is given by the relation (27)

At the left of the initial position

- Case where $S_{r1}>0$ and $S_{r2}=0$:

$$(\ (-\tan(\alpha_0) + 2\beta_1 + \sqrt{(\frac{r_{a1}}{r_{b1}})^2-1}\ ) > \phi_1 > -\frac{r_{s2}}{r_{s1}}(\tan(\alpha_0)-\sqrt{(\frac{r_{a2}}{r_{b2}})^2-1}\ )))$$

Like the previous cases,

$$S_{r1} = b * {A'}_2{G'}_1 \quad (32)$$

$${A'}_2{G'}_1={A'}_2{T'}_1-{G'}_1{T'}_1 \quad (33)$$

with ${A'}_2{T'}_1=\sqrt{{O_1{A'}_2}^2-{rb_1}^2}$, ${G'}_1{T'}_1=rb_1\theta'_1$, $\theta'_1=\text{mes}(\overrightarrow{O_1{A'}_2},\overrightarrow{O_1{T'}_1}) - \text{mes}(\overrightarrow{O_1{A'}_2},\overrightarrow{O_1{J'}_1})$ and $\text{mes}(\overrightarrow{O_1{A'}_2},\overrightarrow{O_1{T'}_1}) = \text{arccos}(\frac{rb_1}{O_1{A'}_2})$

$$\text{mes}(\overrightarrow{O_1{A'}_2},\overrightarrow{O_1{J'}_1}) = \text{mes}(\vec{\imath}, \overrightarrow{O_1{A'}_2}) - \text{mes}(\vec{\imath}, \overrightarrow{O_1{J'}_1}) \quad (34)$$

$\text{mes}(\vec{\imath}, \overrightarrow{O_1{A'}_2})$ =arccos(((x${A'}_2$-0)(1-0))/$O_1{A'}_2$) and $\text{mes}(\vec{\imath}, \overrightarrow{O_1{J'}_1})$=arccos(((x${J'}_1$-0)(1-0))/$O_1{J'}_1$)

- Case where $S_{r1}>0$ and $S_{r2}>0$ ($\phi_1 > -\tan(\alpha_0) + 2\beta_1 + \sqrt{(\frac{r_{a1}}{r_{b1}})^2-1}$)

$$S_{r2} = b * {E'}_2{G'}_2 \quad (35)$$

with ${E'}_2{G'}_2 = {E'}_2{T'}_2 - {G'}_2{T'}_2$, ${E'}_2{T'}_2=\sqrt{{O_2{E'}_2}^2-{rb_2}^2}$, ${G'}_2{T'}_2=rb_2\theta_2$ and

$\theta'_2=\text{mes}(\overrightarrow{O_2E'_2},\overrightarrow{O_2T'_2}) - \text{mes}(\overrightarrow{O_2E'_2},\overrightarrow{O_2J'_2})$, $\text{mes}(\overrightarrow{O_2E'_2},\overrightarrow{O_2T'_2}) = \text{arccos}(\frac{rb_2}{O_2E'_2})$

$$\text{mes}(\overrightarrow{O_2E'_2},\overrightarrow{O_2J'_2})=\text{mes}(\vec{\imath},\overrightarrow{O_2E'_2}) - \text{mes}(\vec{\imath},\overrightarrow{O_2J'_2}) \quad (36)$$

$\text{mes}(\vec{\imath},\overrightarrow{O_2E'_2})$=arccos(((x${E'}_2$-0)(1-0))/$O_2E'_2$) and $\text{mes}(\vec{\imath}, \overrightarrow{O_2J'_2})$= Arccos(((x${J'}_2$-0)(1-0)) /$O_2J'_2$) Sr1 is given by relation (33)

iii. *Calculation of Axial Leakage Surfaces*

Case where $S_{r1}=0$ and $S_{r2}=0$:

$$((-\frac{r_{s2}}{r_{s1}})(-\tan(\alpha_0) - 2\beta_2 + \sqrt{(\frac{r_{a2}}{r_{b2}})^2-1}\ ) \le \phi_1 \le -\frac{r_{s2}}{r_{s1}}(\tan(\alpha_0)-\sqrt{(\frac{r_{a2}}{r_{b2}})^2-1}\ ))$$

- Case where $r_p < r_b$

According to figure 5 and figure 6:

$$\text{Surface axiale}= SC_1B_1{B'}_1C_2A_1{A'}_1C_1 = SO_1C_1A_1{A'}_1C_2O_1 - SO_1C_1B_1{B'}_1C_2O_1 \quad (37)$$

$$S O_1 C_1 A_1 A'_1 C_2 O_1 = \text{triangle}\_O_1 C_2 O_2 O_1 - \text{triangle}\_O_1 C_1 O_2 O_1 - S O_2 C_2 A_1 A'_1 C_1 O_2 \quad (38)$$

Avec triangle$_O_1 C_2 O_2 O_1$ =0.5$O_1 C_2$*E*sin(θ_{C2})et triangle$_O_1 C_1 O_2 O_1$ =0.5*$O_1 C_1$*E*sin(θ_{C1})

$$S O_2 C_2 A_1 A'_1 C_1 O_2 = S O_2 C_2 A'_1 O_2 + S O_2 C_2 A'_1 A_1 O_2 + S O_2 A_1 C_1 O_2 \quad (39)$$

$S O_2 C_2 A'_1 A_1 O_2$ =0.5*r_{a2}^2*(2*θ_{ra2}),$S O_2 A_1 C_1 O_2$ =0.5*r_{b2}^2(($\sqrt{(\frac{r_{a2}}{r_{b2}})^2 - 1}$)^3-$\theta_{C2}{}^3$)/3

and $S O_2 C_2 A'_1 O_2$ =0.5*r_{b2}^2*(($\sqrt{(\frac{r_{a2}}{r_{b2}})^2 - 1}$)^3-$\theta'_{C2}{}^3$)/3

$$S O_1 C_1 B_1 B'_1 C_2 O_1 = S O_1 C_1 B_1 O_1 + S O_1 B_1 B'_1 O_1 + S O_1 B'_1 C_2 O_1 \quad (40)$$

with $S O_1 C_1 B_1 O_1$ =0.5*$\mathrm{rb1}^2$*($\theta_{C1}{}^3$)/3,

$$S O_1 B_1 B'_1 O_1 = (\mathrm{rc1} + \mathrm{rp1}) * \mathrm{o1c} * \sin(\zeta) - \mathrm{rc1}^2 * (\mathrm{qmax} - \mathrm{qmin}) + \mathrm{rp1}^2 * (\mathrm{q2max} - \mathrm{q2min})$$

$$O_1 c = \sqrt{(x_c - 0)^2 + (y_c)^2}$$

$$\mathrm{q2max} = (\pi/2) - (\zeta + \Omega_s) \text{ and } \mathrm{q2min} = (\pi/2) - (\pi/N1)$$

$$\mathrm{qmin} = \mathrm{Arccos}((1*(x_B - x_E) + 0*(y_B - y_E))/EB) \text{ and } \mathrm{qmax} = \mathrm{qmin} + \mathrm{acos}(((x_C - x_E)*(x_D - x_E) + (y_C - y_E)*(y_D - y_E))/\mathrm{rc1}^2)$$

$$S O_1 B'_1 C_2 O_1 = 0.5 * \mathrm{rb1}^2 * (\theta_{C2}{}^3)/3.$$

- Case where $r_p \geq r_b$

According to figures 5 and 6

$$\text{Surface axiale} = S C_1 p_1 p_1{}' C_2 A_1 A'_1 C_1 = S O_1 C_1 A_1 A'_1 C_2 O_1 - S O_1 C_1 p_1 p_1{}' C_2 O_1 \quad (41)$$

$$S O_1 C_1 p_1 p_1{}' C_2 O_1 = S O_1 p_1{}' C_2 O_1 + S O_1 p_1 p_1{}' O_1 + S O_1 C_1 p_1 O_1 \quad (42)$$

with $S O_1 p_1{}' C_2 O_1$ =0.5*$\mathrm{rb1}^2$*(($\theta_{C2}{}^3$) -$\theta_{\mathrm{rp1}}{}^3$)/3,$S O_1 p_1 p_1{}' O_1$ =$\mathrm{rp1}^2$*(q3max-q2min)) and q3max=Arctan(yp1/xp1)

$S O_1 C_1 p_1 O_1$ =0.5*$\mathrm{rp1}^2$*($\theta_{C1}{}^3$-$\theta_{\mathrm{rp1}}{}^3$)/3 with $\theta_{\mathrm{rp1}} = \sqrt{(\frac{r_{p1}}{r_{b1}})^2 - 1}$

IV. Results

a) Simulation Results for the Modeling of a Gear

By applying the equations (1) to (13), we obtain 03 types tooth profile:

- The profile made up of the gear tip, the involute part, a line segment, a circular part, and the tooth root ($r_p < r_b$ and arccos($2r_b * r_p/(r_b{}^2 + r_p{}^2)$)> ζ_{max}).
- The profile made up of the gear tip, the involute part, a circular portion, and the tooth root ($r_p < r_b$ and arccos($2r_b * r_p/(r_b{}^2 + r_p{}^2)$) ≤ ζ_{max}).
- The profile made up of the gear tip and the involute part. Here the involute part is limited at root circle ($r_b \leq r_p$).

For the application, we have chosen 03 types of gears whose respective parameters are recorded in table 1 below.

Table 1: Parameters of 03 gears used for simulation

	Number of teeth	m(module)	α(pressure angle)	x(shift coefficeint)	b(mm)
Gear 1	20	10	20°	0	100
Gear 2	40	10	20°	-0.2	100
Gear 3	76	4	20°	0	100

Figure 8 below is a detailed view of the half of the tooth profile taken from the simulation result for the specific case of gear 1 in table 1.

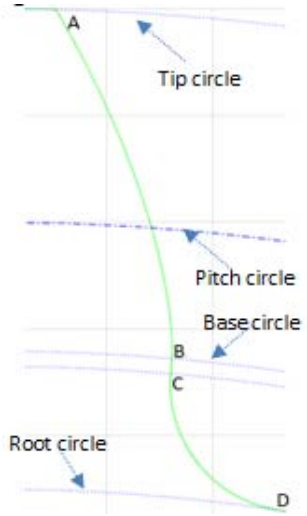

Figure 8: Detailed view of the half of tooth profile of gear 1 of table 1. Here =93,9693mm; =89,5mm

The particularity here is the presence of a straight part on our teeth, namely the segment [BC].

Figure 9 below is a detailed view of the half of the tooth profile taken from the simulation result for the specific case of gear 2 in table 1.

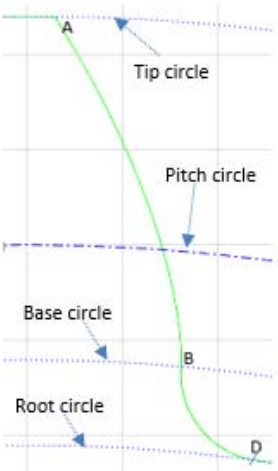

Figure 9: Detailed view of the half of the tooth of gear 2 in table 1. Here, =187.9385 mm; =185.5 mm

The profile is made up of the tooth top, the involute part, the circular part, and tooth root. Here, the straight part no longer exists.

A detailed view of the half of the tooth profile resulting from the simulation result for the particular case of gear 3 of table 1 is represented in figure 10 below.

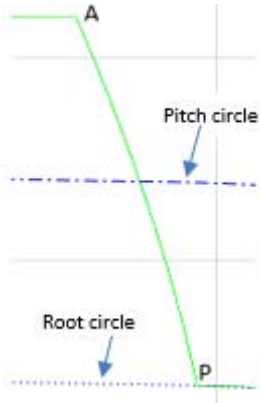

Figure 10: Detailed view of the half of the tooth in gear 3 of table 1. Here=142.8333 mm; = 147 mm

In this particular case, the root radius is greater than the base radius and the tooth profile consists only of the involute part and top part.

b) Results of Calculations of Radial and Axial Leakage Surfaces

To validate our model, the simulation of our equations and formulas developed above (equations (13) to (42)) on Matlab 16 was carried out with the particular case of a gear whose characteristics are grouped in table 2 below.

Table 2: Parameters of the gear used for the simulation

	Number of teeth	m(module)	α(pressure angle)	x(shift coefficient)	b(mm)
pinion	76	4	20°	0	100
gear	76	4	20°	0	100

The application of our model for calculating of the radial leakage surfaces 1 and 2 relative to the gear of table 2 has generated the curves of figure 11 below. This figure gives the evolution of the radial leakage surfaces (S_{r1} and S_{r2}) as a function of the rotation angle of the drive gear on the interval [-13°, 13°].

NB: To facilitate the comparative study with other models, during the simulation, we brought back the initial position at the position where (O_1O_2) passes simultaneously through the middles of the gear tip tooth and the pinion root. That is after rotating the driver gear of β_1 on counterclockwise direction.

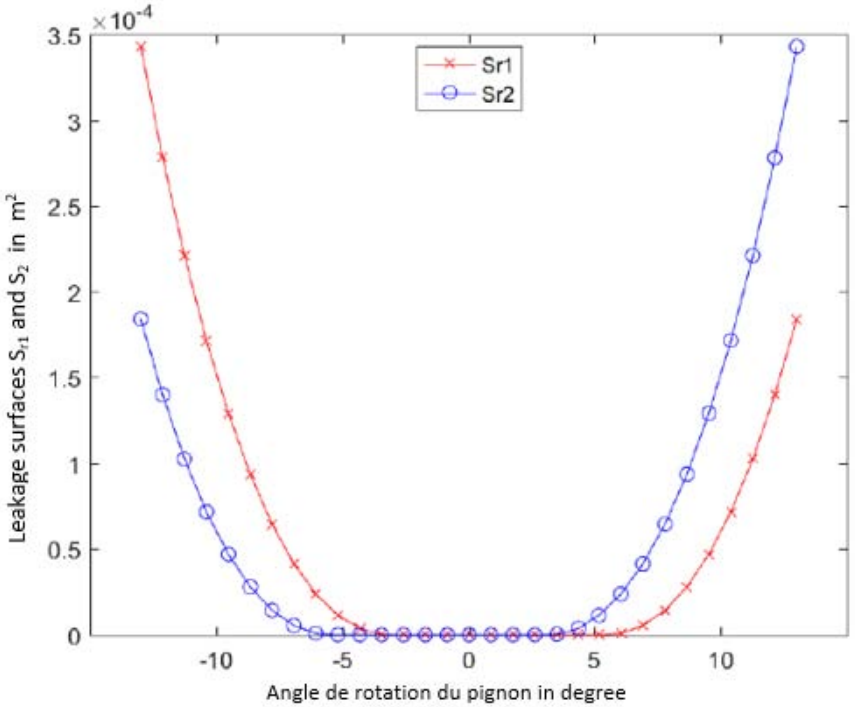

Figure 11: Evolution of the radial leakage surfaces 1 and 2 as a function of the angle of rotation of the driver gear. Case of the gearing system of table 2

The result of our model for calculating the pockets volumes corresponding to the gearing system of table 2 has generated the curve of figure 12 below. This figure gives the evolution of the pockets volumes (axial leakage surface multiplied by the tooth width) as a function of the angle of rotation of the driver gear on the interval [-13°,13°].

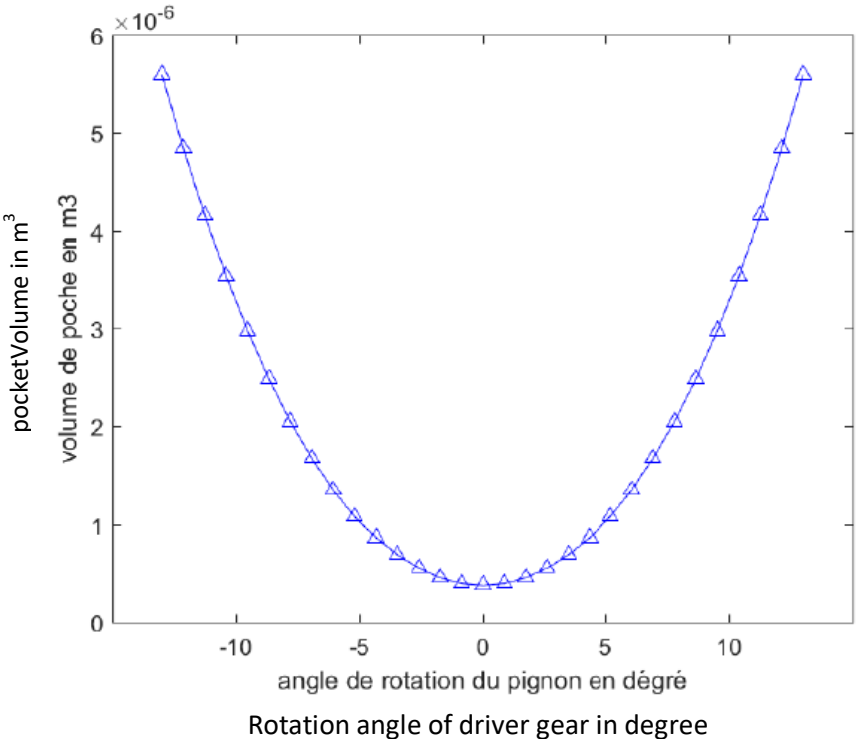

Figure 12: Radial leakage volume corresponding to the parameters in table 2

c) *Results Interpretation*

The curves of Figure 11 justify the similarity of the radial and axial leakage surfaces on each side of the initial position ($\phi_1 = 0$). This result agrees with the surfaces evolution of figure 2. we observe that On figures 2.a) to 2.h) the axial surface reaches its minimum at the initial position ($\phi_1 = 0$). This observation agrees with the curve of figure 12.

More we move away from the initial position ($\phi_1 = 0$), the pockets volumes increase. This result agrees with the observation of figures 2.a) to 2.h).

The curves in figure 11 show that at the left of the initial position, the radial leakage surface one is always greater than the radial leakage surface two and, at the right of the initial position, it is the opposite phenomenon. This result agrees with the observations of figure 2.

In figure 11, the two profiles bordering the radial surface 1 (S_{r1}) meet when ϕ_1 belongs in the interval [-3,75°; 6,5°]. For the radial surface 2 (S_{r1}), this phenomenon occurs in the interval [-6,5°; 3,75°].

V. Model Validation

The validation of our model follows from a comparative study between the results of our model and the results of Abdelilah Lasri and al [13] and Diab Y. and al [10] for the same gear system. We have superimposed the curves of our model and those of the reference models.

a) *Superposition of the Radial Surfaces Curves of our Model and those Resulting from the Model of Abdelilah Lasri [13]*

Figure 13 below is the result of the superposition of the radial leakage surfaces (Sr1 and Sr2). In this figure, the leakage surfaces curves of our model are in blue colour and the curves of Abdelilah Lasri's model [13] are in red.

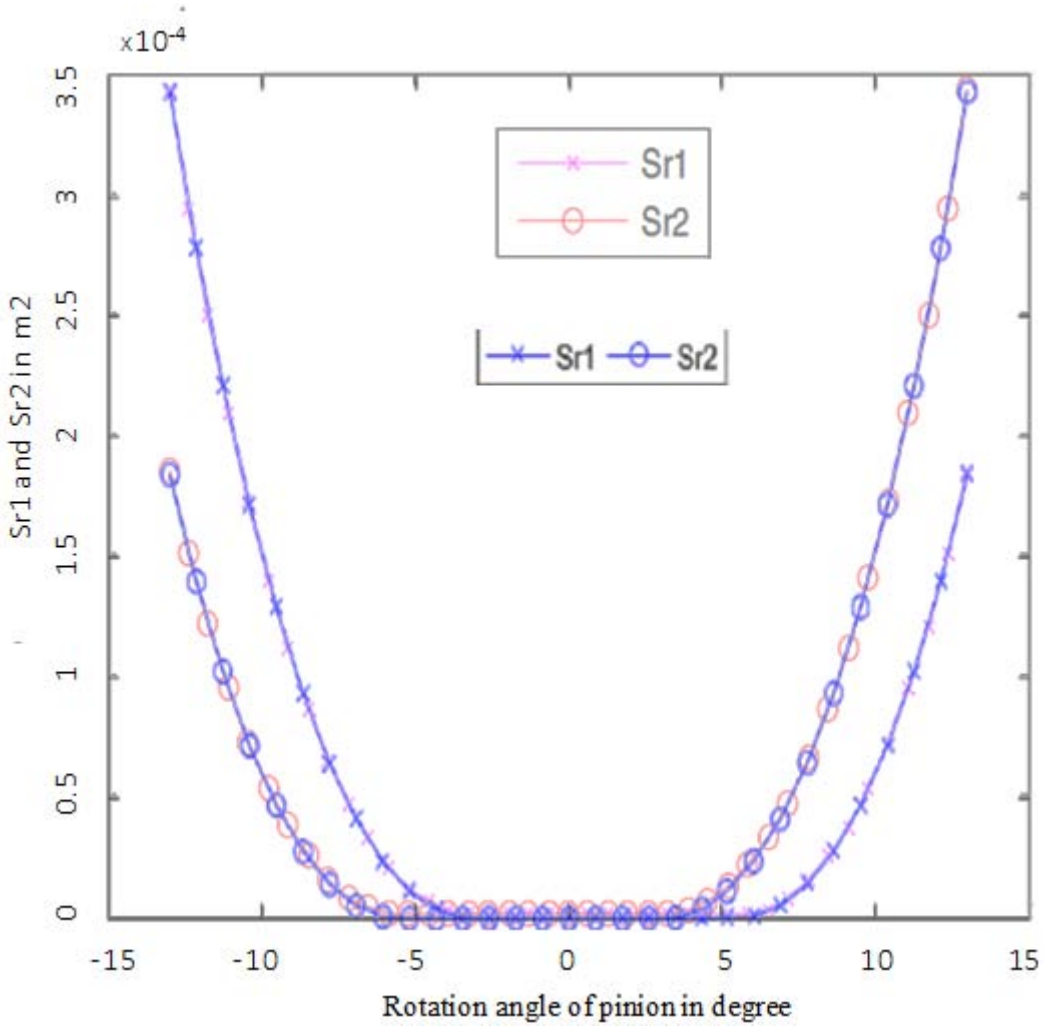

Figure 13: Superposition of radial leakage surfaces from our model (in blue) and those from Abdelilah Lasri's model [13] (in red color)

Looking at Figure 13, the radial leakage surfaces of our model and the reference model are merged. The relative deviations between the values from these two (02) models are of the order of 10^{-2}.

b) Superposition of Pocket Volume Curves from our Model and those from the Diab's Model [10]

Figure 14 below is the result of the superposition of pocket volumes. On this figure, the curve of pocket volumes from our modelis blue and the Diab's model curve [10] is black.

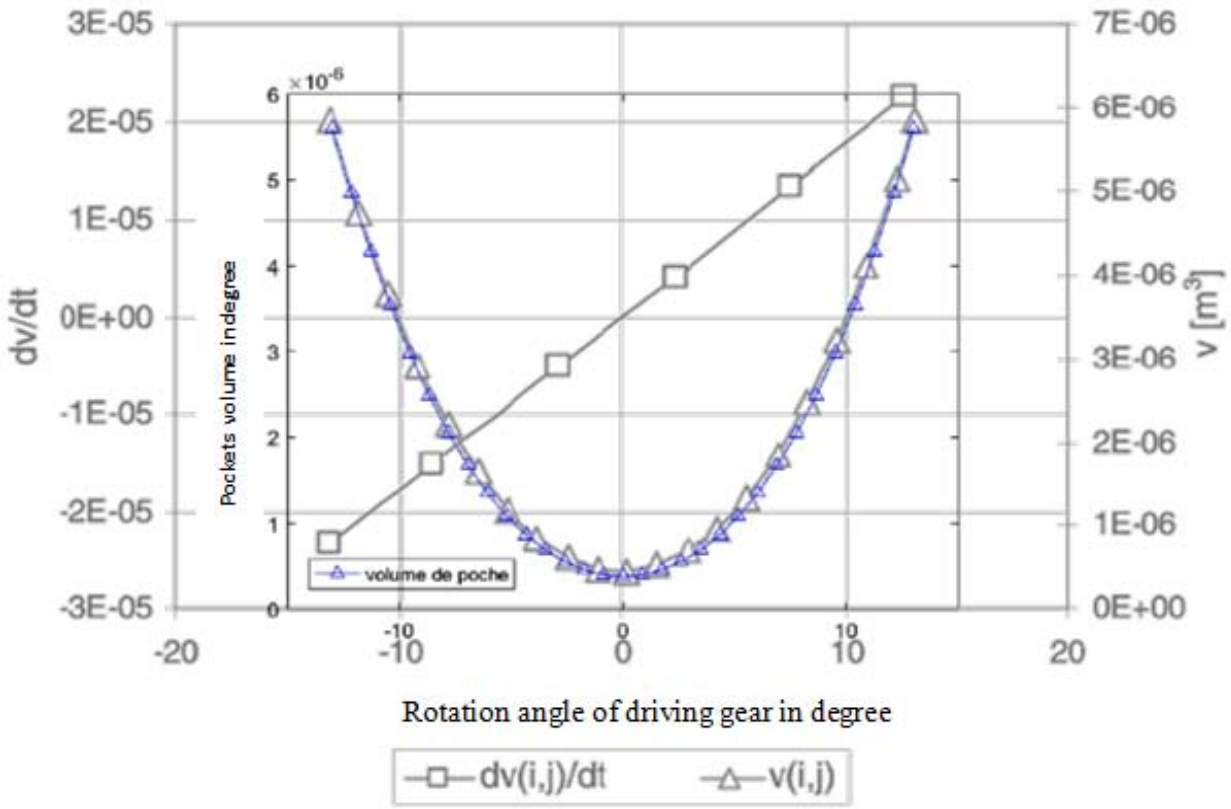

Figure 14: Superposition of pocket volumes from our model (in blue) and those from Y. Diab's[10] model (in black)

On figure 14, the two curves are almost merged. In the neighbourhood of the initial position, there is a minimal difference between the 02 curves. Outside the interval [-10°; -10°] the two curves are identical. The relative deviations between the values from the 02 curves, is at the order of 10^{-2}.

The curves of the figures 13 and 14 and the relative deviations between the results from our model and the reference models allow us to state with certainty that the model developed in this work is valid and meets our set objectives. The model developed in this work allows us to calculate the exact values of the axial and radial leakage surfaces of the lubricant in a gear.

VI. Conclusion

A better optimization of the power losses by the lubricant trapping in the inter-tooth space requires a preliminary work of total lifting of the veil on the gear inter-tooth space during the movement. In this perspective, we have established a purely analytical model allowing to accurately evaluating the radial and axial leakage surfaces of the lubricant in the inter-tooth space of external spur gears.

This model was developed based on the parametric equations of a tooth profile and the exploitation of the involute properties, followed by the surface integrations delimited by the contour representing their exact boundary. The results are presented as curves of the evolution of the leakage surfaces (radial and axial) as a function of the driving gear's rotation angle. The curve of the evolution of the axial leakage surfaces as a function of the rotation angle is a symmetrical parabola, and the two curves of the evolution of the radial leakage surfaces are symmetrical (relative to each other). These results agree with the observation of the lubricant behavior in the inter-tooth space during gear movement. Far from numerical approximations, this model is an analytical formula allowing us to evaluate the exact leakage surfaces directly, according to the geometrical parameters of the gears.

References Références Referencias

1. Devin R. and Hilty B. S., “An experimental investigation of spin power losses of planetary gear sets,” Thesis for the degree Master of Science, The Ohio State University, 2010.

2. Anderson N. E., Loewenthal S. H. and Black J. D., "An Analytical Method To Predict Efficiency of Aircraft Gearboxes," [en ligne]. NASA Technical Memorandum 83716, 1984. Disponible sur:<http://ntrs.nasa.gov/archive/nasa/casi.ntrs.nasa.gov/19840017538_1984017538.pdf>.
3. Krantz T. L., "Experimental and analytical evaluation of efficiency of helicopter planetary stage," [en ligne]. NASA Technical paper 3063, 1990. Disponible sur: <http://ntrs.nasa.gov/archive/nasa/casi.ntrs.nasa.gov/19910003643_1991003643.pdf>.
4. Rohn D. A. and Handschuch R. F., "Efficiency testing of a helicopter transmission planetary reduction stage," [en ligne]. NASA Technical Paper 2795, 1988. Disponible sur: <http://ntrs.nasa.gov/archive/nasa/casi.ntrs.nasa.gov/19880005842_1988005842.pdf>.
5. Terekhov AS, '' Hydraulic losses in gearboxes with oil immersion.'', Russ Eng J 55:7–11, 1975.
6. Mauz W., "Hydraulische Verluste von Stirnradgetriebebei Umfangsgeschwindigkeitbis 60m/s," PhD Dissertation: IMK University of Stuttgart, 209 p., 1987.
7. Butsch M., "Hydraulischeverlusteschnell-laufenderstirnradgetriebe," PhD Dissertation: IMK University of Stuttgart, 157 p., 1989.
8. Maurer J, ''LastunabhängigeVerzahnungsverlusteschnellaufenderStirnradgetriebe.''; 1994, Universität Stuttgart, Stuttgart.
9. Pechersky, M. J., and Wittbrodt, M. J., "An Analysis of Fluid Flow Between Meshing Spur Gear Teeth," Proceedings of the ASME Fifth International Power Transmission and Gearing Conference, Chicago, IL, p. 335–342, 1989.
10. Diab, Y., Ville, F., Houjoh, H., Sainsot, P. and Velex, P., 2005, "Experimental and Numerical Investigations on the Air-Pumping Phenomenon in High-Speed Spur and Helical Gears," Proceedings of the Institute of Mechanical Engineers, 219, pp. 785-800.
11. Diab, Y., Ville, F. and Velex, P., 2006, "Investigations on Power Losses in High Speed Gears," Proc. Inst. Mech.Eng., Part J: J. Eng. Tribol., 220, pp. 191–298.
12. Abdelilah Lasri, Lahcen Belfals, Brahim Najji, Bernard Mushirabwoba, ''Pressure Estimation of the Trapped and Squeezed Oil between Teeth Spaces of Spur Gears'' Applied Mathematical Sciences, Vol. 8, 2014, no. 107, 5317 - 5328 HIKARI Ltd, www.m-hikari.com, http://dx.doi.org/10.12988/ams.2014.47542
13. Abdelilah Lasri, F. Ville, Lahcen Belfals, Brahim Najji, ''Preliminary modeling of the oil trapping between teeth for spur gears'', Mechanics & Industry 15, 393–402 (2014), AFM, EDP Sciences 2014, DOI: 10.1051/meca/2014046, www.mechanics-industry.org
14. A. LASRI, L. BELFALS, B. NAJJI, M. ZAOUI ''Pertes de puissance par piégeage de l'huile lubrifiant dans les engrenages'' 13ème Congrès de Mécanique 11 - 14 Avril 2017. AFM, EDP Sciences 2014, DOI: 10.1051/meca/2014046, www.mechanics-industry.org
15. David C. Talbot, "Theoretical investigation of the efficiency of planetary gear sets", 2012, these de Doctor at à l'université de l'Etatd'Ohio au USA.
16. Seetharaman S. and Kahraman A., "Load-independent spin power losses of a spur gear pair: Model formulation," Journal of Tribology, vol. 131, 2009.
17. Massimo Rundo, ''Theoretical flow rate in crescent pumps'' ELSEVIER, Simulation Modelling Practice and Theory 71 (2017) 1–14, www.elsevier.com/locate/simpat.
18. Faydor L. Litvin, Alfonso Fuentes, ''Gear Geometry and Applied Theory'', SECOND EDITION, Ca,bridge university press, 2004.
19. J.R. Colbourne, The Geometry of Involute Gears, 1987 by Springer-Verlag New York Inc. DOI: 10.1007/978-1-4612-4764-7.
20. Christos A. Spitas and Vasilis A. Spitas, Generating Interchangeable 20° Spur Gear Sets with Circular Fillets to Increase Load Carrying Capacity; JULY/AUGUST 2006 • GEAR TECHNOLOGY • www.geartechnology.com • www.powertransmission.com.
21. Guodong Zhai, Zhihao Liang, and Zihao Fu, ''A Mathematical Model for Parametric Tooth Profile of Spur Gears''; Hindawi, Mathematical Problems in Engineering, Volume 2020, Article ID 7869315, 12 pages, https://doi.org/10.1155/2020/7869315.
22. Marco Ceccarelli Editor, ''Proceedings of EUCOMES 08'', The Second European Conference on Mechanism Science, Springer Science+Business Media B.V. 2009.

Global Journals Guidelines Handbook 2022

www.GlobalJournals.org

Memberships

Fellows/Associates of Engineering Research Council

FERC/AERC Memberships

Introduction

FERC/AERC is the most prestigious membership of Global Journals accredited by Open Association of Research Society, U.S.A (OARS). The credentials of Fellow and Associate designations signify that the researcher has gained the knowledge of the fundamental and high-level concepts, and is a subject matter expert, proficient in an expertise course covering the professional code of conduct, and follows recognized standards of practice. The credentials are designated only to the researchers, scientists, and professionals that have been selected by a rigorous process by our Editorial Board and Management Board.

Associates of FERC/AERC are scientists and researchers from around the world are working on projects/researches that have huge potentials. Members support Global Journals' mission to advance technology for humanity and the profession.

FERC

Fellow of Engineering Research Council

FELLOW OF ENGINEERING RESEARCH COUNCIL is the most prestigious membership of Global Journals. It is an award and membership granted to individuals that the Open Association of Research Society judges to have made a 'substantial contribution to the improvement of computer science, technology, and electronics engineering.

The primary objective is to recognize the leaders in research and scientific fields of the current era with a global perspective and to create a channel between them and other researchers for better exposure and knowledge sharing. Members are most eminent scientists, engineers, and technologists from all across the world. Fellows are elected for life through a peer review process on the basis of excellence in the respective domain. There is no limit on the number of new nominations made in any year. Each year, the Open Association of Research Society elect up to 12 new Fellow Members.

Benefit

To the institution

Get letter of appreciation

Global Journals sends a letter of appreciation of author to the Dean or CEO of the University or Company of which author is a part, signed by editor in chief or chief author.

Exclusive Network

Get access to a closed network

A FERC member gets access to a closed network of Tier 1 researchers and scientists with direct communication channel through our website. Fellows can reach out to other members or researchers directly. They should also be open to reaching out by other.

Career | Credibility | Exclusive | Reputation

Certificate

Certificate, LoR and Laser-Momento

Fellows receive a printed copy of a certificate signed by our Chief Author that may be used for academic purposes and a personal recommendation letter to the dean of member's university.

Career | Credibility | Exclusive | Reputation

Designation

Get honored title of membership

Fellows can use the honored title of membership. The “FERC” is an honored title which is accorded to a person’s name viz. Dr. John E. Hall, Ph.D., FERC or William Walldroff, M.S., FERC.

Career | Credibility | Exclusive | Reputation

Recognition on the Platform

Better visibility and citation

All the Fellow members of FERC get a badge of "Leading Member of Global Journals" on the Research Community that distinguishes them from others. Additionally, the profile is also partially maintained by our team for better visibility and citation. All fellows get a dedicated page on the website with their biography.

Career | Credibility | Reputation

Future Work

Get discounts on the future publications

Fellows receive discounts on the future publications with Global Journals up to 60%. Through our recommendation programs, members also receive discounts on publications made with OARS affiliated organizations.

Career | Financial

GJ Account

Unlimited forward of Emails

Fellows get secure and fast GJ work emails with unlimited storage of emails that they may use them as their primary email. For example, john [AT] globaljournals [DOT] org.

Career | Credibility | Reputation

Premium Tools

Access to all the premium tools

To take future researches to the zenith, fellows receive access to all the premium tools that Global Journals have to offer along with the partnership with some of the best marketing leading tools out there.

Financial

Conferences & Events

Organize seminar/conference

Fellows are authorized to organize symposium/seminar/conference on behalf of Global Journal Incorporation (USA). They can also participate in the same organized by another institution as representative of Global Journal. In both the cases, it is mandatory for him to discuss with us and obtain our consent. Additionally, they get free research conferences (and others) alerts.

Career | Credibility | Financial

Early Invitations

Early invitations to all the symposiums, seminars, conferences

All fellows receive the early invitations to all the symposiums, seminars, conferences and webinars hosted by Global Journals in their subject.

Exclusive

Publishing Articles & Books

Earn 60% of sales proceeds

Fellows can publish articles (limited) without any fees. Also, they can earn up to 70% of sales proceeds from the sale of reference/review books/literature/publishing of research paper. The FERC member can decide its price and we can help in making the right decision.

Exclusive | Financial

Reviewers

Get a remuneration of 15% of author fees

Fellow members are eligible to join as a paid peer reviewer at Global Journals Incorporation (USA) and can get a remuneration of 15% of author fees, taken from the author of a respective paper.

Financial

Access to Editorial Board

Become a member of the Editorial Board

Fellows may join as a member of the Editorial Board of Global Journals Incorporation (USA) after successful completion of three years as Fellow and as Peer Reviewer. Additionally, Fellows get a chance to nominate other members for Editorial Board.

Career | Credibility | Exclusive | Reputation

And Much More

Get access to scientific museums and observatories across the globe

All members get access to 5 selected scientific museums and observatories across the globe. All researches published with Global Journals will be kept under deep archival facilities across regions for future protections and disaster recovery. They get 10 GB free secure cloud access for storing research files.

AERC

ASSOCIATE OF ENGINEERING RESEARCH COUNCIL

ASSOCIATE OF ENGINEERING RESEARCH COUNCIL is the membership of Global Journals awarded to individuals that the Open Association of Research Society judges to have made a 'substantial contribution to the improvement of computer science, technology, and electronics engineering.

The primary objective is to recognize the leaders in research and scientific fields of the current era with a global perspective and to create a channel between them and other researchers for better exposure and knowledge sharing. Members are most eminent scientists, engineers, and technologists from all across the world. Associate membership can later be promoted to Fellow Membership. Associates are elected for life through a peer review process on the basis of excellence in the respective domain. There is no limit on the number of new nominations made in any year. Each year, the Open Association of Research Society elect up to 12 new Associate Members.

Benefit

To the institution

Get letter of appreciation

Global Journals sends a letter of appreciation of author to the Dean or CEO of the University or Company of which author is a part, signed by editor in chief or chief author.

Exclusive Network

Get access to a closed network

A AERC member gets access to a closed network of Tier 1 researchers and scientists with direct communication channel through our website. Associates can reach out to other members or researchers directly. They should also be open to reaching out by other.

Career | Credibility | Exclusive | Reputation

Certificate

Certificate, LoR and Laser-Momento

Associates receive a printed copy of a certificate signed by our Chief Author that may be used for academic purposes and a personal recommendation letter to the dean of member's university.

Career | Credibility | Exclusive | Reputation

Designation

Get honored title of membership

Associates can use the honored title of membership. The “AERC” is an honored title which is accorded to a person’s name viz. Dr. John E. Hall, Ph.D., AERC or William Walldroff, M.S., AERC.

Career | Credibility | Exclusive | Reputation

Recognition on the Platform

Better visibility and citation

All the Associate members of AERC get a badge of "Leading Member of Global Journals" on the Research Community that distinguishes them from others. Additionally, the profile is also partially maintained by our team for better visibility and citation. All associates get a dedicated page on the website with their biography.

Career | Credibility | Reputation

Future Work

Get discounts on the future publications

Associates receive discounts on the future publications with Global Journals up to 60%. Through our recommendation programs, members also receive discounts on publications made with OARS affiliated organizations.

Career | Financial

GJ Account

Unlimited forward of Emails

Associates get secure and fast GJ work emails with unlimited storage of emails that they may use them as their primary email. For example, john [AT] globaljournals [DOT] org..

Career | Credibility | Reputation

Premium Tools

Access to all the premium tools

To take future researches to the zenith, associates receive access to all the premium tools that Global Journals have to offer along with the partnership with some of the best marketing leading tools out there.

Financial

Conferences & Events

Organize seminar/conference

Associates are authorized to organize symposium/seminar/conference on behalf of Global Journal Incorporation (USA). They can also participate in the same organized by another institution as representative of Global Journal. In both the cases, it is mandatory for him to discuss with us and obtain our consent. Additionally, they get free research conferences (and others) alerts.

Career | Credibility | Financial

Early Invitations

Early invitations to all the symposiums, seminars, conferences

All associates receive the early invitations to all the symposiums, seminars, conferences and webinars hosted by Global Journals in their subject.

Exclusive

Publishing Articles & Books

Earn 30-40% of sales proceeds

Associates can publish articles (limited) without any fees. Also, they can earn up to 30-40% of sales proceeds from the sale of reference/review books/literature/publishing of research paper.

Exclusive | Financial

Reviewers

Get a remuneration of 15% of author fees

Associate members are eligible to join as a paid peer reviewer at Global Journals Incorporation (USA) and can get a remuneration of 15% of author fees, taken from the author of a respective paper.

Financial

And Much More

Get access to scientific museums and observatories across the globe

All members get access to 2 selected scientific museums and observatories across the globe. All researches published with Global Journals will be kept under deep archival facilities across regions for future protections and disaster recovery. They get 5 GB free secure cloud access for storing research files.

Associate	Fellow	Research Group	Basic
$4800 **lifetime designation**	$6800 **lifetime designation**	$12500.00 **organizational**	APC **per article**
Certificate, LoR and Momento **2** discounted publishing/year **Gradation** of Research **10** research contacts/day **1 GB** Cloud Storage **GJ** Community Access	**Certificate,** LoR and Momento **Unlimited** discounted publishing/year **Gradation** of Research **Unlimited** research contacts/day **5 GB** Cloud Storage **Online Presense** Assistance **GJ** Community Access	**Certificates,** LoRs and Momentos **Unlimited** free publishing/year **Gradation** of Research **Unlimited** research contacts/day **Unlimited** Cloud Storage **Online Presense** Assistance **GJ** Community Access	**GJ** Community Access

We accept the manuscript submissions in any standard (generic) format.

We typeset manuscripts using advanced typesetting tools like Adobe In Design, CorelDraw, TeXnicCenter, and TeXStudio. We usually recommend authors submit their research using any standard format they are comfortable with, and let Global Journals do the rest.

Alternatively, you can download our basic template from https://globaljournals.org/Template.zip

Authors should submit their complete paper/article, including text illustrations, graphics, conclusions, artwork, and tables. Authors who are not able to submit manuscript using the form above can email the manuscript department at submit@globaljournals.org or get in touch with chiefeditor@globaljournals.org if they wish to send the abstract before submission.

Before and during Submission

Authors must ensure the information provided during the submission of a paper is authentic. Please go through the following checklist before submitting:

1. Authors must go through the complete author guideline and understand and *agree to Global Journals' ethics and code of conduct,* along with author responsibilities.
2. Authors must accept the privacy policy, terms, and conditions of Global Journals.
3. Ensure corresponding author's email address and postal address are accurate and reachable.
4. Manuscript to be submitted must include keywords, an abstract, a paper title, co-author(s') names and details (email address, name, phone number, and institution), figures and illustrations in vector format including appropriate captions, tables, including titles and footnotes, a conclusion, results, acknowledgments and references.
5. Authors should submit paper in a ZIP archive if any supplementary files are required along with the paper.
6. Proper permissions must be acquired for the use of any copyrighted material.
7. Manuscript submitted *must not have been submitted or published elsewhere* and all authors must be aware of the submission.

Declaration of Conflicts of Interest

It is required for authors to declare all financial, institutional, and personal relationships with other individuals and organizations that could influence (bias) their research.

Policy on Plagiarism

Plagiarism is not acceptable in Global Journals submissions at all.

Plagiarized content will not be considered for publication. We reserve the right to inform authors' institutions about plagiarism detected either before or after publication. If plagiarism is identified, we will follow COPE guidelines:

Authors are solely responsible for all the plagiarism that is found. The author must not fabricate, falsify or plagiarize existing research data. The following, if copied, will be considered plagiarism:

- Words (language)
- Ideas
- Findings
- Writings
- Diagrams
- Graphs
- Illustrations
- Lectures

- Printed material
- Graphic representations
- Computer programs
- Electronic material
- Any other original work

Authorship Policies

Global Journals follows the definition of authorship set up by the Open Association of Research Society, USA. According to its guidelines, authorship criteria must be based on:

1. Substantial contributions to the conception and acquisition of data, analysis, and interpretation of findings.
2. Drafting the paper and revising it critically regarding important academic content.
3. Final approval of the version of the paper to be published.

Changes in Authorship

The corresponding author should mention the name and complete details of all co-authors during submission and in manuscript. We support addition, rearrangement, manipulation, and deletions in authors list till the early view publication of the journal. We expect that corresponding author will notify all co-authors of submission. We follow COPE guidelines for changes in authorship.

Copyright

During submission of the manuscript, the author is confirming an exclusive license agreement with Global Journals which gives Global Journals the authority to reproduce, reuse, and republish authors' research. We also believe in flexible copyright terms where copyright may remain with authors/employers/institutions as well. Contact your editor after acceptance to choose your copyright policy. You may follow this form for copyright transfers.

Appealing Decisions

Unless specified in the notification, the Editorial Board's decision on publication of the paper is final and cannot be appealed before making the major change in the manuscript.

Acknowledgments

Contributors to the research other than authors credited should be mentioned in Acknowledgments. The source of funding for the research can be included. Suppliers of resources may be mentioned along with their addresses.

Declaration of funding sources

Global Journals is in partnership with various universities, laboratories, and other institutions worldwide in the research domain. Authors are requested to disclose their source of funding during every stage of their research, such as making analysis, performing laboratory operations, computing data, and using institutional resources, from writing an article to its submission. This will also help authors to get reimbursements by requesting an open access publication letter from Global Journals and submitting to the respective funding source.

Preparing your Manuscript

Authors can submit papers and articles in an acceptable file format: MS Word (doc, docx), LaTeX (.tex, .zip or .rar including all of your files), Adobe PDF (.pdf), rich text format (.rtf), simple text document (.txt), Open Document Text (.odt), and Apple Pages (.pages). Our professional layout editors will format the entire paper according to our official guidelines. This is one of the highlights of publishing with Global Journals—authors should not be concerned about the formatting of their paper. Global Journals accepts articles and manuscripts in every major language, be it Spanish, Chinese, Japanese, Portuguese, Russian, French, German, Dutch, Italian, Greek, or any other national language, but the title, subtitle, and abstract should be in English. This will facilitate indexing and the pre-peer review process.

The following is the official style and template developed for publication of a research paper. Authors are not required to follow this style during the submission of the paper. It is just for reference purposes.

Manuscript Style Instruction (Optional)

- Microsoft Word Document Setting Instructions.
- Font type of all text should be Swis721 Lt BT.
- Page size: 8.27" x 11'", left margin: 0.65, right margin: 0.65, bottom margin: 0.75.
- Paper title should be in one column of font size 24.
- Author name in font size of 11 in one column.
- Abstract: font size 9 with the word "Abstract" in bold italics.
- Main text: font size 10 with two justified columns.
- Two columns with equal column width of 3.38 and spacing of 0.2.
- First character must be three lines drop-capped.
- The paragraph before spacing of 1 pt and after of 0 pt.
- Line spacing of 1 pt.
- Large images must be in one column.
- The names of first main headings (Heading 1) must be in Roman font, capital letters, and font size of 10.
- The names of second main headings (Heading 2) must not include numbers and must be in italics with a font size of 10.

Structure and Format of Manuscript

The recommended size of an original research paper is under 15,000 words and review papers under 7,000 words. Research articles should be less than 10,000 words. Research papers are usually longer than review papers. Review papers are reports of significant research (typically less than 7,000 words, including tables, figures, and references)

A research paper must include:

a) A title which should be relevant to the theme of the paper.
b) A summary, known as an abstract (less than 150 words), containing the major results and conclusions.
c) Up to 10 keywords that precisely identify the paper's subject, purpose, and focus.
d) An introduction, giving fundamental background objectives.
e) Resources and techniques with sufficient complete experimental details (wherever possible by reference) to permit repetition, sources of information must be given, and numerical methods must be specified by reference.
f) Results which should be presented concisely by well-designed tables and figures.
g) Suitable statistical data should also be given.
h) All data must have been gathered with attention to numerical detail in the planning stage.

Design has been recognized to be essential to experiments for a considerable time, and the editor has decided that any paper that appears not to have adequate numerical treatments of the data will be returned unrefereed.

i) Discussion should cover implications and consequences and not just recapitulate the results; conclusions should also be summarized.
j) There should be brief acknowledgments.
k) There ought to be references in the conventional format. Global Journals recommends APA format.

Authors should carefully consider the preparation of papers to ensure that they communicate effectively. Papers are much more likely to be accepted if they are carefully designed and laid out, contain few or no errors, are summarizing, and follow instructions. They will also be published with much fewer delays than those that require much technical and editorial correction.

The Editorial Board reserves the right to make literary corrections and suggestions to improve brevity.

Format Structure

It is necessary that authors take care in submitting a manuscript that is written in simple language and adheres to published guidelines.

All manuscripts submitted to Global Journals should include:

Title

The title page must carry an informative title that reflects the content, a running title (less than 45 characters together with spaces), names of the authors and co-authors, and the place(s) where the work was carried out.

Author details

The full postal address of any related author(s) must be specified.

Abstract

The abstract is the foundation of the research paper. It should be clear and concise and must contain the objective of the paper and inferences drawn. It is advised to not include big mathematical equations or complicated jargon.

Many researchers searching for information online will use search engines such as Google, Yahoo or others. By optimizing your paper for search engines, you will amplify the chance of someone finding it. In turn, this will make it more likely to be viewed and cited in further works. Global Journals has compiled these guidelines to facilitate you to maximize the web-friendliness of the most public part of your paper.

Keywords

A major lynchpin of research work for the writing of research papers is the keyword search, which one will employ to find both library and internet resources. Up to eleven keywords or very brief phrases have to be given to help data retrieval, mining, and indexing.

One must be persistent and creative in using keywords. An effective keyword search requires a strategy: planning of a list of possible keywords and phrases to try.

Choice of the main keywords is the first tool of writing a research paper. Research paper writing is an art. Keyword search should be as strategic as possible.

One should start brainstorming lists of potential keywords before even beginning searching. Think about the most important concepts related to research work. Ask, “What words would a source have to include to be truly valuable in a research paper?” Then consider synonyms for the important words.

It may take the discovery of only one important paper to steer in the right keyword direction because, in most databases, the keywords under which a research paper is abstracted are listed with the paper.

Numerical Methods

Numerical methods used should be transparent and, where appropriate, supported by references.

Abbreviations

Authors must list all the abbreviations used in the paper at the end of the paper or in a separate table before using them.

Formulas and equations

Authors are advised to submit any mathematical equation using either MathJax, KaTeX, or LaTeX, or in a very high-quality image.

Tables, Figures, and Figure Legends

Tables: Tables should be cautiously designed, uncrowned, and include only essential data. Each must have an Arabic number, e.g., Table 4, a self-explanatory caption, and be on a separate sheet. Authors must submit tables in an editable format and not as images. References to these tables (if any) must be mentioned accurately.

Figures

Figures are supposed to be submitted as separate files. Always include a citation in the text for each figure using Arabic numbers, e.g., Fig. 4. Artwork must be submitted online in vector electronic form or by emailing it.

Preparation of Eletronic Figures for Publication

Although low-quality images are sufficient for review purposes, print publication requires high-quality images to prevent the final product being blurred or fuzzy. Submit (possibly by e-mail) EPS (line art) or TIFF (halftone/ photographs) files only. MS PowerPoint and Word Graphics are unsuitable for printed pictures. Avoid using pixel-oriented software. Scans (TIFF only) should have a resolution of at least 350 dpi (halftone) or 700 to 1100 dpi (line drawings). Please give the data for figures in black and white or submit a Color Work Agreement form. EPS files must be saved with fonts embedded (and with a TIFF preview, if possible).

For scanned images, the scanning resolution at final image size ought to be as follows to ensure good reproduction: line art: >650 dpi; halftones (including gel photographs): >350 dpi; figures containing both halftone and line images: >650 dpi.

Color charges: Authors are advised to pay the full cost for the reproduction of their color artwork. Hence, please note that if there is color artwork in your manuscript when it is accepted for publication, we would require you to complete and return a Color Work Agreement form before your paper can be published. Also, you can email your editor to remove the color fee after acceptance of the paper.

Tips for Writing a Good Quality Engineering Research Paper

Techniques for writing a good quality engineering research paper:

1. Choosing the topic: In most cases, the topic is selected by the interests of the author, but it can also be suggested by the guides. You can have several topics, and then judge which you are most comfortable with. This may be done by asking several questions of yourself, like "Will I be able to carry out a search in this area? Will I find all necessary resources to accomplish the search? Will I be able to find all information in this field area?" If the answer to this type of question is "yes," then you ought to choose that topic. In most cases, you may have to conduct surveys and visit several places. Also, you might have to do a lot of work to find all the rises and falls of the various data on that subject. Sometimes, detailed information plays a vital role, instead of short information. Evaluators are human: The first thing to remember is that evaluators are also human beings. They are not only meant for rejecting a paper. They are here to evaluate your paper. So present your best aspect.

2. Think like evaluators: If you are in confusion or getting demotivated because your paper may not be accepted by the evaluators, then think, and try to evaluate your paper like an evaluator. Try to understand what an evaluator wants in your research paper, and you will automatically have your answer. Make blueprints of paper: The outline is the plan or framework that will help you to arrange your thoughts. It will make your paper logical. But remember that all points of your outline must be related to the topic you have chosen.

3. Ask your guides: If you are having any difficulty with your research, then do not hesitate to share your difficulty with your guide (if you have one). They will surely help you out and resolve your doubts. If you can't clarify what exactly you require for your work, then ask your supervisor to help you with an alternative. He or she might also provide you with a list of essential readings.

4. Use of computer is recommended: As you are doing research in the field of research engineering then this point is quite obvious. Use right software: Always use good quality software packages. If you are not capable of judging good software, then you can lose the quality of your paper unknowingly. There are various programs available to help you which you can get through the internet.

5. Use the internet for help: An excellent start for your paper is using Google. It is a wondrous search engine, where you can have your doubts resolved. You may also read some answers for the frequent question of how to write your research paper or find a model research paper. You can download books from the internet. If you have all the required books, place importance on reading, selecting, and analyzing the specified information. Then sketch out your research paper. Use big pictures: You may use encyclopedias like Wikipedia to get pictures with the best resolution. At Global Journals, you should strictly follow here.

6. Bookmarks are useful: When you read any book or magazine, you generally use bookmarks, right? It is a good habit which helps to not lose your continuity. You should always use bookmarks while searching on the internet also, which will make your search easier.

7. Revise what you wrote: When you write anything, always read it, summarize it, and then finalize it.

8. Make every effort: Make every effort to mention what you are going to write in your paper. That means always have a good start. Try to mention everything in the introduction—what is the need for a particular research paper. Polish your work with good writing skills and always give an evaluator what he wants. Make backups: When you are going to do any important thing like making a research paper, you should always have backup copies of it either on your computer or on paper. This protects you from losing any portion of your important data.

9. Produce good diagrams of your own: Always try to include good charts or diagrams in your paper to improve quality. Using several unnecessary diagrams will degrade the quality of your paper by creating a hodgepodge. So always try to include diagrams which were made by you to improve the readability of your paper. Use of direct quotes: When you do research relevant to literature, history, or current affairs, then use of quotes becomes essential, but if the study is relevant to science, use of quotes is not preferable.

10. Use proper verb tense: Use proper verb tenses in your paper. Use past tense to present those events that have happened. Use present tense to indicate events that are going on. Use future tense to indicate events that will happen in the future. Use of wrong tenses will confuse the evaluator. Avoid sentences that are incomplete.

11. Pick a good study spot: Always try to pick a spot for your research which is quiet. Not every spot is good for studying.

12. Know what you know: Always try to know what you know by making objectives, otherwise you will be confused and unable to achieve your target.

13. Use good grammar: Always use good grammar and words that will have a positive impact on the evaluator; use of good vocabulary does not mean using tough words which the evaluator has to find in a dictionary. Do not fragment sentences. Eliminate one-word sentences. Do not ever use a big word when a smaller one would suffice.

Verbs have to be in agreement with their subjects. In a research paper, do not start sentences with conjunctions or finish them with prepositions. When writing formally, it is advisable to never split an infinitive because someone will (wrongly) complain. Avoid clichés like a disease. Always shun irritating alliteration. Use language which is simple and straightforward. Put together a neat summary.

14. Arrangement of information: Each section of the main body should start with an opening sentence, and there should be a changeover at the end of the section. Give only valid and powerful arguments for your topic. You may also maintain your arguments with records.

15. Never start at the last minute: Always allow enough time for research work. Leaving everything to the last minute will degrade your paper and spoil your work.

16. Multitasking in research is not good: Doing several things at the same time is a bad habit in the case of research activity. Research is an area where everything has a particular time slot. Divide your research work into parts, and do a particular part in a particular time slot.

17. Never copy others' work: Never copy others' work and give it your name because if the evaluator has seen it anywhere, you will be in trouble. Take proper rest and food: No matter how many hours you spend on your research activity, if you are not taking care of your health, then all your efforts will have been in vain. For quality research, take proper rest and food.

18. Go to seminars: Attend seminars if the topic is relevant to your research area. Utilize all your resources.

19. Refresh your mind after intervals: Try to give your mind a rest by listening to soft music or sleeping in intervals. This will also improve your memory. Acquire colleagues: Always try to acquire colleagues. No matter how sharp you are, if you acquire colleagues, they can give you ideas which will be helpful to your research.

20. Think technically: Always think technically. If anything happens, search for its reasons, benefits, and demerits. Think and then print: When you go to print your paper, check that tables are not split, headings are not detached from their descriptions, and page sequence is maintained.

21. Adding unnecessary information: Do not add unnecessary information like "I have used MS Excel to draw graphs." Irrelevant and inappropriate material is superfluous. Foreign terminology and phrases are not apropos. One should never take a broad view. Analogy is like feathers on a snake. Use words properly, regardless of how others use them. Remove quotations. Puns are for kids, not grunt readers. Never oversimplify: When adding material to your research paper, never go for oversimplification; this will definitely irritate the evaluator. Be specific. Never use rhythmic redundancies. Contractions shouldn't be used in a research paper. Comparisons are as terrible as clichés. Give up ampersands, abbreviations, and so on. Remove commas that are not necessary. Parenthetical words should be between brackets or commas. Understatement is always the best way to put forward earth-shaking thoughts. Give a detailed literary review.

22. Report concluded results: Use concluded results. From raw data, filter the results, and then conclude your studies based on measurements and observations taken. An appropriate number of decimal places should be used. Parenthetical remarks are prohibited here. Proofread carefully at the final stage. At the end, give an outline to your arguments. Spot perspectives of further study of the subject. Justify your conclusion at the bottom sufficiently, which will probably include examples.

23. Upon conclusion: Once you have concluded your research, the next most important step is to present your findings. Presentation is extremely important as it is the definite medium though which your research is going to be in print for the rest of the crowd. Care should be taken to categorize your thoughts well and present them in a logical and neat manner. A good quality research paper format is essential because it serves to highlight your research paper and bring to light all necessary aspects of your research.

Informal Guidelines of Research Paper Writing

Key points to remember:

- Submit all work in its final form.
- Write your paper in the form which is presented in the guidelines using the template.
- Please note the criteria peer reviewers will use for grading the final paper.

Final points:

One purpose of organizing a research paper is to let people interpret your efforts selectively. The journal requires the following sections, submitted in the order listed, with each section starting on a new page:

The introduction: This will be compiled from reference matter and reflect the design processes or outline of basis that directed you to make a study. As you carry out the process of study, the method and process section will be constructed like that. The results segment will show related statistics in nearly sequential order and direct reviewers to similar intellectual paths throughout the data that you gathered to carry out your study.

The discussion section:

This will provide understanding of the data and projections as to the implications of the results. The use of good quality references throughout the paper will give the effort trustworthiness by representing an alertness to prior workings.

Writing a research paper is not an easy job, no matter how trouble-free the actual research or concept. Practice, excellent preparation, and controlled record-keeping are the only means to make straightforward progression.

General style:

Specific editorial column necessities for compliance of a manuscript will always take over from directions in these general guidelines.

To make a paper clear: Adhere to recommended page limits.

Mistakes to avoid:

- Insertion of a title at the foot of a page with subsequent text on the next page.
- Separating a table, chart, or figure—confine each to a single page.
- Submitting a manuscript with pages out of sequence.
- In every section of your document, use standard writing style, including articles ("a" and "the").
- Keep paying attention to the topic of the paper.

- Use paragraphs to split each significant point (excluding the abstract).
- Align the primary line of each section.
- Present your points in sound order.
- Use present tense to report well-accepted matters.
- Use past tense to describe specific results.
- Do not use familiar wording; don't address the reviewer directly. Don't use slang or superlatives.
- Avoid use of extra pictures—include only those figures essential to presenting results.

Title page:

Choose a revealing title. It should be short and include the name(s) and address(es) of all authors. It should not have acronyms or abbreviations or exceed two printed lines.

Abstract: This summary should be two hundred words or less. It should clearly and briefly explain the key findings reported in the manuscript and must have precise statistics. It should not have acronyms or abbreviations. It should be logical in itself. Do not cite references at this point.

An abstract is a brief, distinct paragraph summary of finished work or work in development. In a minute or less, a reviewer can be taught the foundation behind the study, common approaches to the problem, relevant results, and significant conclusions or new questions.

Write your summary when your paper is completed because how can you write the summary of anything which is not yet written? Wealth of terminology is very essential in abstract. Use comprehensive sentences, and do not sacrifice readability for brevity; you can maintain it succinctly by phrasing sentences so that they provide more than a lone rationale. The author can at this moment go straight to shortening the outcome. Sum up the study with the subsequent elements in any summary. Try to limit the initial two items to no more than one line each.

Reason for writing the article—theory, overall issue, purpose.

- Fundamental goal.
- To-the-point depiction of the research.
- Consequences, including definite statistics—if the consequences are quantitative in nature, account for this; results of any numerical analysis should be reported. Significant conclusions or questions that emerge from the research.

Approach:

- Single section and succinct.
- An outline of the job done is always written in past tense.
- Concentrate on shortening results—limit background information to a verdict or two.
- Exact spelling, clarity of sentences and phrases, and appropriate reporting of quantities (proper units, important statistics) are just as significant in an abstract as they are anywhere else.

Introduction:

The introduction should "introduce" the manuscript. The reviewer should be presented with sufficient background information to be capable of comprehending and calculating the purpose of your study without having to refer to other works. The basis for the study should be offered. Give the most important references, but avoid making a comprehensive appraisal of the topic. Describe the problem visibly. If the problem is not acknowledged in a logical, reasonable way, the reviewer will give no attention to your results. Speak in common terms about techniques used to explain the problem, if needed, but do not present any particulars about the protocols here.

The following approach can create a valuable beginning:

- Explain the value (significance) of the study.
- Defend the model—why did you employ this particular system or method? What is its compensation? Remark upon its appropriateness from an abstract point of view as well as pointing out sensible reasons for using it.
- Present a justification. State your particular theory(-ies) or aim(s), and describe the logic that led you to choose them.
- Briefly explain the study's tentative purpose and how it meets the declared objectives.

Approach:

Use past tense except for when referring to recognized facts. After all, the manuscript will be submitted after the entire job is done. Sort out your thoughts; manufacture one key point for every section. If you make the four points listed above, you will need at least four paragraphs. Present surrounding information only when it is necessary to support a situation. The reviewer does not desire to read everything you know about a topic. Shape the theory specifically—do not take a broad view.

As always, give awareness to spelling, simplicity, and correctness of sentences and phrases.

Procedures (methods and materials):

This part is supposed to be the easiest to carve if you have good skills. A soundly written procedures segment allows a capable scientist to replicate your results. Present precise information about your supplies. The suppliers and clarity of reagents can be helpful bits of information. Present methods in sequential order, but linked methodologies can be grouped as a segment. Be concise when relating the protocols. Attempt to give the least amount of information that would permit another capable scientist to replicate your outcome, but be cautious that vital information is integrated. The use of subheadings is suggested and ought to be synchronized with the results section.

When a technique is used that has been well-described in another section, mention the specific item describing the way, but draw the basic principle while stating the situation. The purpose is to show all particular resources and broad procedures so that another person may use some or all of the methods in one more study or referee the scientific value of your work. It is not to be a step-by-step report of the whole thing you did, nor is a methods section a set of orders.

Materials:

Materials may be reported in part of a section or else they may be recognized along with your measures.

Methods:

- Report the method and not the particulars of each process that engaged the same methodology.
- Describe the method entirely.
- To be succinct, present methods under headings dedicated to specific dealings or groups of measures.
- Simplify—detail how procedures were completed, not how they were performed on a particular day.
- If well-known procedures were used, account for the procedure by name, possibly with a reference, and that's all.

Approach:

It is embarrassing to use vigorous voice when documenting methods without using first person, which would focus the reviewer's interest on the researcher rather than the job. As a result, when writing up the methods, most authors use third person passive voice.

Use standard style in this and every other part of the paper—avoid familiar lists, and use full sentences.

What to keep away from:

- Resources and methods are not a set of information.
- Skip all descriptive information and surroundings—save it for the argument.
- Leave out information that is immaterial to a third party.

Results:

The principle of a results segment is to present and demonstrate your conclusion. Create this part as entirely objective details of the outcome, and save all understanding for the discussion.

The page length of this segment is set by the sum and types of data to be reported. Use statistics and tables, if suitable, to present consequences most efficiently.

You must clearly differentiate material which would usually be incorporated in a study editorial from any unprocessed data or additional appendix matter that would not be available. In fact, such matters should not be submitted at all except if requested by the instructor.

Content:

- Sum up your conclusions in text and demonstrate them, if suitable, with figures and tables.
- In the manuscript, explain each of your consequences, and point the reader to remarks that are most appropriate.
- Present a background, such as by describing the question that was addressed by creation of an exacting study.
- Explain results of control experiments and give remarks that are not accessible in a prescribed figure or table, if appropriate.
- Examine your data, then prepare the analyzed (transformed) data in the form of a figure (graph), table, or manuscript.

What to stay away from:

- Do not discuss or infer your outcome, report surrounding information, or try to explain anything.
- Do not include raw data or intermediate calculations in a research manuscript.
- Do not present similar data more than once.
- A manuscript should complement any figures or tables, not duplicate information.
- Never confuse figures with tables—there is a difference.

Approach:

As always, use past tense when you submit your results, and put the whole thing in a reasonable order.

Put figures and tables, appropriately numbered, in order at the end of the report.

If you desire, you may place your figures and tables properly within the text of your results section.

Figures and tables:

If you put figures and tables at the end of some details, make certain that they are visibly distinguished from any attached appendix materials, such as raw facts. Whatever the position, each table must be titled, numbered one after the other, and include a heading. All figures and tables must be divided from the text.

Discussion:

The discussion is expected to be the trickiest segment to write. A lot of papers submitted to the journal are discarded based on problems with the discussion. There is no rule for how long an argument should be.

Position your understanding of the outcome visibly to lead the reviewer through your conclusions, and then finish the paper with a summing up of the implications of the study. The purpose here is to offer an understanding of your results and support all of your conclusions, using facts from your research and generally accepted information, if suitable. The implication of results should be fully described.

Infer your data in the conversation in suitable depth. This means that when you clarify an observable fact, you must explain mechanisms that may account for the observation. If your results vary from your prospect, make clear why that may have happened. If your results agree, then explain the theory that the proof supported. It is never suitable to just state that the data approved the prospect, and let it drop at that. Make a decision as to whether each premise is supported or discarded or if you cannot make a conclusion with assurance. Do not just dismiss a study or part of a study as "uncertain."

Research papers are not acknowledged if the work is imperfect. Draw what conclusions you can based upon the results that you have, and take care of the study as a finished work.

- You may propose future guidelines, such as how an experiment might be personalized to accomplish a new idea.
- Give details of all of your remarks as much as possible, focusing on mechanisms.
- Make a decision as to whether the tentative design sufficiently addressed the theory and whether or not it was correctly restricted. Try to present substitute explanations if they are sensible alternatives.
- One piece of research will not counter an overall question, so maintain the large picture in mind. Where do you go next? The best studies unlock new avenues of study. What questions remain?
- Recommendations for detailed papers will offer supplementary suggestions.

Approach:

When you refer to information, differentiate data generated by your own studies from other available information. Present work done by specific persons (including you) in past tense.

Describe generally acknowledged facts and main beliefs in present tense.

The Administration Rules

Administration Rules to Be Strictly Followed before Submitting Your Research Paper to Global Journals Inc.

Please read the following rules and regulations carefully before submitting your research paper to Global Journals Inc. to avoid rejection.

Segment draft and final research paper: You have to strictly follow the template of a research paper, failing which your paper may get rejected. You are expected to write each part of the paper wholly on your own. The peer reviewers need to identify your own perspective of the concepts in your own terms. Please do not extract straight from any other source, and do not rephrase someone else's analysis. Do not allow anyone else to proofread your manuscript.

Written material: You may discuss this with your guides and key sources. Do not copy anyone else's paper, even if this is only imitation, otherwise it will be rejected on the grounds of plagiarism, which is illegal. Various methods to avoid plagiarism are strictly applied by us to every paper, and, if found guilty, you may be blacklisted, which could affect your career adversely. To guard yourself and others from possible illegal use, please do not permit anyone to use or even read your paper and file.

Criterion for Grading a Research Paper (Compilation) by Global Journals

Please note that following table is only a Grading of "Paper Compilation" and not on "Performed/Stated Research" whose grading solely depends on Individual Assigned Peer Reviewer and Editorial Board Member. These can be available only on request and after decision of Paper. This report will be the property of Global Journals.

Topics	Grades		
	A-B	**C-D**	**E-F**
Abstract	Clear and concise with appropriate content, Correct format. 200 words or below	Unclear summary and no specific data, Incorrect form Above 200 words	No specific data with ambiguous information Above 250 words
Introduction	Containing all background details with clear goal and appropriate details, flow specification, no grammar and spelling mistake, well organized sentence and paragraph, reference cited	Unclear and confusing data, appropriate format, grammar and spelling errors with unorganized matter	Out of place depth and content, hazy format
Methods and Procedures	Clear and to the point with well arranged paragraph, precision and accuracy of facts and figures, well organized subheads	Difficult to comprehend with embarrassed text, too much explanation but completed	Incorrect and unorganized structure with hazy meaning
Result	Well organized, Clear and specific, Correct units with precision, correct data, well structuring of paragraph, no grammar and spelling mistake	Complete and embarrassed text, difficult to comprehend	Irregular format with wrong facts and figures
Discussion	Well organized, meaningful specification, sound conclusion, logical and concise explanation, highly structured paragraph reference cited	Wordy, unclear conclusion, spurious	Conclusion is not cited, unorganized, difficult to comprehend
References	Complete and correct format, well organized	Beside the point, Incomplete	Wrong format and structuring

Index

save our planet

Global Journal of Researches in Engineering

Visit us on the Web at www.GlobalJournals.org | www.EngineeringResearch.org
or email us at helpdesk@globaljournals.org

ISSN 9755861